UNIVERSITY OF CAPE TOWN

DEPARTMENT OF CIVIL ENGINEERING

EVALUATION OF THE RESIDUAL PRESTRESS FORCE IN AGED RAILWAY CONCRETE SLEEPERS CONSIDERED FOR REUSE

---

10 June 2025

A Thesis Submitted in Partial Fulfilment of The Requirements of the Degree of

Master in Engineering

In

The Faculty of Engineering and Built Environment

Course: CIV5017Z – Minor Dissertation

Prepared by: Nonofo Olefile Seketema (sktnon003)

Supervisor: Professor Hans Beushausen

Co-Supervisor: Joanitta Ndawula

Submission Date: 10 June 2025

A journey of 1000 miles begins with a single step

PLAGIARISM DECLARATION

I, the undersigned, hereby declare that:

1. I know that plagiarism is wrong. Plagiarism is to use another's work and to pretend that it is one's own.
2. I have used the Harvard Convention for citation and referencing. Each significant contribution to and quotation in this report from the work or works of other people has been attributed and has been cited and referenced.
3. This report is my work. I have not allowed and will not allow anyone to copy my work with the intention of passing it as his or her own work.

Signature of student

Name of student : Nonofo Seketema

Student number : SKTNON003

Date : 10 June 2025

ACKNOWLEDGEMENTS

The journey of this research was made possible by the assistance and collaboration of many individuals to whom I extend my sincere gratitude.

Firstly, I would like to express my heartfelt thanks to my supervisor, Professor Hans Beushaunsen, and co-supervisor, Joanitta Ndawula, for their valuable guidance, encouragement, and constructive feedback. Their expertise and dedication were instrumental in shaping the direction of this research.

I would also like to thank Transnet for permitting the resources and environment to conduct this research. A very special thank you to the support staff for the support and collaboration. I would also like to thank Deepak Budhram for permitting the use of experimental resources, and Nelson Tapala and his team for participating in the research work. Your contribution was invaluable to the success of this study. I thank Mr. Jeff van der Merwe from TANDM for his input on strain gauging and for providing the strain gauges used in this research.

I am grateful to my friends, peers and former colleagues, in particular Alvino Bezuidenhout, Tembelihle Ntangana, Modibedi Tshukudu and Valentine Kaupa for their companionship and varied support, such as editing, proofreading, and considerate check-ins from afar. I also extend my heartfelt thanks to my family, whose unwavering support, patience, and encouragement have been a source of strength throughout this journey.

While some individuals are acknowledged by name, many others remain unnamed; each has made meaningful contributions and is deeply appreciated. Thank you all for being an integral part of this accomplishment.

ABSTRACT

The increasing demand for railway transport in South Africa has led to the expansion and upgrade of the existing track infrastructure in recent years. Given the high costs associated with new development or refurbishment of existing infrastructure, asset owners and managers are faced with the challenge of optimising expenditures while extending the service life of their infrastructure.

One of the essential structural components of a conventional railway track is the prestressed concrete sleeper. In South Africa, these sleepers are designed to last for 40 years, and their replacement plan is aligned with their design life. Given the desire to extend the useful life of sleepers, aged concrete sleepers are often removed from primary running lines for second-hand use in branch, sidings and yard lines. However, the current quality assurance system for reusing sleepers relies mainly on visual condition assessments, which only consider the external surface of the concrete, neglecting the internal condition of the reinforcing and prestress steel and, critically, the remaining prestress force, which is crucial for the flexural strength.

To address this gap, a study was conducted to determine the prestressing force of concrete sleepers post-design life using the dynamic relaxation method. The study involved sampling 21 P2 concrete sleepers, comprising eighteen old sleepers (manufactured in 1977) and three new sleepers (manufactured in 2006). Six of the 21 sleepers were used to determine compressive and tensile strength values of concrete and steel wires, respectively, while the remaining 15 sleepers were subjected to dynamic relaxation testing.

Visual condition assessment revealed several types of concrete damage caused by operation and maintenance activities, with notable bending cracks propagating from the sleeper base around the rail seat region. Additionally, concrete surface abrasion was identified on the base, sleeper sides, and on the rail seat area. The two steel components, wires and cast-iron, extracted from the concrete were found to have corroded to varying degrees.

The results of the dynamic relaxation method demonstrated significant reduction of the prestress force in both aged and new sleepers when compared to the requirements of the BBG8755 specification. The mean loss of prestress force was 77% and 65% for old and new sleepers, respectively. Whilst prestress loss was expected for aged sleepers, the high loss for new sleepers was unexpected. Further testing is therefore recommended to identify contributing factors and verify the results through expanded testing.

The prestress force loss over the useful life of concrete sleepers confirmed the need for a robust second-hand sleeper classification system. The proposed guideline for evaluating reusable prestressed concrete sleepers incorporates both visual condition assessment and the concrete and steel materials strength and durability confirmation tests.

TABLE OF CONTENTS

LIST OF TABLES

LIST OF FIGURES

LIST OF ABBREVIATIONS AND ACRONYMS

Abbreviations	Definition
AC	Alternating Current
COD	Crack Opening Displacement
DC	Direct Current
FCSR	Functional Condition Scale Rating
GPR	Ground Penetrating Radar
NDT	Non-Destructive Testing
PCS	Prestressed Concrete Sleepers
SA	South Africa
SATS	South African Transport Services
SG	Strain Gauge
Tal	ton axle load

1 INTRODUCTION

1.1 Background

Railway transportation provides a safe and economical means of hauling freight and transporting passengers, using wagons that run on a rail track structure. It is similar to road transportation in principle, where vehicles run on a directionally prepared surface. In railway transportation, locomotives and wagons run on a constructed rail track composed of different layered materials. In order of structural arrangement from top to bottom as shown in Figure 1.1, these include: the rails upon which the wheels make contact, sleepers, fasteners supporting and securing the rails to the sleepers, underlain by ballast and the ground subgrade layers (Gebeyehu, 2017).

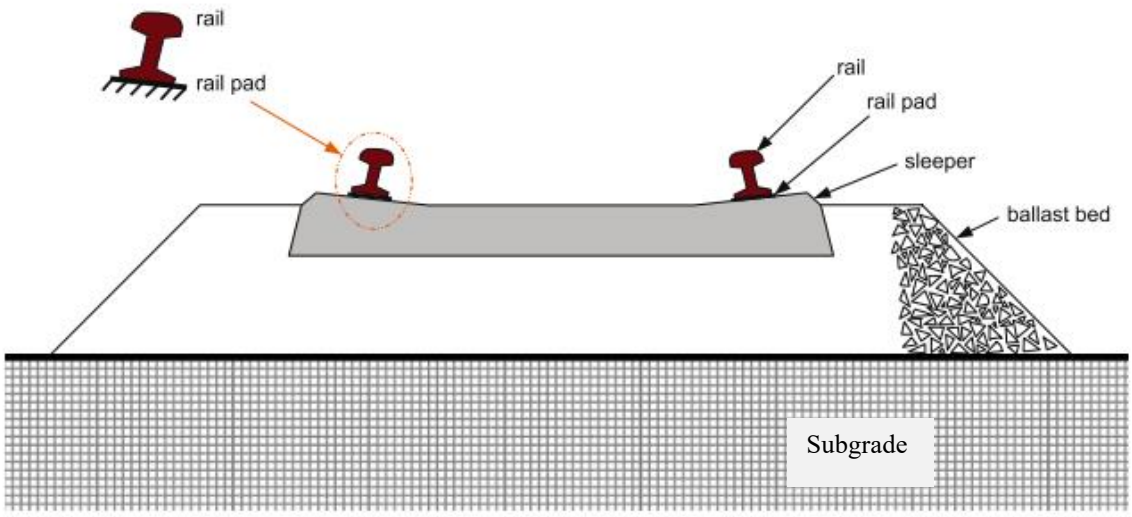

Figure 1.1: Components of the conventional railway track structure (Remennikov & Kaewunruen, 2006)

Sleepers are one of the main structural components of the conventional railway track, designed to transfer static and dynamic loads from the rail to the underlying sub-structures. Moreover, they provide the correct track gauge and horizontal alignment through the fastening systems. Sleepers are generally subjected to enormous vertical, lateral and axial loads during their service life (Zakeri & Rezvani, 2012).

The sleepers are primarily made from steel, timber or concrete. In comparison to the preferred concrete sleepers, timber and steel sleepers have limited strength and durability as required for the structural performance of the railway (Camille et al., 2022). Concrete sleepers have demonstrated the ability to increase track stiffness and improve stability in the longitudinal and lateral planes (Gräbe et al., 2016).

Demand for railways in South Africa has grown decade after decade resulting in expansion of the existing track and train infrastructure. However, due to the considerable cost associated with infrastructure development and rehabilitation, and considering the adverse economic conditions, asset owners and affected parties are interested in the residual life of existing infrastructure; and how its service life may be extended.

In South Africa, it has become common ad-hoc practice to replace the steel and timber sleepers on branch, sidings and yard lines with aged prestressed concrete sleepers uninstalled from primary running lines. Primary lines are characterised by high frequency traffic and greater axle loading capacity, whereas branch and yard lines have moderate to low traffic frequency and lower axle loading capacity. Railway sidings carry variable axle loads but operate at slower speeds. Examples of the reuse of aged concrete sleepers in South Africa are depicted in the figures below. Figure 1.2 shows aged concrete sleepers that were selected and stored at the rail yard line, where installation was planned.

Figure 1.2: Stacked aged concrete sleepers removed from service; awaiting installation in the yard/station

The planning of concrete sleeper installation in the yard proceeds by placing the sleepers adjacent to the track, as shown in Figure 1.3.

Figure 1.3: Concrete sleepers placed alongside the wooden sleeper track in preparation for replacement

An example of railway sleeper removal carried out manually is depicted in Figure 1.4.

Figure 1.4: The replacement of deteriorated wooden sleepers with used concrete sleepers

South African prestressed concrete sleepers are designed elastically according to the BS CP 110 and SATS Specification, CCE 1/57 (Dunaiski, 1985). Both BS CP 110 and SATS Specification CCE 1/57 have since been updated and replaced by newer standards, including

BS 8110 and the Specification for Monolithic Prestressed Concrete Sleepers used on 1065 mm gauge railway tracks (BBG8755). Sleepers in South Africa have an expected lifespan of up to 40 years as per design (Wildenboer et al., 1989) and are required to withstand the design bending moment without cracking. The required strength in bending is derived from the expected flexural behaviour, resulting from the combination of prestressed steel wires and concrete. Nonetheless, the loss of prestress can be a significant structural safety and serviceability concern, as it can affect strength and functionality of the sleeper. The most important variable in prestressed concrete applications is the prestressing force. It has been observed that this force decreases over time due to various factors, such as anchorage slip, friction loss, steel relaxation, creep, and shrinkage of concrete (Ngamkhanong & Kaewunruen, 2018).

Four methods for determining residual prestress force in a concrete sleeper are discussed in literature. These include the flexural cracking, direct tension, dynamic relaxation and the change in extracted wire length techniques (Remennikov & Kaewunruen, 2015; Scott, 2019).

To quantify the residual prestress force and ultimately justify the re-use of aged concrete sleepers following a structural strength assessment, current research adopts the dynamic relaxation approach. This method is preferred due to its potential to be conducted at a suitable location on site, eliminating the logistical challenge of transporting sleepers to a laboratory, which may be located far from site, considering the remoteness and geographical sparseness of the railway infrastructure.

1.2 Problem Statement

The growing focus on sustainability practices has led the railway sector to explore ways to reuse railway components and materials, thus reducing material waste and optimising asset life cycles (UIC, 2021). A key strategy in this effort in South Africa involves reusing concrete railway sleepers, which constitute a substantial portion of the overall materials utilised in track systems, beyond their design service life. This practice is motivated by potential cost savings and derived environmental benefits.

However, there are engineering flaws in this practice. Pretensioned concrete structures undergo reduction of prestress force over their useful life (Ngamkhanong & Kaewunruen, 2018) due to factors such as material aging, cyclic loading, environmental exposure, concrete creep and shrinkage effects. This is also true for railway concrete sleepers, leading to reduced prestress force and consequently, a decline in structural capacity (Remennikov & Kaewunruen, 2015; Scott, 2019). Without quantitative structural condition evaluation methods

to assess the remaining strength of concrete sleepers, it is challenging to make informed decisions about their continued use.

The assessment method for the condition of concrete sleepers in South Africa, both during operational use and at the point of selection for reuse, is typically conducted through visual inspection guided by a functional condition scoring system detailed in Appendix E. This approach is inadequate to capture the complex deterioration mechanisms that affect the performance of the sleepers over time. Furthermore, internal damages such as cracking or prestress loss cannot be identified. The absence of a comprehensive concrete sleeper structural evaluation constrains decision-making but also increases the likelihood of track instability or failure.

Whilst the reuse of sleepers may have positive environmental impact, limited structural assessment can have negative safety and financial consequences. Structurally inadequate sleepers can lead to track defects and occasionally in worst cases may cause derailments. The intended cost saving of reuse can be undermined by the same sleepers, resulting in costly maintenance and service disruptions. A more methodical, evidence-based approach to assessing the residual structural performance of prestressed concrete sleepers is obviously necessary in light of the risks that have been highlighted. By developing and validating such a framework, sleeper maintenance will be able to incorporate data-driven decisions that balance sustainability, safety, and cost.

1.3 Research Objectives

The objective of this research was to evaluate the residual prestress force in aged railway concrete sleepers removed from primary running rail lines prior to their re-use in branch lines, yard lines and sidings. The specific objectives of this study were to:

a) Evaluate the general condition of concrete sleepers visually.
b) Estimate the prestress force in the concrete sleepers using the dynamic relaxation method.
c) Compare the estimated residual stresses in (b) with the theoretical design calculations and requirements of the concrete sleeper specification, BBG8755.
d) Determine the mechanical properties(strength) of concrete and steel wires.
e) Propose criteria for the classification of second-hand concrete sleepers.

1.4 Research Question

Considering the loss of prestressing force with time in pre-tensioned concrete elements, what is the residual prestress force in railway concrete sleepers at the end of their design service

life? How do visually assessed material degradation, environmental exposure, and repeated loading affect this residual prestress force? Additionally, how can the structural performance and safety of selected aged concrete railway sleepers be evaluated, and what are the criteria for their viability in secondary use?

1.5 Conceptual Framework

The conceptual framework presented in Figure 1.5 provides a contextual overview of the fundamental aspects considered in this research to achieve the set objectives. The initial step to take in understanding the structural behaviour of railway concrete sleepers in service is to examine information related to their design. This involves exploration of the design philosophy, specifically in terms of the stress regime and material specifications. As depicted in Figure 1.5, the considerations made during the design phase affect and are related to the in-service performance of a structure.

A key focus of this study is the prestress force, which is a critical strength parameter of concrete sleepers. It is essential to understand that prestress loss over time can impact the structural integrity of pretensioned structures. Therefore, this study proposes experimental work to determine the residual stress force in concrete sleepers at and beyond their design life.

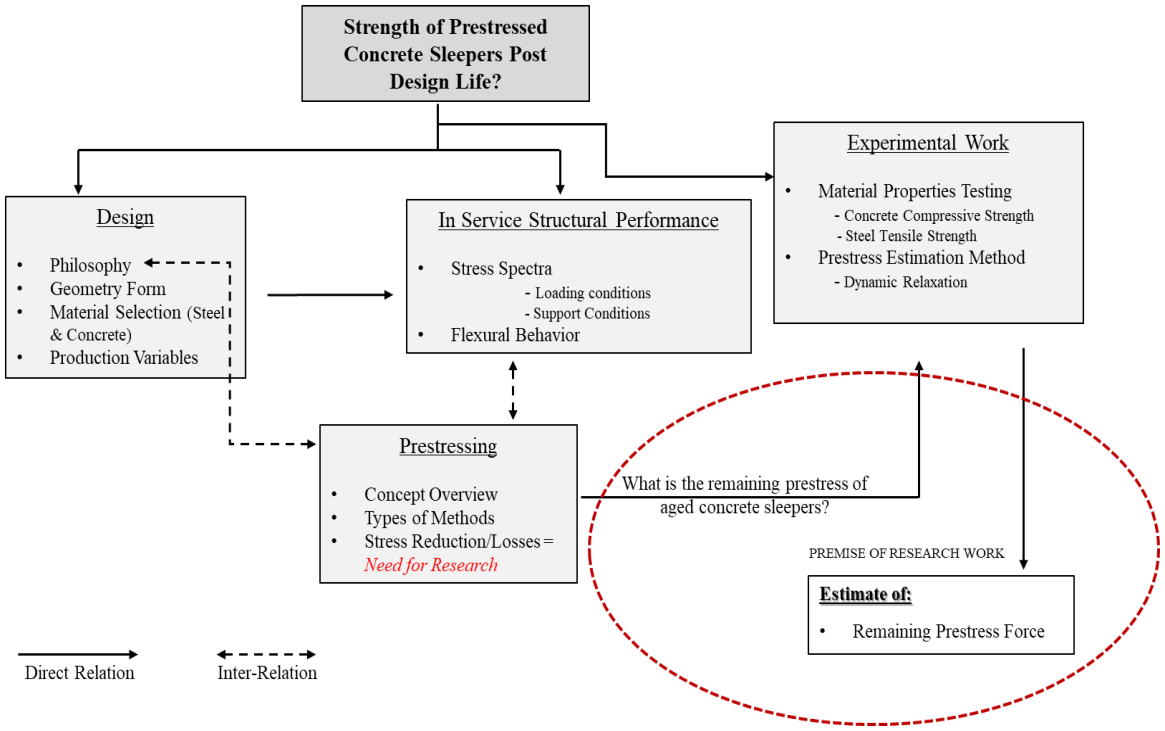

Figure 1.5: Research conceptual framework

1.6 Scope and Limitations of the Study

This research focuses on evaluating the residual prestress force in aged railway concrete sleepers using the dynamic relaxation technique, following the method described in this report. The adopted methodology follows the approaches used in previous studies conducted by other researchers, while exercising discretion and making informed modifications in instances where existing research offers limited information. Therefore, the study findings are valid under the specific conditions of the experiment and may not be applicable in other settings or conditions.

1.7 Organisation of the Report

Chapter 2 of this report reviews the literature related to factors influencing the design of prestressed concrete structures, as well as methods for estimating the residual force in prestressed concrete sleepers. The experimental methods used in this research are outlined in Chapter 3. Results from strain measurements and discussions of these findings are presented in Chapter 4. The study proposes criteria for evaluating old concrete sleepers intended for reuse, which are discussed in Chapter 5. Based on the study's objectives and findings, conclusions are drawn in Chapter 6, and recommendations for future research are provided in Chapter 7. Additional documentation related to testing data and the condition assessments of the sampled sleeper specimens is provided in the Appendices.

2 LITERATURE REVIEW

2.1 Introduction

This chapter reviews literature relevant to the planned experimental work discussed in the subsequent chapters. It covers four broad sections presenting:

a) The evolution of concrete sleepers in South Africa.
b) A detailed summary of the design, manufacture, and operation of concrete sleepers.
c) An overview of the concrete prestressing concept to provide insight into the behaviour of sleepers.
d) Properties of materials focused on the strength of concrete and steel.
e) A review of concrete prestressing force testing methods.

2.2 Railways and the Evolution of Concrete Sleepers in SA

South Africa (SA) has a vast rail network, of about 30 000 km single-track lines. This network comprises primary running main lines and secondary running lines, including branch, sidings and yard lines. The primary running lines are constructed predominantly of concrete sleepers, while the majority of the non-core lines remain steel and wooden sleepers. Figure 2.1 depicts the South African map of rail network categories.

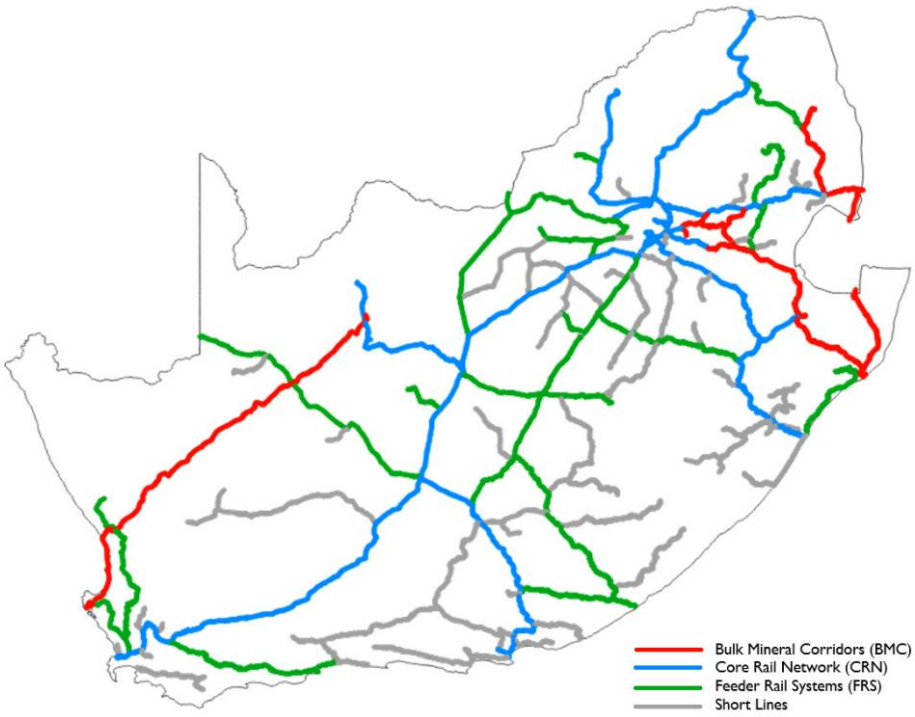

Figure 2.1: South African Rail Network (Republic of South Africa, 2023)

2.2.1 Evolution of Sleepers in South Africa

In the pioneer days of railway construction in South Africa between 1872 and 1877, wooden and steel sleepers were used, with steel sleepers being the most popular at the time due to the simple design, availability, and longer life span. Wooden and steel sleepers were utilised from then until the introduction of concrete sleepers in 1948. Between 1948 and 1952, a small number of twin block concrete sleepers (reinforced) and later monolithic sleepers (prestressed) were ordered from Europe and introduced on the mainlines as a trial on their performance. The satisfactory results led to the procurement of more concrete sleepers between 1955 and 1978. A few of these were twin block sleepers, which were discontinued completely in 1967. Monolithic sleepers were standardised in 1968 (Lombard & Wildenboer, 1981) . After a period of evolution of about 20 years, South African railways standardised two types of concrete sleepers produced domestically, the P-type and F-type sleepers differing in the fastening systems used. The P2/F4 are standard sleepers, whereas PY/FY are heavy-duty sleepers suited for lines with 26 ton/axle loads. Figure 2.2 shows examples of the first two concrete sleeper designs ordered by the South African railways in 1955.

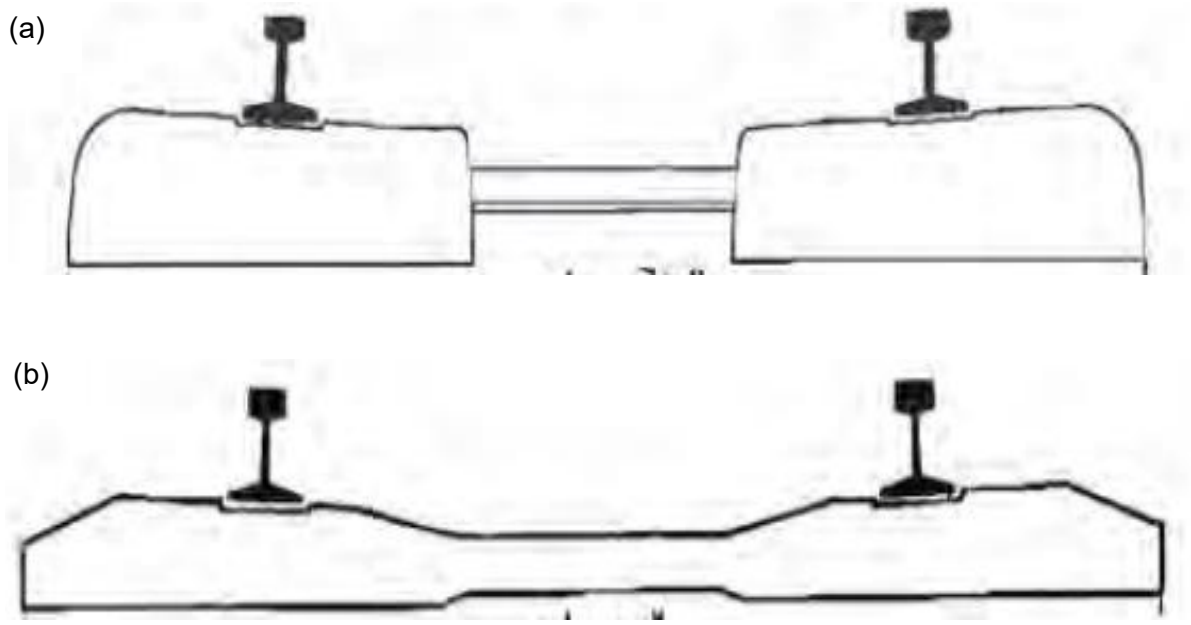

Figure 2.2: (a) Twin block concrete sleeper sonneville design (b) Monolithic concrete sleeper stupp design (Hay, 1962)

2.3 Prestressed Concrete Sleepers

The use of prestressed concrete sleepers (PCS) became popular after their introduction in the 1940s. This was because of their increased track stiffness (Gräbe et al., 2016), owing to the improved flexural capacity, adequate development of prestressing forces (Hurst, 1988) and high self-weight. This sub-section deals exclusively with the design considerations for monolithic prestressed concrete sleepers.

2.3.1 Design Approach

The global design approach for PCS uses the allowable stress state philosophy, which considers simplistic impact factors. The exception is noted in the European (EN 13230) standard which uses the limit state concept (Muchinsky & Stevens, 2012). In the design of PCS, two main loads are considered, including vertical loads imparted by trains and counteracted from ballast support, and lateral loads which are more significant at the curves where centrifugal forces exist. Generally, the PCS derive lateral resistance from the sleeper ends bearing pressure against ballast, self-weight and friction developed between the sleeper and ballast (Taherinezhad et al., 2013).

Various standards governing the design of PCS, including the European (CEN 13230, 2009), North American (AREMA, 2006) and Australian (AS 1085.14, 2012) codes follow the same procedural specification (Muchinsky & Stevens, 2012). The similarities noted in the standards pertain to the following specified details provided to the manufacturer by the purchaser (Taherinezhad et al., 2013):

- Provision of the basic track and train information
- Estimation of vertical loads
- Assumption for ballast support distribution pattern
- Bending moments and permissible stresses
- Materials to be used
- Manufacturing process to be adopted and recommended quality assurance testing

2.3.2 Loading

Prestressed concrete sleepers are expected to withstand enormous static and dynamic loads under harsh environments. Static loading is generally easier to account for in the design calculations. In contrast, dynamic loading presents challenges as it invokes a non-uniform stress response generated from the interaction between the rail and the wheel. The source of dynamic impact loads can be from abnormalities found on the wheels, rails and support

conditions. The weight of the sleeper is generally considered to be insignificant in various analyses (Taherinezhad et al., 2013).

2.3.2.1 Applied Loads at Rail Seat

Muchinsky and Stevens (2012) highlighted typical information considered for the vertical load, such as the annual gross tonnage, maximum axle load, maximum operational speed, track gauge, sleeper spacing and rail size. These are factored to produce the maximum static wheel load, which in turn is compounded with a service or safety factor to yield the vertical design load. This load is shared by a set of sleepers depending on the track stiffness, rail dead weight and sleeper spacing.

2.3.2.2 Ballast Distribution Support Effect

The counter vertical load action offered by the ballast support underneath the sleeper influences the structural design of the sleeper significantly, considering its variation over time. A newly constructed or recently tamped track has ballast supporting the sleeper uniformly along its longitudinal dimension. In this circumstance, all critical areas (rail seats and mid-span) remain supported. This is the case used for determining the rail seat positive bending moment. As time progresses and the track experiences some noticeable level of deterioration, the ballast settles underneath the rail seat region, reducing support under the rail seats. The negative bending moment is calculated from this case. The two moments are used as the main criteria in the design of sleepers. However, computation of the rail seat negative moment and midspan positive moment is not ignored in design (Taherinezhad et al., 2013). Figure 2.3 shows proposed stress distribution patterns underneath sleepers.

Item No.	Proposed Stress Distribution Pattern	Researcher or Standard	Remarks
1	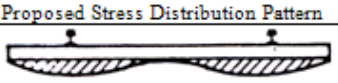	UIC,Talbot	Distribution pattern according to laboratory tests
3		UIC,Talbot	Maximum stress under the rail
4	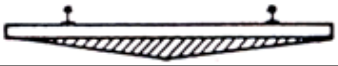	Talbot	Maximum stress on in the middle of sleeper
5	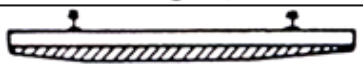	Talbot	Stress concentration in sleeper center
6		Talbot	Valid for flexible sleepers
7		UIC,Talbot	Trapezoid distribution
8	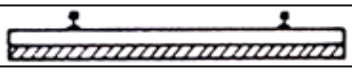	AREA,Raymond,talbot	Uniform stress distribution

Figure 2.3: Resultant bending moment along the sleepers from applied train load and ballast support (Zakeri and Sadeghi, 2007)

2.3.3 Other Considerations

In addition to the concrete sleeper structural requirements discussed in Section 2.2.1 and Section 2.2.2, there are other considerations made in the design of concrete sleepers. As mentioned by Gylltoft (1987), these include durability and electrical insulation.

2.3.3.1 Durability

Durability is defined as the ability of the material to remain serviceable in the surrounding environment during its useful life without damage or unexpected maintenance. It is required that the material used for the manufacture of sleepers, concrete and steel tendons be of high quality and durability.

2.3.3.2 Electrical Insulation

Concrete sleepers are extensively used in electrified and automated signal-controlled running lines. Therefore, it is necessary to provide insulation between the track and the different electrical systems, i.e., traction and signalling. In this case, protection against potential short-circuiting of signal systems, electrical leakage or transmission between the rail and sleeper or with the signalling system is achieved using plastic insulators positioned between the rail and the sleeper rail, and in between the rail and fastening systems.

2.4 Concrete Prestressing

The technical advantages of prestressed concrete stem from the practice of loading a structure with compressive forces prior to service. The resulting, intentionally introduced compressive load counteracts, in full or partially, the induced tensile stresses in a member, consequently improving the tensile property of concrete. Furthermore, with prestressing concrete structures of longer spans, smaller cross-sectional dimensions and lower deflections can be produced. Nevertheless, prestressed concrete applications involve a complex design process and require a high level of quality control during construction or manufacture (Kraľovanec et al., 2021; Nawy, 2009).

2.4.1 Pre-Tensioning Method of Manufacturing Concrete Sleepers

Pre-tensioning of concrete is the construction process in which the member is cast around the straightened strands or wires placed in a mould and tensioned between anchors. Once the concrete has hardened enough and the prestressing tendons are released from the anchors, the prestressing force is transferred into the pre-tensioned structure through the bond between the steel reinforcement and concrete. This technology finds its application in short-span or medium-span bridges, structures, or railway sleepers (Kral'ovanec et al., 2021). Figure 2.4 illustrates the three stages in the construction of prestressed members. Stage 1 in (a) is the initial phase where steel wires are pretensioned. The second stage, (b), involves concrete

being cast around the tensioned wires. Finally, the prestress is transferred to the concrete once it has hardened in the third stage, (c) (Jhatial, 2022) .

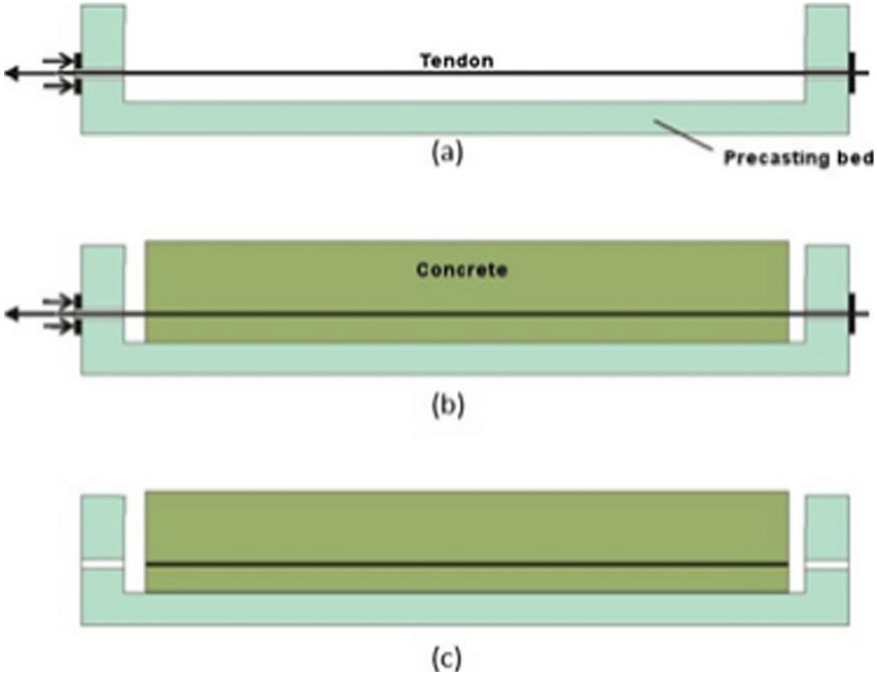

Figure 2.4: Schematic pre-tensioning diagram of concrete sleeper (Jhatial, 2022)

2.4.2 Prestress Losses

Prestressed structures have been observed to undergo a reduction of stress over time, from construction until end of service life. Consequently, it is essential that prestress losses are determined at each loading stage, from initial release of tensioned reinforcement (i.e., at transfer) to different stages at service load and up to the ultimate end of service life (see Figure 2.5). Fundamentally, prestress losses can be classified into two groups, namely, the short-term (immediate) and long-term (time-dependent) losses (Hurst, 1988; Nawy, 2009; Kraľovanec et al., 2021).

i. Short-term loss of prestressing occurs immediately at or just after construction, resulting from elastic shortening, anchorage slip, short-term steel relaxation, frictional and temperature losses.

ii. Long-term prestressing loss occurs gradually with time due to concrete dimensional change (i.e., creep and shrinkage), temperature effects and long-term steel relaxation.

Another factor that may result in loss of prestress, although not considered in the short or long-term loss factors approach for determining remaining prestress force, is corrosion.

Deterioration of steel tendons by corrosion can be dire for the serviceability and safety of a prestressed member. Corrosion of prestressing steel is difficult to ascertain visually and thus requires regular non-destructive means for its detection, location and quantification along the length of the tendon (Kraľovanec et al., 2021). Figure 2.5 depicts the idealised stress-versus-time relation for a prestressed member.

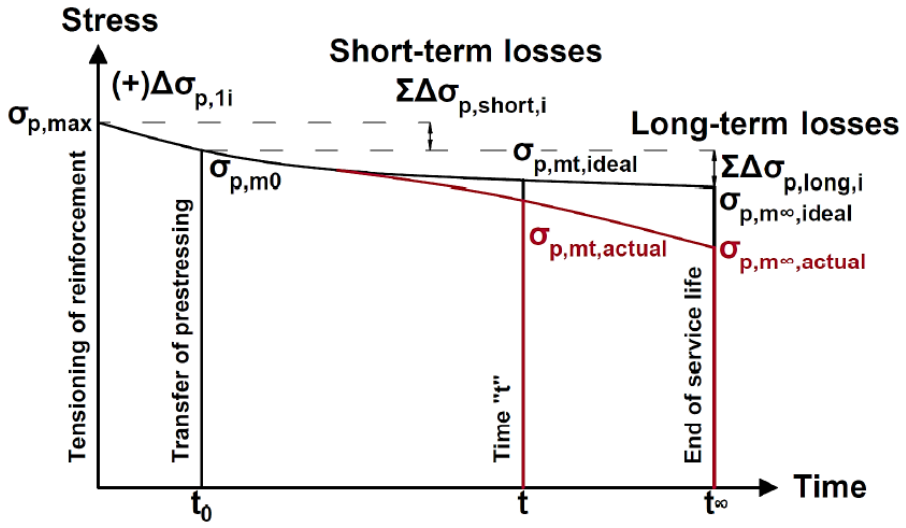

Figure 2.5: Prestressing loss in a member over time (Kraľovanec et al.,2021)

According to Caro et al. (2013), prestress losses are generally accepted to have minimal effect on the ultimate design capacity of prestressed members. However, the losses can affect the service conditions. In light of that, overstressing a member may not be a solution to prevent prestress losses as it is uneconomical and can result in excessive camber under service loads. Conversely, under-stressing a member can lead to excessive deflections and premature cracking of concrete. Abdel-Jaber and Glisic (2019) further stated that under-stressing may result in other consequential damages such as corrosion or rupture of steel strands.

2.5 Properties of Materials

Concrete is a composite material comprising selected aggregates bound together by a continuous hydrated cement paste matrix. Inherently, concrete has an impressive compressive strength, but is limited in tensile strength (Alexander, Bentur & Mindess, 2017). To improve the latter characteristic, steel is introduced as reinforcement to produce a composite material that performs well in compression and tension. This sub-section deals with the properties of concrete and prestressing steel.

2.5.1 Strength of Concrete

Concrete strength can be affected by the choice of design mix and adherence to prescribed construction processes. In the case of concrete design, the water/cement ratio plays a major role in the strength of concrete. Higher strength is obtained from a lower water/cement ratio, and the typical relationships between water/cement ratio and compressive cylinder strength at different drying ages are shown in Figure 2.6. The properties of cement and aggregates are important to ensure homogenous interaction at the interfaces.

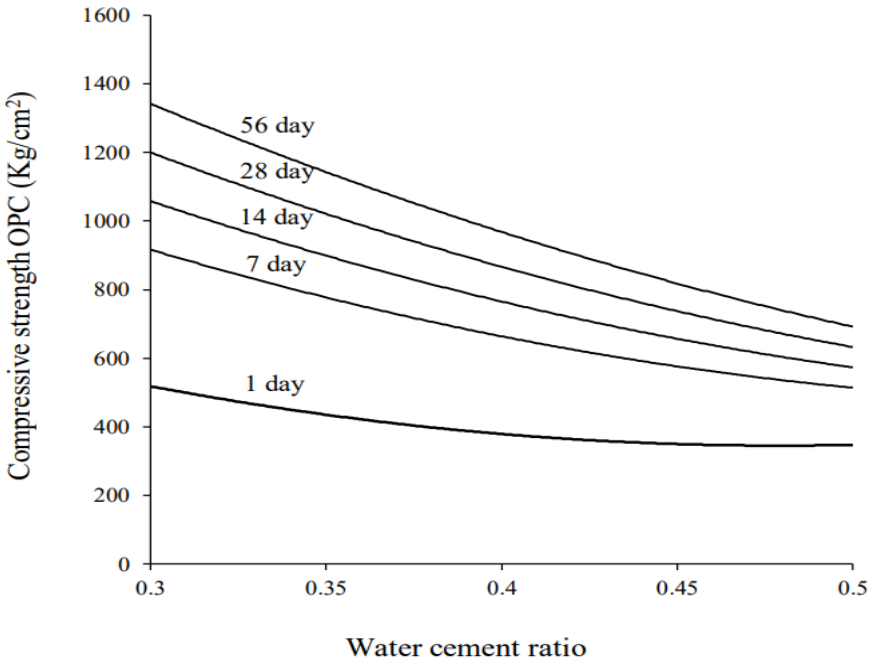

Figure 2.6: Strength of dry cast OPC concrete in relation to the water-cement ratio and curing age (Amhudo, Tavio and Putu Raka, 2018)

In construction, two of the most important factors considered are compaction and curing. Compaction is required to minimise air voids in concrete. The more air volume contained in concrete, the lower its strength, as the material becomes more compressible. It is therefore essential that concrete is compacted as fully as possible. Not only does compaction affect concrete strength but also the bond developed between the concrete and any steel embedded within it. This is particularly important for pretensioned members, where the bond is relied upon to transfer the prestress force to the concrete (Hurst, 1988).

Neville (2011) stated that the strength of concrete is dependent on time. It increases with age, but the rate at which it increases is greatly affected by the curing conditions (Hurst, 1988). Ideally, concrete should be kept in a moist environment and at an appropriate temperature to allow for optimum hydration of cement.

Most concrete members are cured for the first few days under moist covering and then cured in air. For railway sleepers, concrete is steam cured at a pre-set temperature, usually close to 40 °C, for a defined period, not exceeding 12 hours. At the end of steam curing, concrete sleepers would have attained over 50 MPa as a minimum compressive strength. This is well close to the prescribed 60 MPa compressive strength required for concrete sleepers in South Africa.

2.5.1.1 Concrete Creep

Creep refers to a phenomenon in which deformation in a solid increase with time under a constant load (ACI Committee 209, 2008). Over time, the accumulated strain can be significantly larger than the initial strain. In relation to concrete, creep is a considerable factor that affects the long-term displacements (serviceability) and loss of prestress force (stress redistribution) in prestressed members (Hurst, 1988). Depending on the severity, failure of structural elements can occur (ACI Committee 209, 2008). Bhatt (2011) explains that under constant load and subject to creep, concrete deformation can increase gradually with time, reaching a value three to four (3 to 4) times greater than that of the initial displacement. The initial strain is characterised as the immediate elastic deformation. Thus, creep deformation is considered the inelastic deformation under constant load. Figure 2.7 depicts the effect of creep in concrete over time.

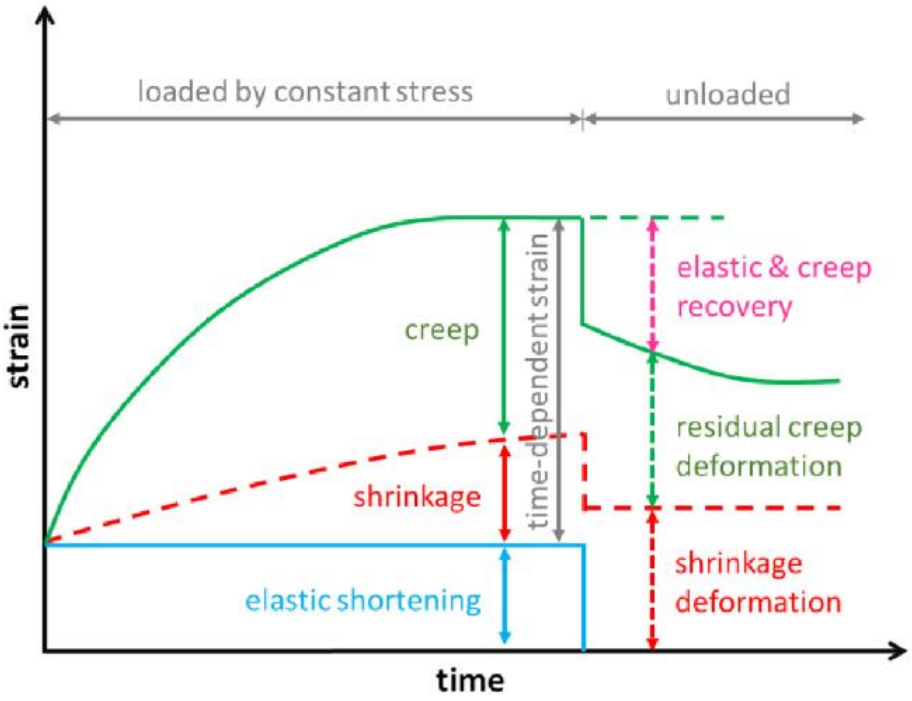

Figure 2.7: Concrete creep and shrinkage effects over time (Li et al., 2020)

Creep is commonly described as one overarching process; however, it is important to recognise that it comprises two distinct mechanisms. The first is basic creep, which is defined as “the total deformation of loaded, sealed specimens minus elastic deformation and autogenous shrinkage” (Mutungi, 2023). This creep mechanism occurs under 100% relative humidity, making it independent of moisture (Mehta & Monteiro, 2006). The second creep mechanism, known as drying creep, refers to additional deformation that occurs when the specimen is subjected to constant load and exposed to drying conditions (Mehta & Monteiro, 2006).

Creep is influenced by a number of factors ranging from concrete mix design to loading and environmental conditions. A common observation made of creep is that it is inversely proportional to concrete compressive strength in which higher strength is related to less creep (Li et al., 2020). The effects of creep are more prevalent in prestressed structures than reinforced structures due to a greater proportion of the member cross-section being in compression (Hurst, 1988).

2.5.1.2 Concrete Shrinkage

Concrete shrinkage is the time-dependent strain in an unloaded and unrestrained specimen at a constant temperature. It is dissimilar to concrete creep in that it is not entirely reversible. However, the two, creep and shrinkage, are affected by environmental conditions and concrete mix design (Li et al., 2020), except for the loading condition (Hurst, 1988). Shrinkage can be classified into several forms, including inelastic (or plastic) shrinkage, chemical shrinkage, autogenous shrinkage, thermal shrinkage, drying shrinkage and carbonation shrinkage (Markovski et al., 2012). For shrinkage strain analysis, drying, chemical and thermal shrinkage components are usually considered (Wallah, 2010).

In relation to prestressed concrete sleepers that must (amongst other functions) ensure the correct rail gauge, excessive creep and shrinkage arising from improper concrete mix design and/or unexpected material responses due to environmental and loading conditions can negatively affect the rail gauge (for instance, too tight rail gauge and splitting cracks at fasteners) (Li et al., 2020).

2.5.2 Steel for Prestressing

Steel used for prestressing members usually consists of high tensile wires, stands or bars. According to SANS 2001-CC1 (2007), prestressing steel ought to comply with the following British Standards:

- BS5896:2012 – for wire and strands
- BS4486:1980 – for bars

The tensile strength of steel is dictated by its chemical composition. Steel is an alloy material consisting of iron and carbon as the primary chemical constituents, mixed with one or more non-metals or metals. High tensile steel usually contains a carbon content ranging from 0.6 – 0.85% fused with 0.7 – 1% of manganese, and 0.05% of sulphur and phosphorus. A marginal increase in carbon content in steel results in an increase in tensile strength.

Apart from the chemical composition, the manufacturing process of high carbon steel contributes to the final tensile strength. At the factory, steel ingots are hot rolled into rods and thereafter cooled to make them suitable for drawing. Once cold, a die forming process is employed to reduce the diameter sizes, increase the tensile strength and improve the durability of drawn wires, termed “as drawn”. The “as drawn” wires are generally available in nominal diameters of 2.5 to 8 mm.

Further processing of steel takes place when “as drawn” wires are heat-treated to improve their properties, such as increasing the elastic range and consequently, the tensile strength. As drawn wires are known as “normal-relaxation” and post-treated “as drawn” wires are known as “low-relaxation” wires (Hurst, 1988).

The shape of the prestressing wire matters for the case of prestressed concrete structures when the prestress force is transferred to the concrete by the bond between steel and concrete. This bond is substantially increased if indentations are made on the wire surface, and if the wire is ‘crimped’, that is, given an undulating, instead of a smoothened surface.

A strand is produced by spinning several individual wires around a central core wire. Modern strands comprise seven wires with overall diameters ranging from 8 to 18 mm. A strand can be spun from as-drawn wires to produce an “as-spun” strand, or it can be heat treated after spinning to produce either a normal- or low-relaxation strand (Hurst, 1988).

2.5.2.1 Steel Relaxation and Stress-Strain Curves

Relaxation’ is defined as a reduction in load under constant deformation. Similar to concrete creep, relaxation of steel is a time-dependent change under constant load. In addition to time and stress, the amount of steel relaxation is also dependent on temperature. Steel relaxation values can be obtained by performing a standard test for relaxation or from a manufacturer’s quality assurance certificate. The British Standards Institution (2012) specifies three classes of steel relaxation, Class 1 and 2 corresponding to normal relaxation and low relaxation wires respectively. Class 3 corresponds to bars.

A typical stress-strain relationship for prestressing steel is illustrated in Figure 2.8. The stress-strain curve for high-strength steel does not have a well-defined yield point but rather provides the proof stress. Hurst (1988) defines proof stress as the stress at which permanent

deformation is sustained by steel when the load is removed. The BS5896:2012 specifies deformation of prestressing steel to have 0.1% elongation which corresponds to 0.1% proof stress of prestressing steel (see Figure 2.8).

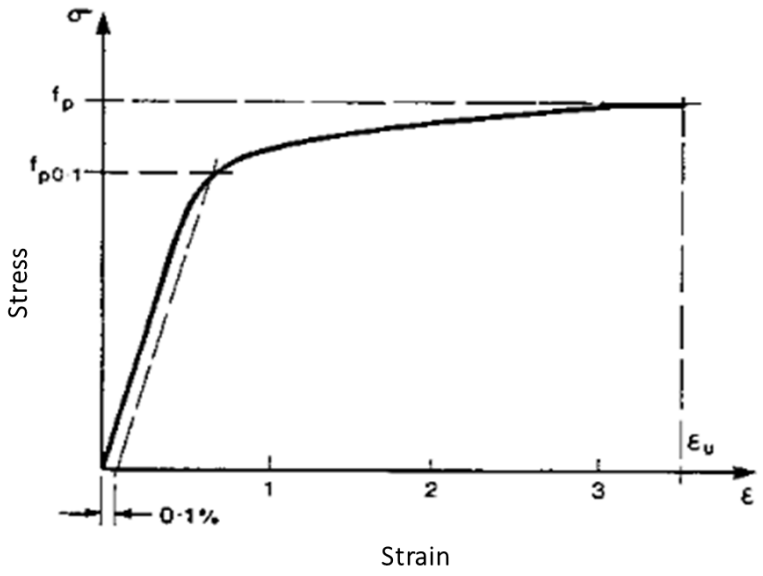

Figure 2.8: Stress-strain relation for prestressing steel (BSI 5889, 2012)

As mentioned, in Section 2.4.2, the heat-treatment of cold-drawn wires increases the elastic range of prestressing wires. This translates to a decrease in relaxation of steel and an increase in the proof stress. Although the elastic modulus for different steel types may vary, EC2 provides the modulus of elasticity to be assumed in design for all steel types as 200 x 10^3 N/mm^2.

2.5.2.2 Corrosion of Steel

As with steel used in reinforced concrete, prestressing steel must be protected from corrosion damage (Hurst, 1988). The ingress of moisture and ions known to initiate corrosion must be prevented. This is achieved by having adequate cover and using good quality concrete, which has an adequate low water cement ratio (Alexander et al., 2017). These two factors, cover depth and cover quality, govern the permeability of concrete.

2.6 Residual Prestressing Force Determination Methods

There are numerous experimental methods that can be used to determine the prestress force in a structural member at any given time. The methods vary in complexity and accuracy levels. For this study, four (4) applicable techniques—identified from Caro et al. (2013) and Scott (2019)—are discussed below.

2.6.1 Flexural Cracking

A common technique often used to estimate the prestress force in structures, bridges in particular, is through observing cracking during flexural tests. The load required for crack initiation or crack reopening can be used to calculate the prestressing force using statics. Flexural crack initiation and crack reopening methods differ in the way stresses are computed. The crack initiation method considers an equilibrium case between the rupture modulus and the tensile stresses on the bottom side of the concrete. The prestress load, *P,* can therefore be calculated for a member subjected to flexural stresses using Equation 2.1:

$$-\frac{P}{A}+\frac{Pey_t}{I}+\frac{My_t}{I}=Q_t \qquad (2.1)$$

Where:

P - Prestress Load
A - Cross-sectional area of the member,
e - Eccentricity of the wire group
I - Moment of inertia,
y_t - Distance from centroid to extreme steel fibre in tension
M - Applied moment
Q_t - Tensile force in concrete

The negative sign preceding the axial stress from prestress, $\frac{P}{A}$, in Equation 2.1, indicates the compressive force introduced by prestressing wires, thereby reducing tensile stresses. The crack initiation method requires pre-cracking and reloading of the prestressed member, in which case Q_t would equal zero as there would effectively be no tensile stresses when the crack is fully opened. With that in mind, *P* then becomes the only unknown in Equation. (2.1). Rearranging Equation (2.1) yields Equation 2.2:

$$P=-\frac{My_tA}{Aey_t-1} \qquad (2.2)$$

On the contrary, the crack reopening method does not consider the tensile stresses as this is effectively zero when crack opening reoccurs, after full cracking has already occurred on a member. The decompression load that corresponds with the crack reopening region, can be approximated using the applied load versus crack opening displacement (COD) curve which tends to display the bilinear contour. The prestress load may be read off at the intersection point between the two linear curves or at the end point of the first linear curve. The accuracy level of the two methods depends highly on the technique and instrumentation used to measure the crack opening displacement at initiation or at reopening. A comparison of the two

methods has shown an overestimation of prestressing loss by both, with the crack initiation displaying a greater error margin.

2.6.2 Direct Tension

Scott (2019) developed the direct tension test method to overcome the shortfalls associated with the flexural cracking method. In this technique, sleepers are pre-cracked at the centre and thereafter loaded in direct tension. The tension load is applied using the hydraulic jacks to push the constructed blocks encasing each end of the sleeper. Figure 2.9 depicts the construction set up of the casing and cast casing around the sleeper.

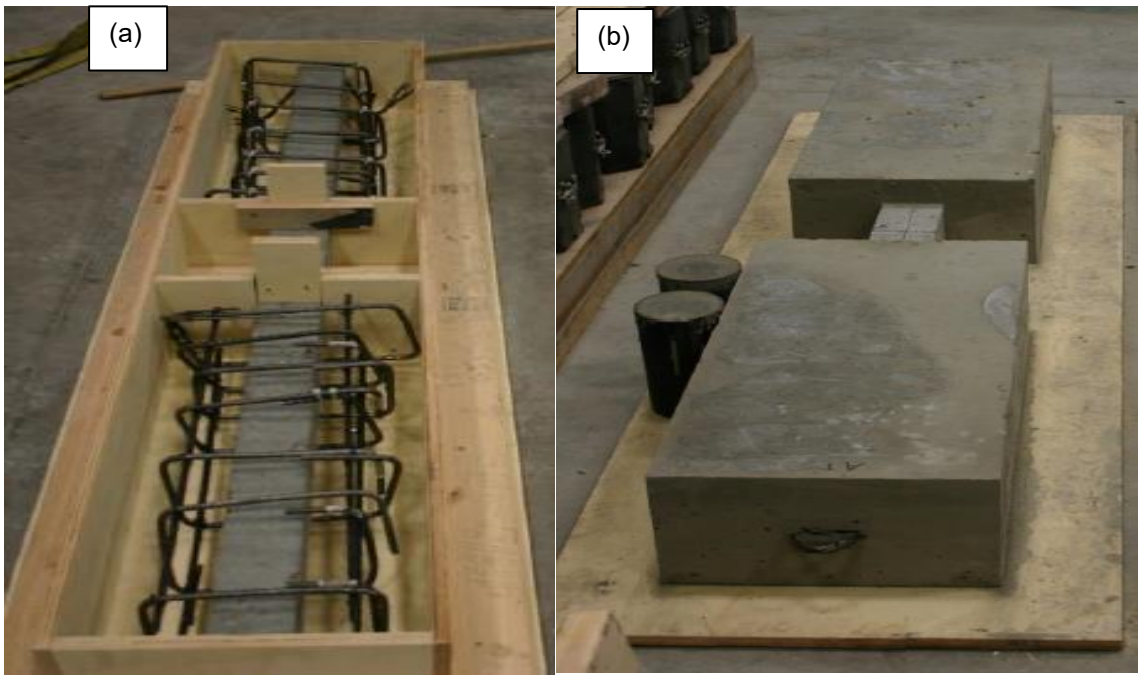

Figure 2.9: (a) Formwork with reinforcement for casting of sleeper casing blocks (b) Cast concrete block (Scott, 2019)

As the sleeper is pulled apart by the tensile load, the COD at the sleeper centre is measured. It is anticipated that the crack will fully open when the prestress force is exceeded by the applied load. The resulting relational plot between the applied load and the COD yields a curve with two linear segments representing two different stress resistance cases. The first part of the linear curve relates to the resistance provided by both concrete and prestressing steel at the pre-cracking state (represented by the green line, Figure 2.10-b). The second portion relates to the resistance provided by prestressing only at the post-cracking state (represented by the red line, Figure 2.105-b). The beginning of the second part of the linear curve corresponds to the load, which serves as an upper limit approximation of the prestress force in the sleeper. Figure 2.10 illustrates the example showing estimation of prestress force from the COD theory, using results of experimental work obtained from Scott (2019).

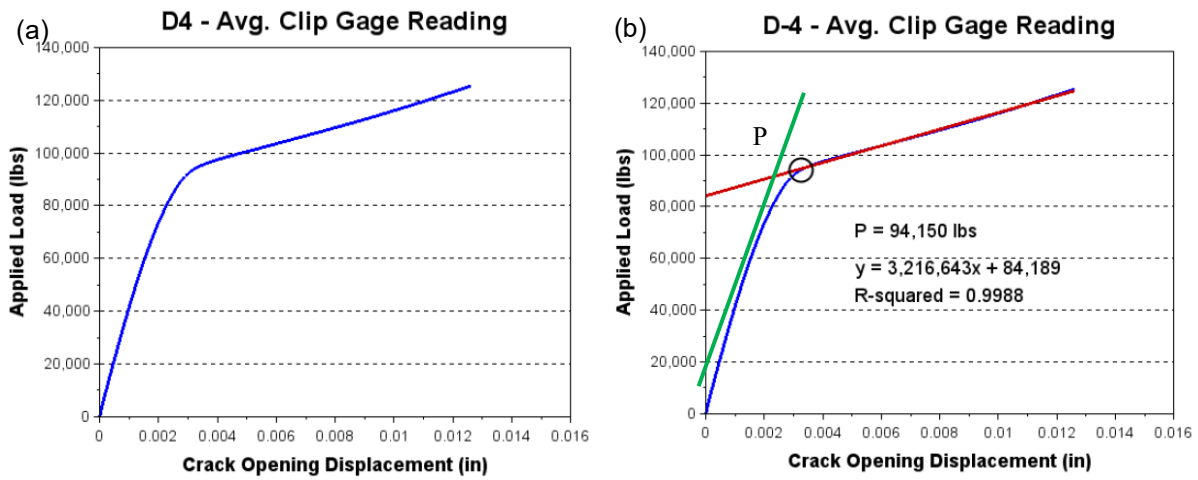

Figure 2.10: (a) Load vs crack opening displacement and (b) Prestress force estimated from the line (red) of best fit (Scott, 2019)

2.6.3 Dynamic Relaxation

Khayal (2019) defines dynamic relaxation as the numerical method commonly used for form-finding of one-, two- and three-dimensional structures (i.e., plates, shells, membrane structures etc.). The method considers the body mass of a structural system as combined discretised nodes that oscillate around the equilibrium point at the influence of induced constant force. With the introduction of non-natural inertia and damping effects, the oscillation continues until the system comes to a displaced stationary position of static equilibrium. The resulting static equilibrium state serves as a solution to the analysis of damped structural vibrations (Papadrakakis, 1978).

Dynamic relaxation can adopt two damping approaches in the problem-solving process, namely, kinetic and viscous. The two tactics are different in that kinetic damping traces the kinetic energy of the system whilst velocities are reset to zero at each energy peak. This occurs until a balance of forces, external and internal, is reached to bring the system to rest. The aim is to, therefore, attain kinetic energy peaks quicker by optimising the defined system mass matrix. In contrast, viscous damping does not use velocity but rather tries to find the optimum viscous damping coefficient, *K*, required to damp oscillations effectively. Viscous damping is preferred to kinetic damping as it closely models real life system behaviour (Khayal, 2019).

Analysis of structural forms using dynamic relaxation methods coupled with finite difference involves extensive use of a set of ordinary or partial differential equations expressed in single or group equations. The basis of dynamic relaxation equations is derived from the principles of elastic isotropic materials, and its application requires transformation of differential equations into dynamic equations by incorporating effects from viscous damping and inertia.

Scott (2019) cited an example of a dynamic relaxation application in a one-dimensional scenario involving a steel bar under tensile loading (Otter, Cassell & Hobbs, 1966). In this case, the bar was sectioned into multiple elements having displacement and velocity as initial boundary conditions. Time was a variable, at zero (t = 0), all boundary conditions were zero (v = 0; d = 0). Stress analysis was conducted for small increments of time, resulting in varying displacements and velocities at a particular point in time, *t*. After some time of iterations, the sought stresses and displacements were found when the dynamic equation solution converged. This approach simplified using the steel bar, provided the basis of using dynamic relaxation for approximating tensile stress and can be used to solve complex engineering problems. However, equivalent results can be obtained from the application of Hooke's law. An example of dynamic relaxation application on axial load; considering the effect of the different values of damping factor K is depicted in Figure 2.11.

According to Hooke's law, the tensile stress of a uniform steel bar is proportional to the strain in the elastic region, where the slope of the resulting curve is Young's modulus. The mathematical expression of Hooke's law is presented in Equation 2.3.

$$\sigma = E.\varepsilon \tag{2.3}$$

Where:

σ - Stress

ε - Strain

E - Elastic Modulus

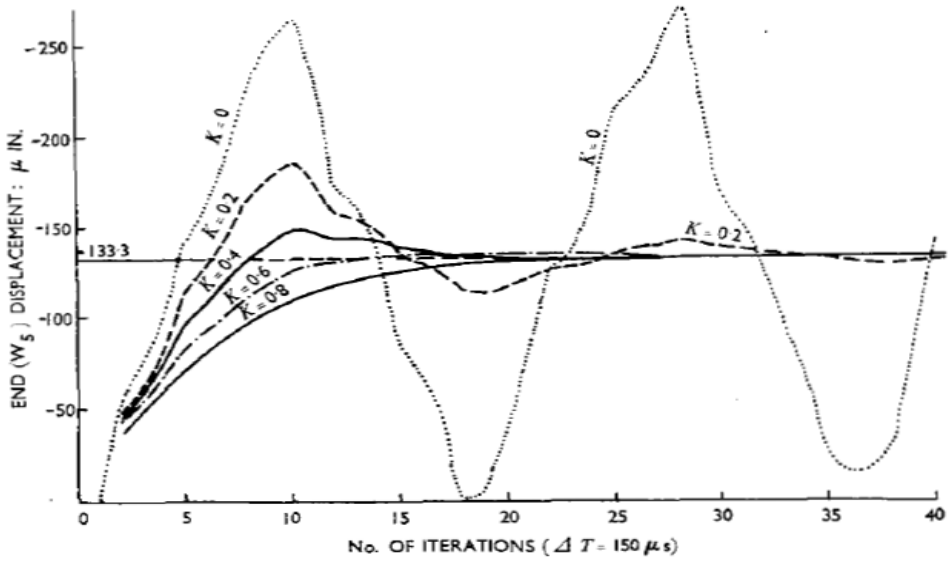

Figure 2.11: Example of dynamic relaxation application on axial load; effect of the different values of damping factor K (Otter et al., 1966)

Attempts by Remennikov and Kaewunruen (2015) and Scott (2019) to use dynamic relaxation in estimating the remaining prestress force in concrete sleepers produced varying results. The prestressed tendons of sleepers were exposed at the sleeper centre and instrumented with strain gauges to measure strains as the tendons were cut. Remennikov and Kaewunruen (2015) tested a sleeper extracted from heavy-haul service and yielded 60% of prestress loss. This was higher than expected. They verified their results with a sleeper that was in service for 10 years under suburban loads, and the obtained results were found to be comparable. It was concluded that the method is suitable for use to determine the prestress force in aged sleepers. Scott (2019) tested three sleepers of different designs removed from service after 25 years. The results obtained indicated an error margin of 18 to 26% in the estimation of prestress force.

2.6.4 Extracted Wire Length Change

The wire length change method was studied by Scott (2019), where the length of the extracted wire was used to estimate the prestress force in a sleeper. The method evaluates the change in length (ΔL) of the wire before and after extraction, while excluding the influence of concrete. Once the wire is removed and isolated from the concrete, it may undergo contraction or elongation, reflecting the presence of the axial load and changes in its initial length owing to its elastic properties. Thus, the mechanics formula, in Equation 2.4, which describes axial displacement in an isolated, linearly elastic bar, is used to determine the force, (*P)*.

$$\Delta L = \frac{PL_i}{AE} \qquad (2.4)$$

Where*:*

P - Prestress load in the wire

E - Elastic modulus of the wire

A - Cross-sectional area of the wire

L_i - Initial length of the wire measured while the wire is still embedded in concrete.

Having solved for *P*, the total prestress force in a sleeper can be estimated by multiplying the force obtained for a single wire by the number of wires in the sleeper. It is essential to employ precision instruments to measure the expected strains accurately when determining the prestress force using this method. Besides the measurement inaccuracy, non-uniform stress along the wire's length and slip or bond loss can further compromise the technique's accuracy. In comparison to the dynamic relaxation approach, Scott (2019) observed an inaccuracy of 9%. To quantify the error reported by Scott (2019) with certainty, testing of the

wire's elastic modulus and determination of the transfer length would be necessary as these were assumed.

2.7 Summary

The literature reviewed in this chapter relates to the aspects outlined in the conceptual framework in Figure 1.5 and listed in Section 2.1.

Prestressed concrete sleepers are designed to transfer the train load from the rail to the underlying sub-structures. In doing so, they are repeatedly subjected to static and dynamic impact loading. To keep the sleeper in equilibrium, the two downward forces are counteracted by the upward ballast pressure which is assumed to be uniformly distributed underneath the sleeper. These loading spectra serve as input to the design of concrete sleepers. The global design approach for prestressed sleepers follows the allowable stress state which considers the simplistic safety factors, except for the European (EN 13230) standard, which assumes the ultimate design philosophy.

The desired strength of prestressed concrete is achieved from the good quality concrete and adequate prestressing force. However, prestressing load has been observed to decrease over time owing to material changes of both concrete and steel. The reduction of prestressing force has the potential to result in unwanted structural serviceability and strength issues.

To better understand the structural behaviour of concrete sleepers in relation to prestressing, the properties of the materials forming the composite structure were reviewed. The material properties of the designed concrete and selected prestressing steel are key to the successful functionality of sleepers. Good quality concrete achieved through control of the water-cement ratio, high-strength cement, clean and optimal aggregate size, free of alkali agents, can ensure minimal effects of dimensional and volumetric changes. In addition, compaction and curing effects contribute to the quality of concrete achieved. Thus, their management during manufacture is equally important. The metallurgical composition, manufacturing process and diameter of the prestressing wires or tendons govern their strength in terms of tensile capabilities and relaxation level.

The four methods applicable to the estimation of prestress force loss in concrete sleepers were reviewed. These included the flexural cracking, direct tension, dynamic relaxation and the change in extracted wire length methods. Dynamic relaxation was adopted in the study as the method to determine the remaining prestress stresses in sleepers due to its ease of application and suitability for in-situ application. Given favourable environmental conditions and logistical feasibility, the study can be conducted on site.

3 METHODOLOGY

3.1 Introduction

This chapter outlines the methodology used in the study to determine the residual prestress force in concrete sleepers. It covers the sampling of sleepers, criteria for assessing their condition and the experimental procedure used to determine the residual prestressing force.

3.2 Concrete Sleeper Specimen

The study involved two experimental sample groups, including old and new P2 concrete sleeper type. The old concrete sleepers were sampled from a population of 11 200 concrete sleeper units removed from an 8 km section of railway track, in the Northern Cape Province, between Kimberley and De Aar. The inspection report supported the argument for removing the sleepers as they had surpassed their intended service life and showed concrete material deterioration. The new P2 concrete sleepers were retrieved from the storage yard located in Krugersdorp, Gauteng Province. It is important to note that the old and new sleepers had been exposed to different environmental and loading conditions. Table 3.1 shows the typical dimensions, and Figure 3.1 illustrates the typical configuration of P2 concrete sleeper design.

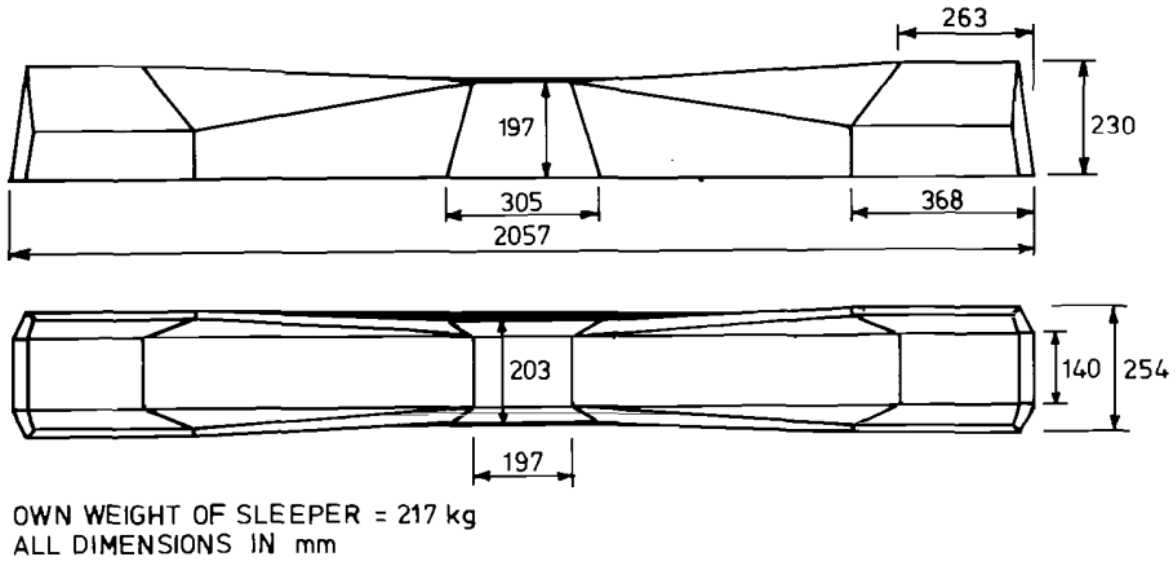

Figure 3.1: Typical design of concrete sleepers used in South African mainlines (Dunaiski, 1985)

Table 3.1: Standard dimensions of the P2 concrete sleeper type

Mass (kg)	Gauge Length (mm)	Total Length (mm)	Rail Seat Position		Centre Position	
			Width (mm)	Depth (mm)	Width (mm)	Depth (mm)
220.0	1 310.0	2 057.0	254.0	230.0	203.0	197.0

3.2.1 Variables

In this study, the independent variable is the age of concrete sleepers, classified by the production date (e.g., old sleepers - those manufactured in 1977 versus new sleepers manufactured in 2006). The primary dependent variable is the residual prestress force in the concrete sleepers. Controlled variables include the testing environment and procedure, ensuring consistency by using the same apparatus and measuring protocols across all samples.

3.2.2 Sample Selection

Random sampling was adopted because of logistical and financial limitations. The 11 200 sleeper units extracted from service were stacked in seven batches of approximately 1 600 sleeper units. From each batch, two to three sleepers were selected, limited to the top sleepers due to ease of access. A total of 18 aged sleepers were extracted and tested for prestress loss and material strength. This sampling strategy ensured representative coverage across the stacks of sleepers while adhering to resource limitations.

To determine the material characteristics, six sleepers were selected from the 18 aged concrete sleepers. Of these, three sleepers underwent concrete rebound hammer testing to determine their compressive strength, while one steel wire taken from each of the other three sleepers was subjected to tensile strength testing. Using the dynamic relaxation technique, the remaining 12 sleepers, numbered 1 to 12, were evaluated for the prestressing force. To further validate and contrast the performance of aged sleepers with that of assumed newer sleepers, three additional P2 concrete sleepers manufactured in 2006 were sourced. These sleepers were numbered 13 to 15 and underwent dynamic relaxation testing. As a result, the total number of sleepers included in the study was 21.

3.3 Assumptions

The following assumptions were made in this research:

- The average concrete compressive strength and average steel tensile strength were assumed to be the same for all tested sleepers, since they were manufactured at the same time, likely from the same production batch and removed from the same railway section, having experienced similar loading histories.
- The sampled aged concrete sleepers were assumed to be over 40 years old, with a manufacture date of 1977. It was further assumed that they were installed on the track shortly after manufacture and were subjected to operational loads until their replacement. Additionally, the concrete sleepers used for validation, manufactured in 2010, were considered new since they had never been used.

3.4 Condition Assessment of Sleepers

The current condition assessment of railway concrete sleepers in South Africa mainly relies on visual inspection, as prescribed by the Manual for Infrastructure Condition Assessment (MICA: version 4, 2018) alongside the Manual for Track Maintenance (MTM: version 2, 2012 - BBB0481). The MICA BBC 8266 is a multi-discipline document that provides guidance through details of numerous condition assessments and promotes uniformity and conformity in conducting condition assessments of railway infrastructure. For concrete sleepers, the standard document, BBC 8175 version 2 derived from MICA, is used to record the condition assessment information (see form attached in Appendix E).

The inspection form, BBC 8175, uses the condition and functional category rating from a score of one up to five, where one represents excellent condition, and five denotes the worst or unserviceable condition. However, the form does not provide a detailed list of typical defects or link them directly to the condition and functionality ratings. To address this, the condition assessment in this study focused on identifying typical concrete structural defects associated with operational ageing. These included cracking (indicating the type, size and location on the structural membe*r*), chipping and abrasion around the sleeper, particularly at the base and rail seat positions. The durability was assessed through visual inspection of cast iron products (such as steel wire and rail fasteners) and concrete deterioration resulting from ballast tamping works. Figure 3.2 depicts the condition of failed and degraded sleepers removed from service.

Figure 3.2: (a) A sleeper exhibiting significant cracking and compromised steel wire due to stress corrosion (b) Rupture around the rail seat position (c) Rail seat abrasion (d) Chipped concrete sleeper on the shoulder (Lutch, Harris and Ahlborn, 2009)

To achieve a more comprehensive visual examination of the mono-block concrete sleepers, the assessment focused on four critical areas considered essential to the functionality and overall performance of the railway track in this study. These sections included the:

- Rail Seat Area (from top to bottom) – area where the rail load is highest
- Centre Area (from top to bottom)
- Shoulder Area (from the end points)

3.5 Mechanical Properties

3.5.1 Compressive Strength

The compressive strength of the concrete sleepers was estimated using the rebound hammer method, in accordance with the HT-255 A manual and guided by the BS 1881-202 standard. Due to the varying load conditions experienced by critical parts of the sleeper throughout its service life, and the resulting fatigue from cyclic loading, test points were selected at key areas, including the shoulder, rail seat, and centre sections. These points were strategically chosen

to avoid interference with the first layer of embedded prestressing wires, the locations of which were determined through destructive exposure. The overall dataset consisted of impact points grouped by test zone and combined across the three sleepers. The rebound hammer readings were taken within a confined area not exceeding 60 mm × 90 mm, with impact points evenly spaced at 30 mm intervals. Figure 3.3 illustrates the selected rebound hammer impact locations.

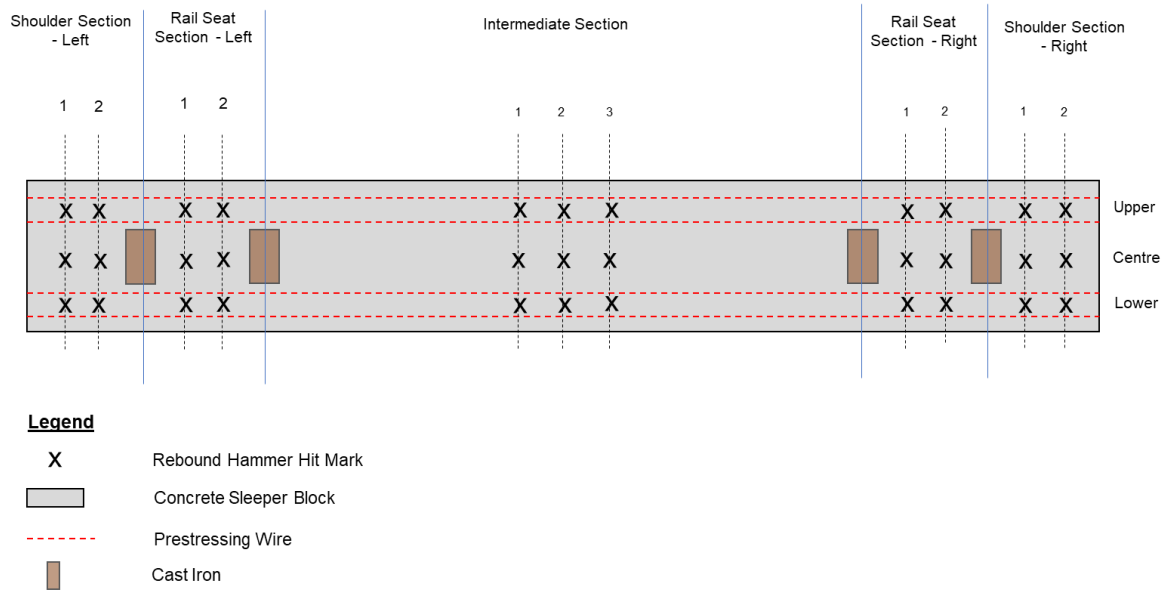

Figure 3.3: Schematic concrete outline indicating the locations of concrete hammer impacts

To account for surface roughness and potential variability in measurements, given the slightly abraded surface of the concrete sleepers, the test areas were carefully prepared by removing surface contaminants to ensure a more uniform surface texture. Additionally, extra test points were collected to improve measurement reliability, and statistical outliers were excluded from the dataset. The relationship between rebound number and concrete compressive strength was established by correlating the measured rebound values with the reference data provided in the “Conversion Table of Concrete Strength Value of Test Zone” (Appendix D), specifically for the −90° impact orientation. The resulting line of best fit equation was then used to estimate the compressive strength corresponding to the mean rebound value for each test section.

3.5.2 Tensile Strength

To obtain the tensile properties of the prestressing wires in the sleepers, steel tensile strength testing as specified in the EN 10204 was undertaken. A total of three (3) steel wires were extracted from three of the sampled sleepers (i.e., one from each sleeper).

3.6 Experimental Procedure

The experimental procedure was designed to investigate the residual prestress force in concrete sleepers of different ages using the dynamic relaxation method. All experiments were conducted using calibrated equipment and standardised procedures in an uncontrolled environment at a Transnet freight depot facility in City Deep, an industrial area south of Johannesburg in Gauteng Province. This section outlines, in a systematic manner, the processes followed for specimen preparation, prestress measurement, and data capture, with particular care given to consistency in all test conditions. The equipment and apparatus used in the experiments, along with their respective functions are listed in Table 3.2.

Table 3.2: Equipment and apparatus used in the experimental procedures

Item	Equipment/Tools	Use/Role
1	Angle Grinder and concrete cutting disc	To induce cracking or profile line where concrete was to be removed, and to cut off the wires
2	Chisel and Hammer	To break off the concrete covering the wire
3	Bolt Cutter	To cut off the wires
4	Heat Gun	To blow off concrete debris around the exposed wires region after the concrete breakout & to accelerate the drying of X60 cold glue once the strain gauges were pasted
5	1.5/120LY13 HBM Strain Gauges	To measure the strains as the wires were cut
6	Phosphoric Acid & Neutraliser	To clean the freshly exposed wires before application of the acetone
7	RMS1 Acetone	To clean the exposed wires after application of phosphoric acid and neutraliser
8	Cotton	Soaked with solutions, items listed in 6 & 7 above and used to clean off the sand off the wire.
9	X60 Adhesive	To affix the strain gauge to the prestressing steel
10	Cellotape	To temporarily affix and position the strain gauge before permanent fixation on the wire
11	Tweezer	To handle the strain gauges
12	Data Acquisition System - MX840B	To capture and record strains
13	Laptop and CATMAN Software	For data acquisition and display
14	12kW Generator	To provide power on site
15	Bolt Cutter	To cut off the strain-gauged wires
16	ABM75	Covering Material for Strain Gauges
17	Soldering Gun	To attach the connecting wires to the strain gauges

3.6.1 Preparation of the Testing Site and Concrete Sleepers

The preparation of the testing site involved cleaning of the designated area, which was a concrete-paved and brick-walled shed with one large opening along its longest side. Additionally, the loose soil-covered ground in front of the shed's entrance was watered to minimise dust, given the cool and dusty weather conditions at the time. The sleepers were to be positioned and aligned on 40 mm square wooden branding that had been laid on the floor. Subsequently, the sleeper specimens were aligned and numbered for identification purposes before concrete was removed. Figure 3.4 depicts the set up at the testing site.

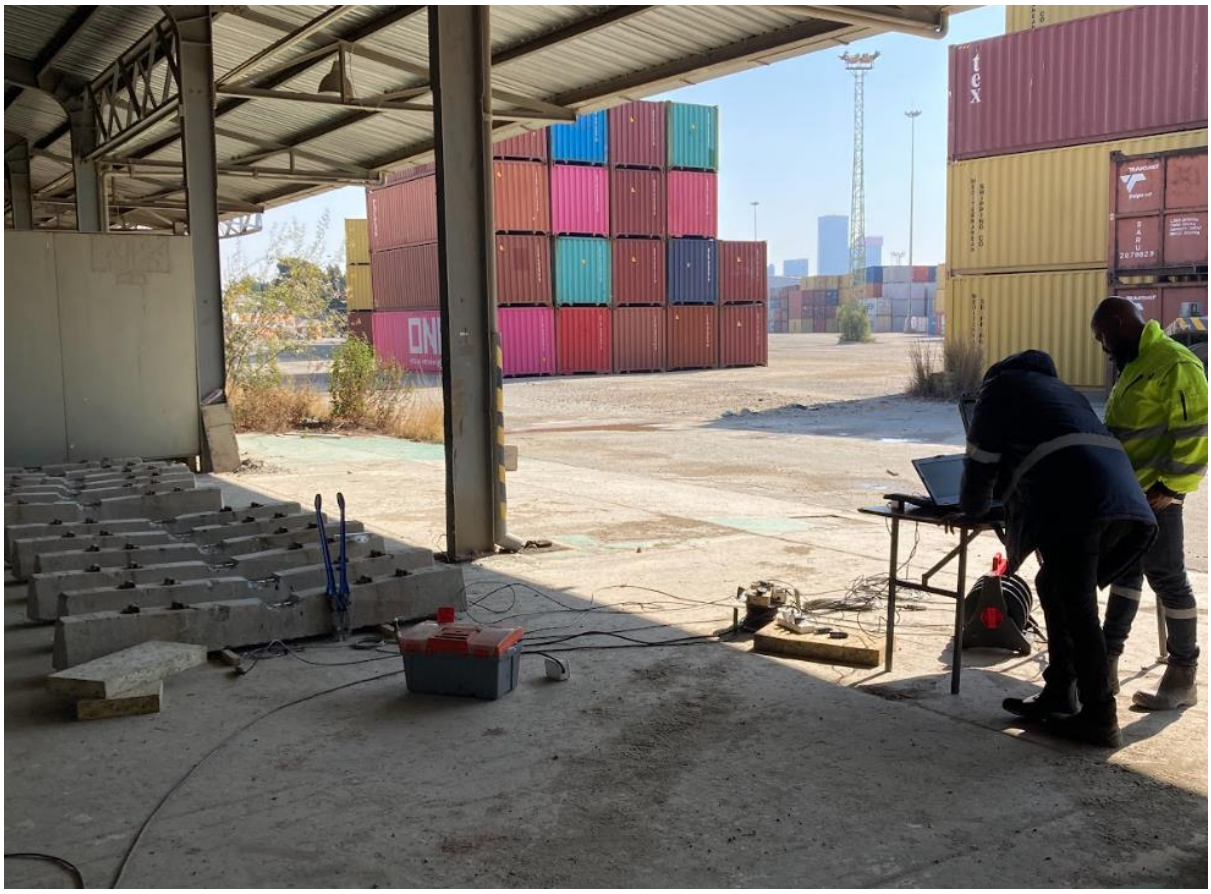

Figure 3.4: Establishment of the experimental site

3.6.2 Concrete Removal

The concrete at mid-span of each sleeper was removed to a maximum length of 150 mm and a depth of less than 40 mm. This was adequate to expose and free the top row of prestressing wires of concrete bondage, which allowed axial displacement. The test zone was carefully chosen to be at mid-span to ensure enough anchorage for the tendons. Less than 10% of the sleeper’s concrete was removed along its longitudinal axis to ensure that the prestress level and eccentricity were not affected by the concrete removed. Figure 3.5 presents a photographic summary of the concrete removal process.

Figure 3.5: (a) Marking of the portion of the concrete removed with a 150 mm ruler (b) Grinding of concrete at the marked transverse contours (c) Concrete removal using a 2.7 kg hammer and bull-pointed chisel (d) Exposed prestressed wires.

To prevent damage to the prestressing wires during the concrete removal process, using an angle grinder and chisel, one sleeper was intentionally broken in an uncontrolled manner at the centre to expose the first (top) and underlying second layer of prestressing wires. This method was employed to accurately map the location and cover depth of the wires. The longitudinal extent of the removal and the maximum cut depth, which was carefully limited to avoid exceeding the cover depth or reaching the wires, were marked, as depicted in Figure 3.5(a). A diamond blade angle grinder was used to create a transverse crack along the top surface of the sleeper, which helped to restrict the length of the concrete removal. The sleeper was rotated to its side to induce another longitudinal crack on the sides.

A chisel was used at this stage to remove concrete in small, manageable pieces to avoid removing large sections at once. This served to provide greater control over the process and minimise the risk of damaging the reinforcement. Various methods could potentially be used to remove concrete to expose prestressing wires. These include rotary hammer drills,

hydraulic splitters, sandblasting, and high or low-pressure water jetting. However, these methods were not explored in this context. Instead, the use of an angle grinder and chisel was more cost-effective, given the available resources.

3.6.3 Strain Gauge Attachment

Once exposed, the wires were cleaned of concrete debris and rust by grinding with a fine sandpaper and wiped with a cotton cloth moistened with acetone. Given the delicate nature of the strain gauges (SGs), tweezers were used throughout the handling process from unpackaging to application. For temporary fixation and positioning on the wire, a cellotape was utilised. The SGs were fixed 10 mm from the cutting point centre using X60 cold curing adhesive to ensure consistent and precise measurement of strain.

To accelerate the drying process of the adhesive, heat from a heat gun was applied. The heat gun served a secondary purpose in cleaning the sleeper testing zone by blowing off concrete debris. After the installation of the strain gauges, short lead wires were soldered to the gauge terminals utilising a soldering iron. Considering the uncontrolled environmental conditions at the testing site, and the timing of the testing, which occurred a day after the application of the strain gauges, a mastic tape (ABM75) was used to cover and safeguard the wire-connected strain gauges against potential damage. Figure 3.6 provides a visual summary of the strain gauge affixing process.

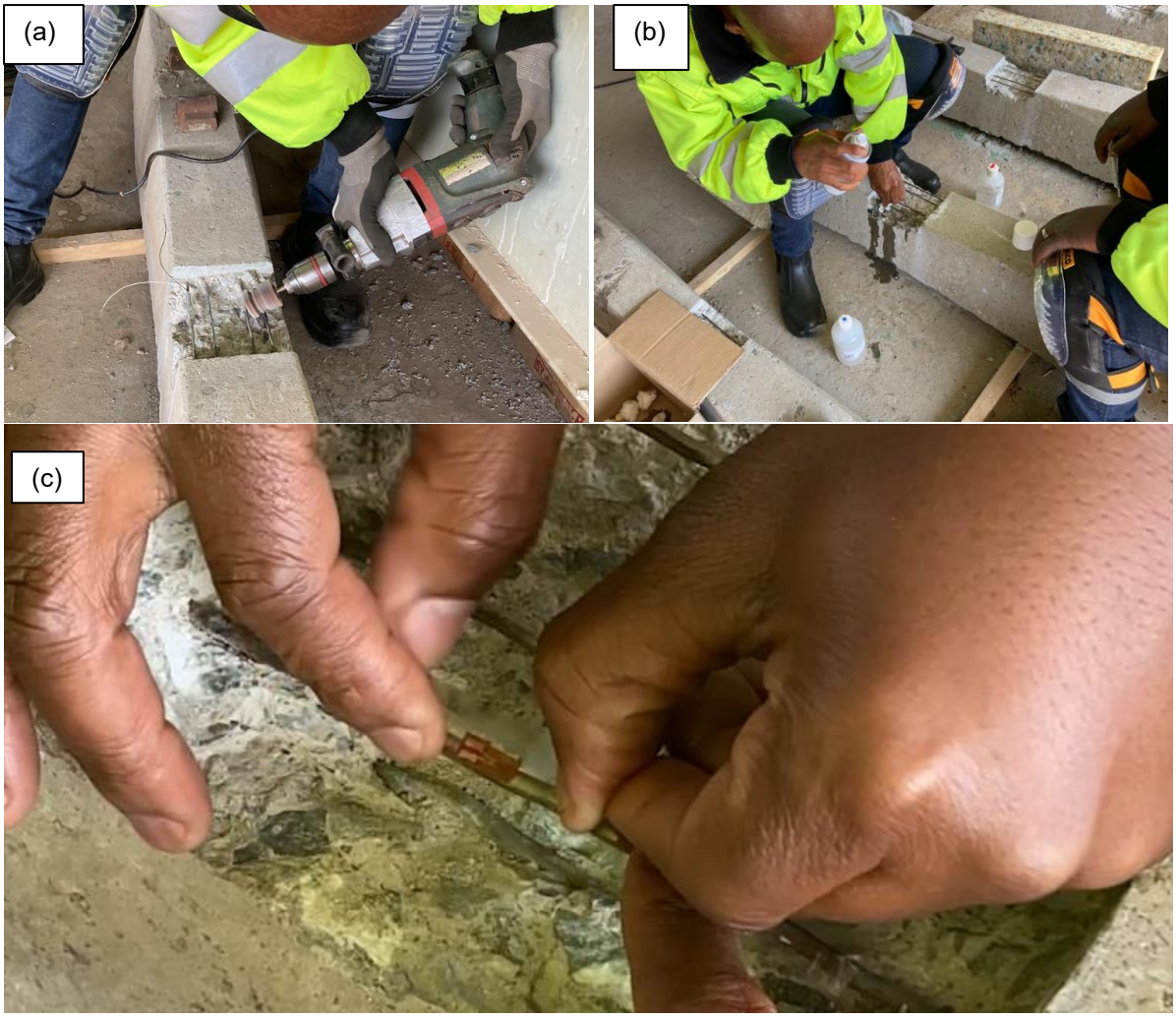

Figure 3.6: (a) Sanding of the prestressed wire (b) Cleaning off the pressed wire (c) The temporary attachment of the wire using cellotape

Figure 3.7 depicts the completed strain gauge pasting setups.

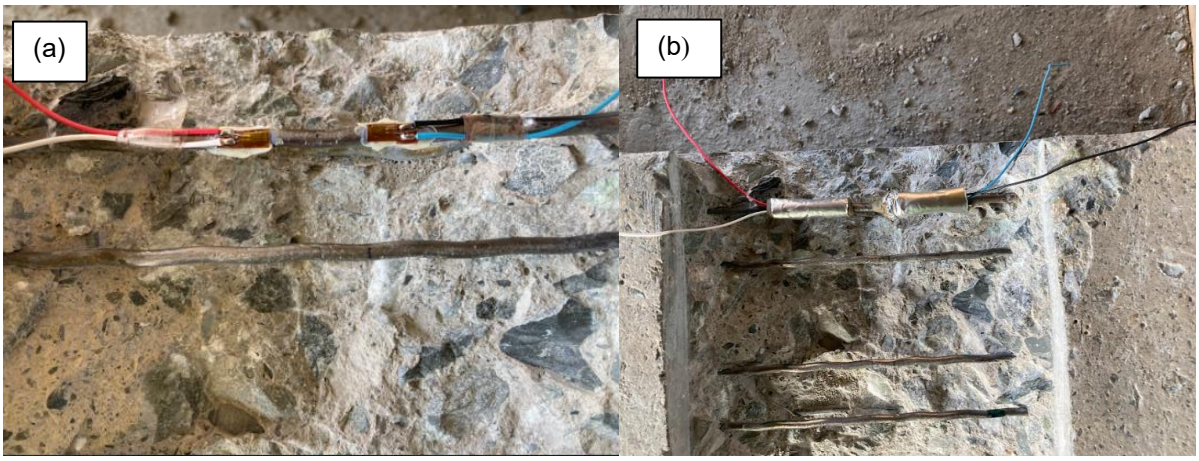

Figure 3.7: (a) Attachment of strain gauges with connected lead wires (b) Strain gauges covered with mastic tape

For ease of reference and recording purposes, the strain gauges were identified by position relative to the sleeper centre or cutting point. Figure 3.8 illustrates the strain gauge placement oriented as South or North. Due to budgetary constraints, five sleepers were instrumented with two strain gauges each and the rest had one strain gauge mounted on each, except for Sleeper 12. Details on Sleeper 12 are covered in Chapter 4 under Sub-Section 4.4.3.2.

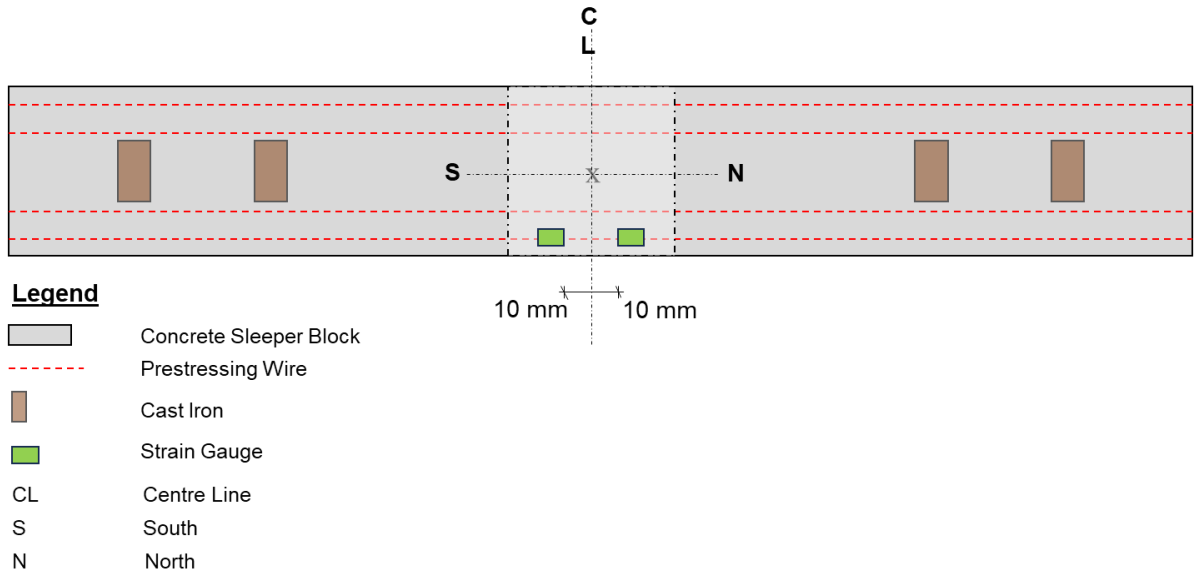

Figure 3.8: Orientation of Strain Gauges - Southern and Northern Positions

3.6.4 Strain Gauge Configuration and Calibration

The strain gauges (SG) with properties shown in Appendix G were used to measure strains of prestressed wires. The sensors were integrated into a half-bridge Wheatstone bridge circuit, where one SG was affixed to the test prestress wire while the second SG served as a dummy to complete the Wheatstone bridge configuration. The data acquisition system (DAQ) included an integrated database storing predefined sensor types, configurations and associated material data sheets. Following the selection of the appropriate SG sensors and the finalisation of the Wheatstone bridge configuration, the DAQ, applied the relevant settings automatically.

The MX840B Universal Amplifier was evaluated in the laboratory using the K148 Unit prior to field testing to confirm its operational and calibration status. The K148 device is used to verify the calibration of amplifier scanners, ensuring they function correctly. The amplifier scanner enhances the quality of measurement by increasing voltage levels, so that the signal range is aligned with the analog-to-digital converter (ADC), thereby improving resolution and sensitivity. The amplifier measures the change in resistance of the strain gauge sensor and subsequently converts this into a voltage or other designated units, depending on the applied testing method.

Calibration of the strain gauge sensor and the data acquisition equipment was performed using the calibration signal from the MX840B Universal Amplifier. These measuring amplifiers are equipped with a switch or a pushbutton that allows a defined signal to be introduced into the measurement circuit. This calibration signal can be expressed in either strain units (μm/m) or bridge unbalance units (mV/V) (Hoffman, 1989). In this study, the calibration signal from the MX840B indicated the following calibration: 1 mV/V is equivalent to 2000 μm/m assuming a strain gauge factor of K = 2. All installed strain gauges had a gauge factor of K = 2, and the settings on the amplifier confirmed this value. Therefore, the MX840B amplifier autonomously calibrated the sensors to convert millivolt/volt measurements into micro strain values.

3.6.5 Data Collection and Measurement

The 16-channel data acquisition system, MX840B was configured to operate at a frequency of 10 Hz and used to capture strains as the wires were cut. The wires were cut individually using a bolt cutter and the grinder, as shown in Figure 3.9, to allow for data capture and recording. The lower frequency was chosen in anticipation of the sudden relaxation behaviour of the wires.

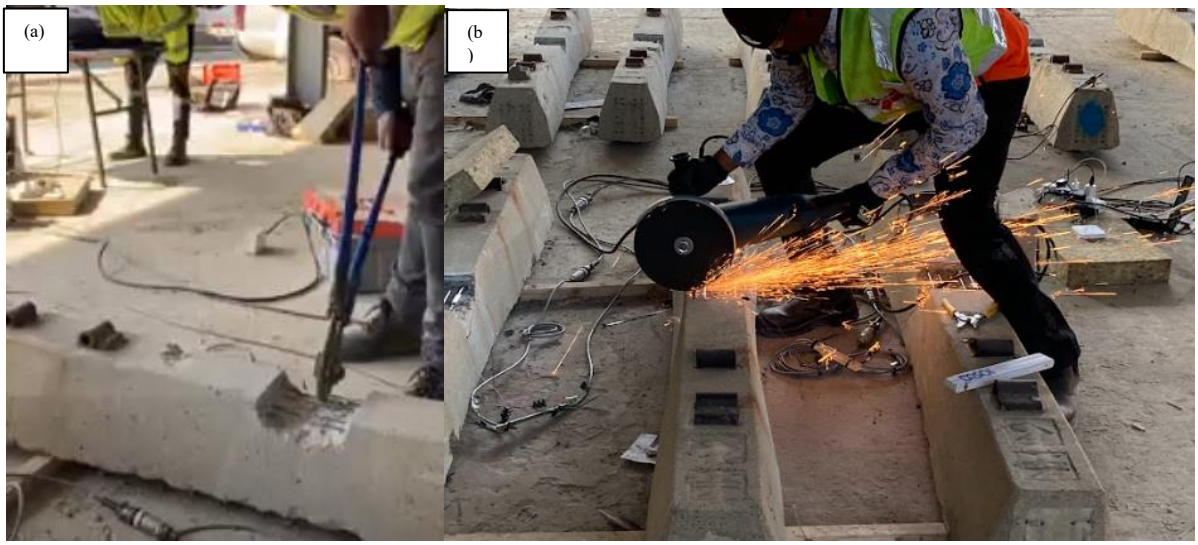

Figure 3.9: The cutting of steel wires to induce relaxation (a) Using the bolt cutter (b) Using the grinder

Figure 3.10 shows the setup of the data acquisition system used in the study and wire connection between the measuring equipment and specimen.

Figure 3.10: (a) Connectivity to the data acquisition system (b) Data acquisition system setup

3.7 Data Analysis

Based on the equilibrium strain state measured in the cut prestressed wire and applying Hooke's law, the corresponding prestressed stress was determined. The calculated stress results were subsequently compared with the theoretical design values derived from the South African sleeper specification: Specification for Monolithic Pre-Stressed Concrete Sleepers used on 1065 mm Gauge Railway Track.

3.8 Summary

The methodology employed to achieve the study objectives is covered in Chapter 3. To visually evaluate the condition of concrete sleepers, a defect descriptive assessment was defined and adopted, focusing on critical sections of the sleeper, specifically the rail seat, centre, and shoulder areas. To ascertain the material properties, the rebound hammer method was utilised to estimate the compressive strength of concrete, while tensile testing was conducted for steel wire parameters, in accordance with the BS 1881-202 and EN10204 standards, respectively. The estimation of prestress loss was conducted following a defined procedural dynamic relaxation method, which involved exposing the wires through the removal of concrete, the attachment of strain gauges, and the connection to the data acquisition system, followed by the cutting of wires as measurements were recorded. The results obtained through this methodology are presented in Chapter 4, aligned with the objectives of the study.

4 RESULTS AND DISCUSSIONS

4.1 Introduction

This chapter presents and discusses results obtained from the visual condition assessment, material tensile and compressive strength testing, and strain measurements used to estimate the residual prestress force.

4.2 Visual Condition Assessment

A defect-based descriptive evaluation approach was implemented in this study, as it proved to be more effective in determining the condition of visually inspected sleepers than the too simple functional scoring technique employed in South Africa.

Using the proposed concrete sleeper evaluation criteria, a range of defects was observed among the sleeper samples. These defects were classified by different deterioration mechanisms such as cracking, abrasion, chipping, roundness, corrosion, and deformity of cast-iron shoulders (i.e., fastening anchors) and corrosion of the wires. Furthermore, the defects were further identified by their position on the sleeper. To facilitate the evaluation of the steel and concrete components, considering the complexity of the composite nature of the prestressed concrete sleeper, the concrete and steel materials were evaluated separately. However, this approach did not preclude the reporting of observations that indicated composite behaviour, such as cracking of the sleeper and corrosion of the steel wires. A summary of the sleeper condition is provided below. Sleeper-specific conditions are provided in Appendix C.

4.2.1 Cracking

All the sleepers displayed transverse cracks originating from the sleeper base around the rail seat area and extending upward to a height of about 75 mm – 85 mm. The cracks were widest (≈ 1.0 mm) at the bottom of the sleeper and progressively narrowed along the path becoming less than 0.1 mm near mid-height. While the width of the crack (1mm in this case) is an important factor, the depth of the crack is equally critical. Shallow cracks that do not extend into the reinforcement may not pose a great danger; but cracks that approach or reach the prestressing wires must be carefully evaluated for the potential for corrosion risk. Under continued cyclic loading, a consideration when deciding to reuse sleepers, small cracks can propagate resulting in larger and wider cracks. At these points of damage, the load will be redistributed to the unaffected sections, increasing the vulnerability to corrosion due to the potential ingress of water.

The observed 1 mm cracks likely went undetected to the condition assessors during the service life of the concrete sleepers due to their location, size and the fact that they remain

buried in ballast. This highlights the need for alternative inspection methods, as many such cracks may remain hidden and unknown to track inspectors or infrastructure managers. Non-Destructive Techniques (NDTs), i.e., ultrasonic testing or ground penetrating radar (GPR), should be considered for identifying these defects. Integrating NDTs with other design or refurbishment options for preventing water ingress, such as grouting, may provide timely and cost-effective mitigation measures.

The cracks observed are likely attributable to excessive bending and shear stresses at the rail seat area owing to increased traffic loading and frequency over the years within the corridor. Additionally, track geometry and ballast maintenance practices such as tamping and screening, have likely contributed to uneven stress distribution beneath the sleepers. No visible cracking was observed at the centre of the sleeper. This phenomenon could possibly be explained by assuming constant ballast support directly underneath the rail seat area, adequate to minimise the negative bending moment acting at the centre of the sleeper. A glass-magnified crack originating from the sleeper base is depicted in Figure 4.1.

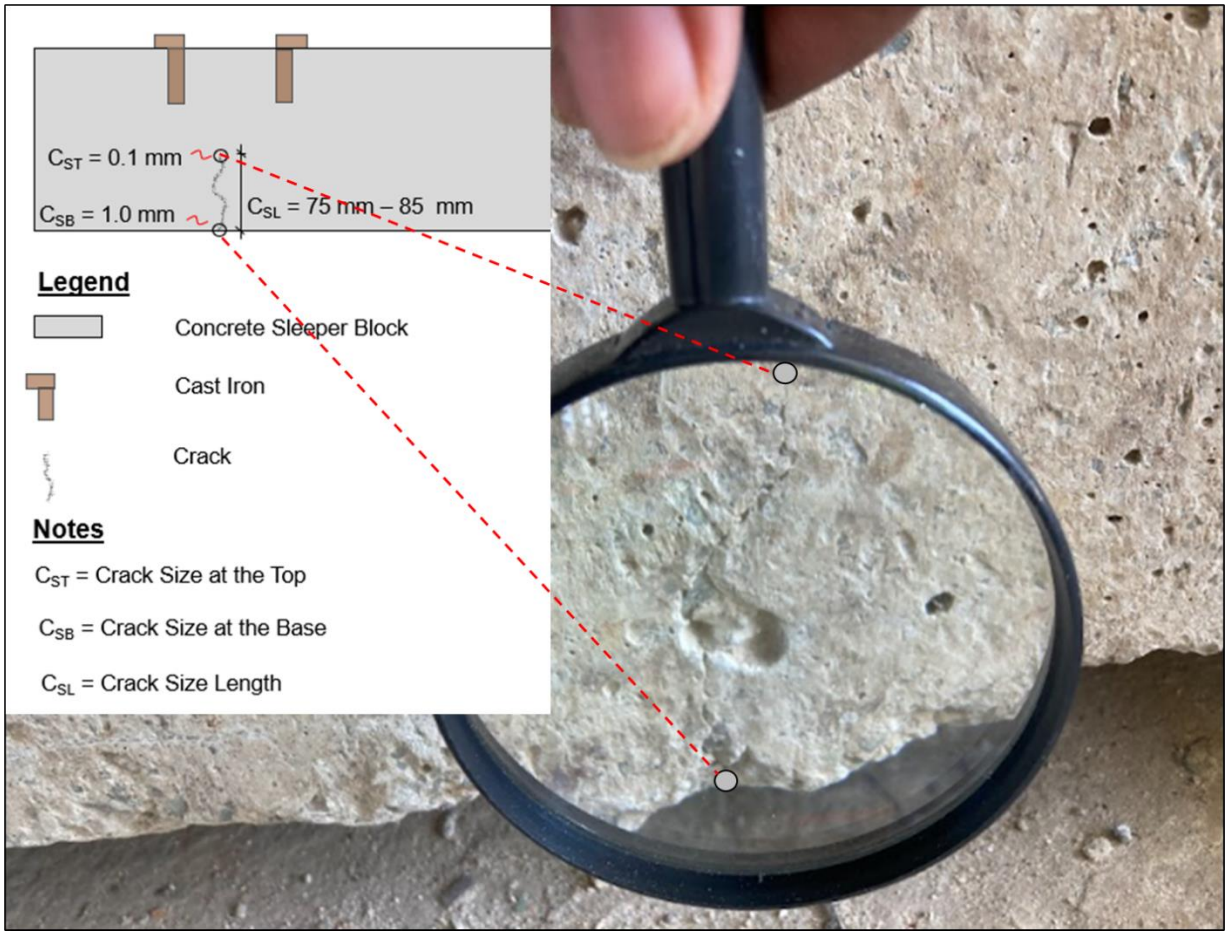

Figure 4.1: A typical concrete crack exploded using a magnifying glass

4.2.2 Rail Seat Abrasion

For most of its life in operation, the rail seat area is always in contact with the pad, which provides insulation and cushions the stresses transferred from the rail. In this study, very light abrasion was observed on the rail seat area, and its impact on the local pad movement remains undetermined.

A notable and previously undocumented phenomenon observed for all sleepers was the irregular sleeper pad residual, ranging from 0.1 mm to 0.3 mm in thickness. As illustrated in Figure 4.2, this residual material defined as the remains of the sleeper pad material, appears as a uniformly or non-uniformly spread thin paste on the concrete surface at the rail seat area. The staining of the rail seat concrete surface by the sleeper pad material suggests slippage of the pad likely due to high frictional forces under externally induced and internally generated elevated temperatures. This might have occurred alongside the shifting of rails under excessive longitudinal stresses. The presence of the pad residual certainly would reduce the frictional coefficient required for adequate resistance between the pad and concrete materials.

Figure 4.2: A typical slightly abraded rail seat area exhibiting residual rail-sleeper pad material

4.2.3 Shoulder Area (the Ends)

The structural integrity of sleepers depends on the state of the shoulder ends, which serve as anchors for the prestressed wires. The evaluation revealed no cracking at the sleeper ends for all sleepers, except for an interesting observation made on sleeper number 6 (Figure 4.3), which exhibited evidence of patch repair on the southern side. However, no information could be obtained for the specific sleeper or to confirm whether patch repair of sleepers was standard practice in the past.

Figure 4.3: Substandard patch repair observed on the southern side of sleeper number 6

Figure 4.4 illustrates the typical steel arrangement and compares the condition of the sleeper base edges at sleeper ends between the old and new sleepers. Over time, the sleeper-interaction results in ballast breakdown and noticeable wear on the sleeper edges at the base (termed sleeper roundness) and the abraded sleeper underside.

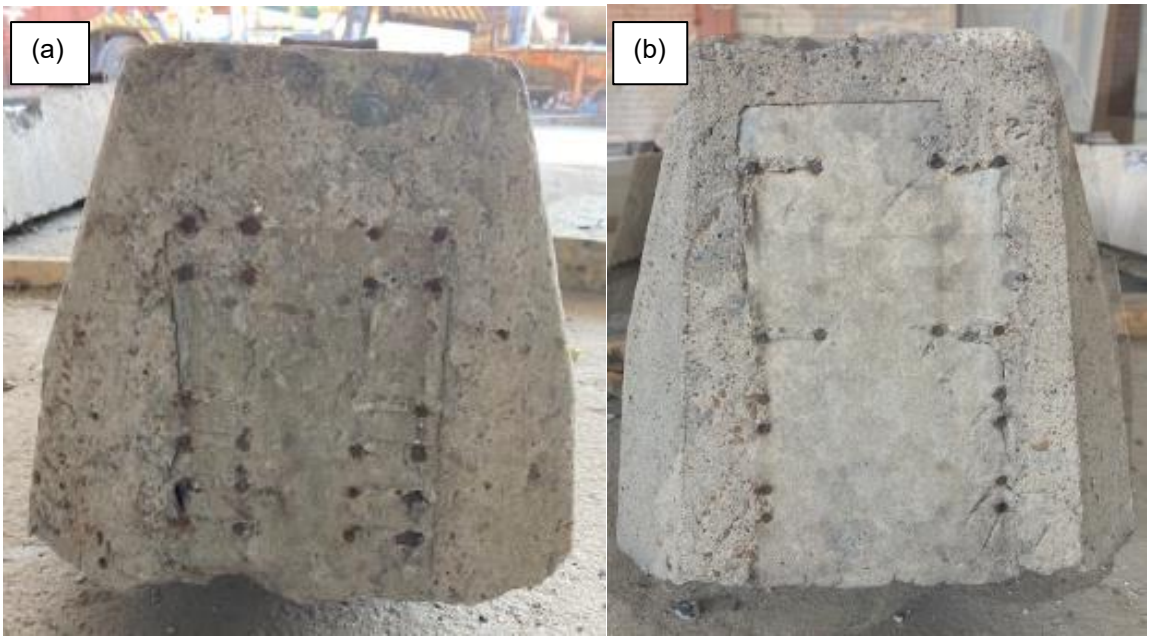

Figure 4.4: A comparative analysis of steel arrangement and the roundness of sleepers (a) Old sleepers (b) New sleepers

4.2.4 Concrete Breakage and Chippings

Another common form of damage observed was concrete breakage or chippings that likely resulted from either maintenance or operational derailments as seen in Figure 4.5. The sleepers themselves showed friction marks that are a result of sleeper-ballast interaction.

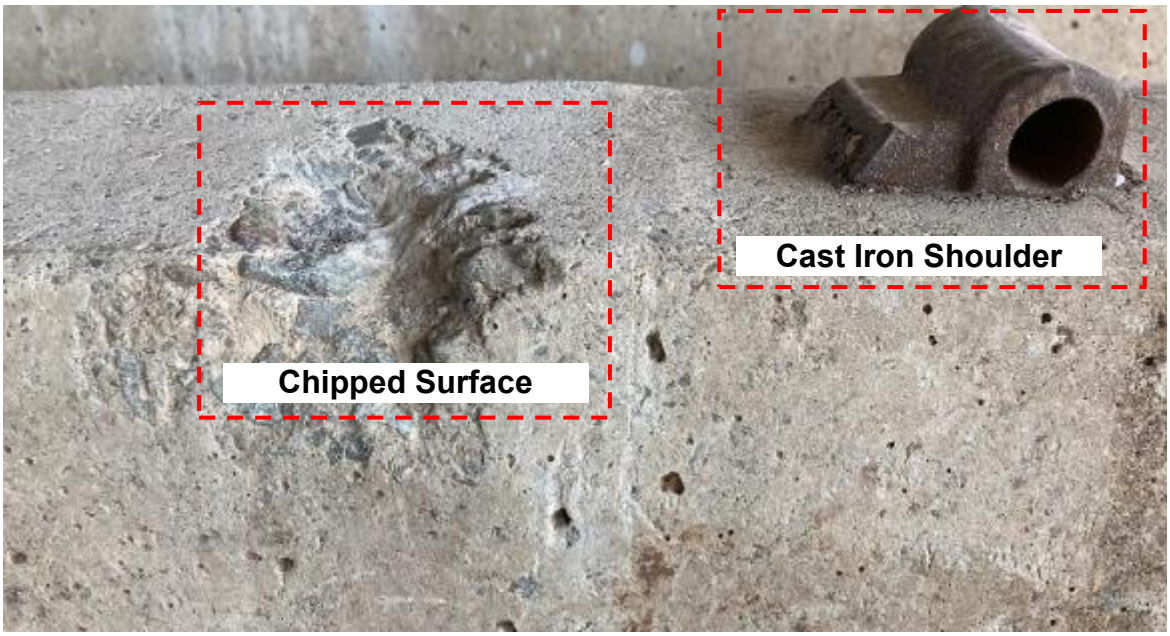

Figure 4.5: Chipped concrete edge/surface and intact cast Iron shoulder

4.2.5 Corrosion

Corrosion of embedded steel is the leading cause of deterioration in concrete. For concrete sleepers, prestressed steel wires and cast-iron components are the two embedded metals susceptible to corrosion, which can subsequently impact the overall condition of the surrounding concrete.

4.2.5.1 Cast Iron Shoulder

The embedded part of the cast iron was exposed, and its condition assessed visually. Based on the evaluation, the cast iron appeared to be intact and in good condition, i.e., no deformation had occurred. The exposed and embedded sections of the cast iron material both exhibited a uniform, thin layer of rust. However, the covered part of the cast iron remained comparatively intact structurally and retained its original condition. In contrast, the exposed area displayed signs of advanced corrosion, including a noticeably roughened surface. At the foot of the cast iron, where it made direct contact with the outside concrete surface, this corrosion was especially noticeable.

This observation suggests that early stages of corrosion may have resulted in the formation of an oxide layer either before or after the manufacture of sleepers. This oxide layer acts as a protective shield, slowing down further damage to the underlying metal. Given the exposure to environmental factors such as moisture and oxygen, which are necessary to initiate or accelerate corrosion, it was inevitable for the external section of the cast iron to corrode. Additionally, it is not surprising that the cast iron foot, which rests on the concrete surface, showed advanced corrosion, due to the prolonged presence of moisture at the interface between the sleeper and the cast iron.

Notably, the concrete sleepers examined in this study were removed from a 25 kV AC electrified railway line located in a remote, semi-arid area. This environmental and operational context suggests minimal exposure to aggressive chemicals, such as chlorides, which could otherwise penetrate the concrete matrix and initiate corrosion of the cast iron inserts or prestressing wires. Furthermore, the use of an AC electrification system inherently reduces the risk of stray current corrosion. Commonly associated with the 3 kV DC system, stray current-induced corrosion occurs when leaked current from the traction power supply travels through conductive materials, including water, to reach other corrosive materials. Stray currents can initiate or accelerate electrochemical corrosion of embedded steel reinforcement, enabled by the presence of concrete cracks or inadequate concrete cover. Ultimately, the residual strength of the prestressing wires can be reduced and lead to premature structural failure. In this study, however, the absence of a DC system and the low environmental

aggressiveness indicate negligible chances of such degradation mechanisms. Figure 4.6 shows the condition after the cast iron portion was removed.

Figure 4.6: Condition of the cast iron immediately following extraction from concrete

4.2.5.2 Steel Wires

The condition of the wires was visually assessed at two stages during the study. The first evaluation, conducted at partial level, occurred during the test specimen preparation, i.e., during the removal of concrete at the sleeper centre. The second, more comprehensive examination took place when the steel wires were extracted fully from the sleepers for testing. The top layer of steel wires did not exhibit signs of corrosion when exposed only at the sleeper centre. However, once the wires were removed completely and freed from concrete bondage, scattered patches of rust were observed along their length, with varying degrees of deterioration.

Whilst some spots displayed the onset of corrosion, others indicated more advanced pitting corrosion, as reduction in the wire cross-section could be seen. A misconception about the condition of the wires would have been to assume no presence of corrosion as was presumed

in the initial phase of the assessment. The severity of corrosion on wires also varied with the depth within the sleeper. Relative to the sleeper's mid-height of the sleeper, the bottom layered wires exhibited more advanced stages of pitting corrosion compared to the top layered wires. Figure 4.7 depicts the condition of the visually assessed steel wires following their extraction.

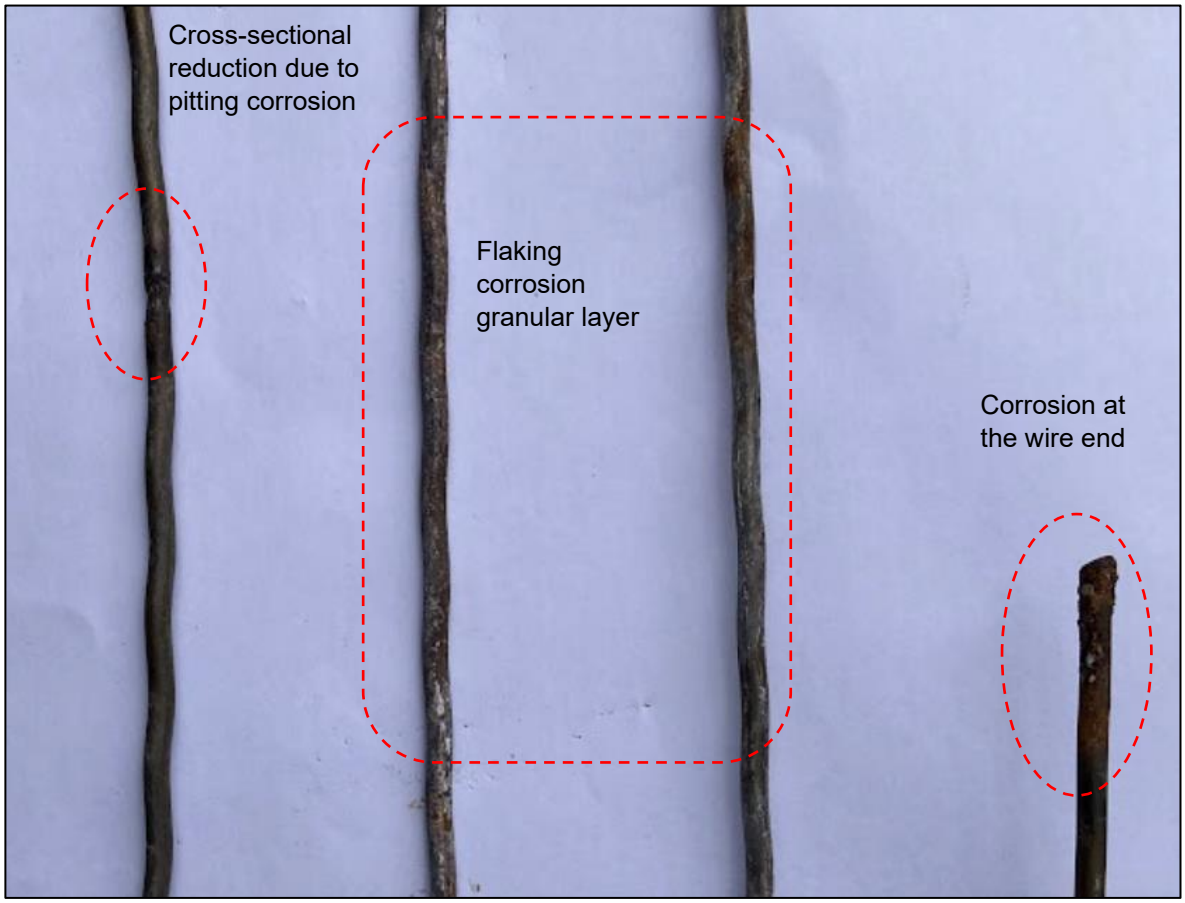

Figure 4.7: Condition of the wire immediately following extraction from concrete

Profiling of corrosion on the wires and in relation to the concrete condition revealed the presence of corrosion in areas where the wires were exposed, as was the case at sleeper ends, and localised around the rail seat section where structural cracks were present. The corroded spots extended from underneath the sleeper to the around the rail seat region, which is where the rail load is highest. This was due to the penetration of moisture through the cracks or concrete pores, considering the cover depth of only 20 mm.

The degree of corrosion deterioration varied with the vertical position of the sleeper, with the worst condition of corrosion found on the bottom layers of steel wires, where the cracks were widest. Moderate corrosion damage was found in the mid-layer of wires and decreased towards the top layer of wires. Figure 4.8 shows the schematic corrosion profile in terms of severity.

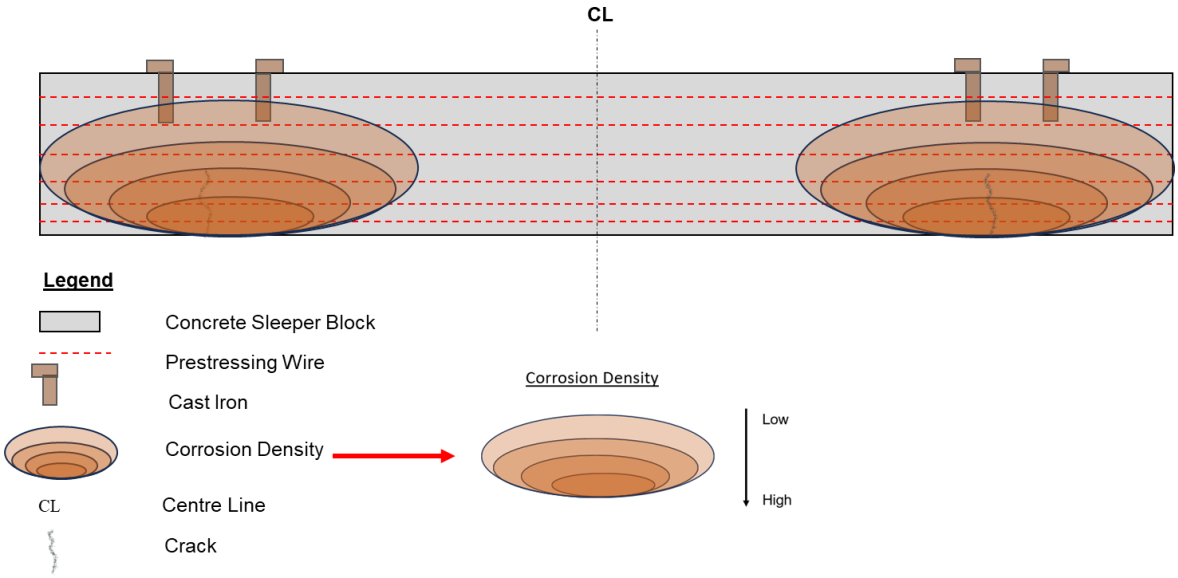

Figure 4.8: Corrosion density in the rail seat zone

4.3 Mechanical Properties

4.3.1 Concrete

As described in Section 3.5.1, the rebound hammer technique was used to estimate the compressive strength of the concrete. The mean rebound values for the tested concrete regions were all above 50, ranging from 50 to 54. The standard deviations for the sections ranged from 2.21 to 4.04, indicating that the rebound values were closely grouped around the mean. The coefficient of variation ranged from 4.22% to 7.96%, reflecting a very high consistency in the measurements. The line of best fit achieved was linear and was expressed by the equation $y = 1.763x – 22.58$, with a strong correlation coefficient of $R^2 = 0.99221$. From this equation, the respective compressive strengths were estimated to range from 60 to 67 MPa, which is higher than the 28-day strength requirement of 60 MPa. Detailed calculations for the rebound hammer approach are provided in Appendix D, and the average compressive strengths for sleepers tested are given in Table 4.1.

Table 4.1: Estimation of concrete compressive strength

Rebound Test Location	Mean Rebound (Resilience) Value per Test Zone, Nα	Standard Deviation	Coefficient of Variation	Stress Conversion (MPa): Equation. of Best Fit Line
Shoulder Section (Left)	50.75	4.04	7.96%	60.72
Rail Seat Section (Left)	52.59	2.76	5.25%	63.96
Intermediate Section	53.48	3.17	5.93%	65.54
Rail Seat Section (Right)	52.24	2.21	4.22%	63.34
Shoulder Section (Right)	54.38	2.50	4.59%	67.13

4.3.2 Ribbed Steel Wires

The tensile test was performed on three prestressing wires following the EN10204 standard, and the average yield tensile strength and ultimate tensile strength obtained were 1340 MPa and 1907 MPa, respectively. The calculated standard deviation of the steel wire tensile strength is 18 MPa, indicating a cluster of the measured values around the mean. Additionally, the calculated coefficient of variation is 0,96%, suggesting a high level of consistency among the measured tensile strengths. Detailed experimental results are in Appendix D. Table 4.2 presents the material yield and ultimate tensile strength for the three wires.

Table 4.2: Steel material strength properties

Material	Ultimate Tensile Strength (MPa)	Mean (MPa)	Standard Deviation	Coefficient of Variation
Wire Number 1	1 902	1 907	18	0.96%
Wire Number 2	1 931			
Wire Number 3	1 887			

4.4 Residual Prestressing Force

This section provides an analysis of the results obtained from the experiment. It also explains observations found to be different from the expectation.

4.4.1 Design Prestress

For railway concrete sleepers to be approved for use, the BBG8755 specification demands particular design information. This includes the characteristic ultimate tensile strength of the reinforcing steel, the initial and final stresses in the concrete and reinforcement. The following criteria must be adhered to concerning the initial and final stresses in the reinforcement:

a. The Initial stress must not exceed 75% of the characteristic strength.

b. The final stress, after accounting for losses, must not be less than 60% of the characteristic strength for all open line sleepers, except for the Low Profile (LP) sleeper, which may be 54%.

It is assumed that the condition stated in 4.4.1 (b) applies to the LP sleepers used in this study. Given the ultimate tensile strengths obtained for the new and old sleepers, the design prestress force in the concrete sleeper is determined using Equation 4.1:

$$\sigma = 0.6\sigma max \qquad \text{Equation 4.1}$$

where: σmax - represents the ultimate tensile strength.

The calculated prestress results are provided in Table 4.3.

Table 4.3: Design prestress values for new and old concrete sleepers after accounting for losses

	Ultimate Tensile Strength (MPa)	Prestress after losses (MPa)
New Sleepers	1 700	1 020
Old Sleepers	1 906	1 140

4.4.2 Experimental Results

The data presented effectively demonstrates the use of strain gauge measurements to estimate the residual prestress force in railway concrete sleepers. Special attention is given to the levels of measured strains, which are subsequently converted into residual prestress values. These values are then compared to the theoretical measurements detailed in Section 4.4.1, providing a comprehensive analysis of the findings.

4.4.2.1 Signal Tracing Analysis

The signal tracing analysis confirms that the strain gauge setup was correctly configured to capture strain data from the axially loaded prestressing wire. All tests were initialised to zero before cutting the wires, and measurements were collected at a frequency of 10 Hz. The strain gauge measurements demonstrated a contraction of the prestressing wire, which is consistent with the theoretical understanding that when a steel bar is tensioned and securely fixed at both ends, it contracts immediately upon being cut in a shock or impact mode, followed by a speeded settling period. Once settled, the tension within the wire remains stable over time. This measurement behaviour aligns with findings from previous experimental work (Remennikov & Kaewunruen, 2015; Scott, 2019). The exception was Sleeper number 1 (S1), which exhibited a positive value indicative of expansion (see Section 4.4.2.4 for details). Figure 4.9 presents the signal traces for all tested sleepers, highlighting an initial contraction and subsequent state of equilibrium.

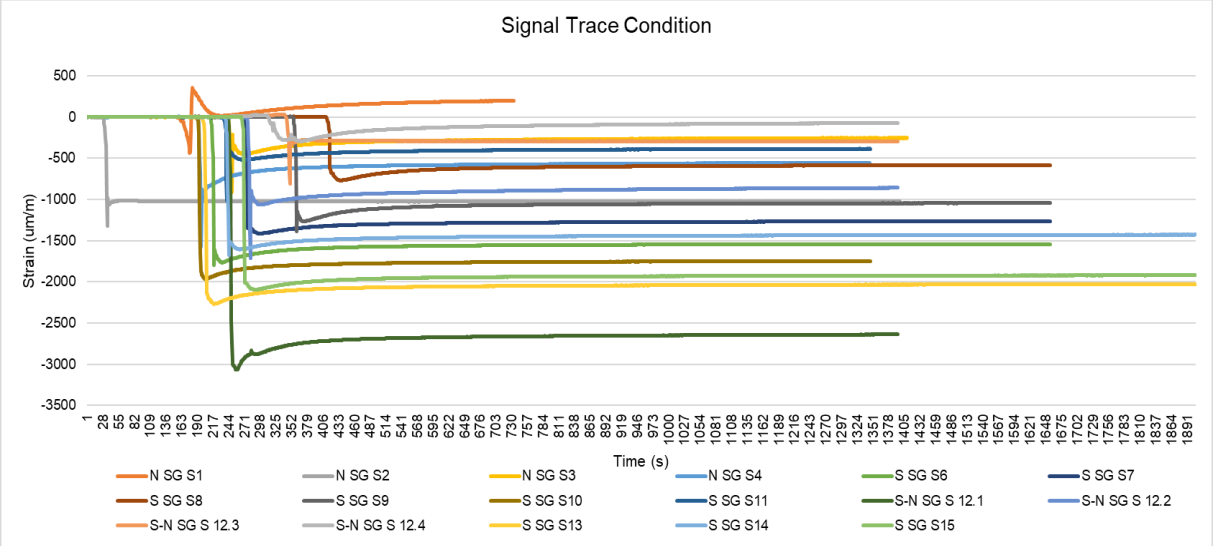

Figure 4.9: Signal tracing analysis for all sleepers

In contrast, Figure 4.10 displays experimental data on dynamic relaxation derived from (a) Scott (2019) and (b) Remennikov and Kaewunruen (2015). There are observable general trends that bear a resemblance to those depicted in Figure 4.9, specifically regarding the overall shape of the relaxation curves. Differences, however, exist in both the magnitude and rate of relaxation when comparing the findings of the current study. Notably, Scott's (2019) results exhibit a more gradual decline in the time trend for dynamic response, whereas Remennikov and Kaewunruen (2015) report an immediate sharp decrease followed by a plateau. Both cases differ from the pattern identified in the present research.

These discrepancies imply that, while the fundamental mechanisms remain consistent, the dynamic characteristics revealed in this study indicate differing material or structural responses, likely attributable to variations in experimental setup, boundary conditions, or material properties. Such variations underscore the necessity for context-dependent analysis when evaluating the dynamic relaxation behaviour of structural systems.

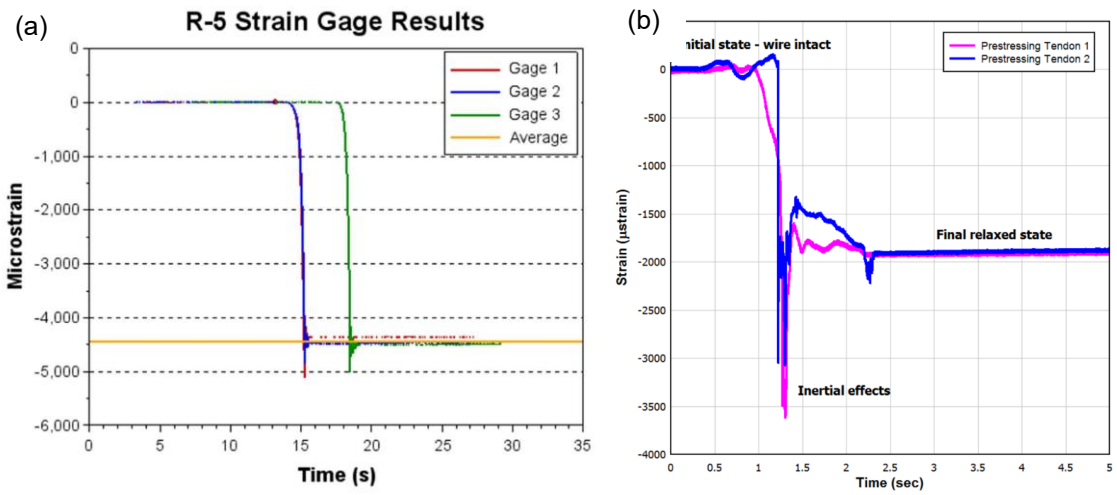

Figure 4.10: Dynamic relaxation experimental studies by (a) Scott (2019) and (b) Remennikov and Kaewunruen (2015)

4.4.2.2 Residual Prestress of Aged Sleepers

The results presented in Figure 4.11 indicate that the prestress levels in the 40-year-old concrete sleepers, as determined from measured strain data, varied considerably but remained significantly below the theoretical design stress of 1140 MPa in all cases.

Figure 4.11: The residual prestress of aged concrete sleepers

The mean strain measured at the sleeper centre for aged sleepers was -1273.0 μm/m, corresponding to the mean residual prestress of 254.6 MPa. This represents an average loss of 77.7%. The data exhibited a range of 2 255 μm/m and a standard deviation (STDEV) of 635.5 μm/m. This is indicative of the high variability of the dataset. This is further underscored by the coefficient of variation (CV) calculated at 49.9%. The high dispersion of data relative to the mean may be attributed to several factors, including random sampling of sleepers with

unknown in-service exposure conditions. Influential variables may include the ballast condition and profile underneath the sleeper and the condition of the rail. For instance, a concrete sleeper overlain by a defective rail may experience high dynamic stresses compared to one supporting a good, conditioned rail, thereby affecting the prestress force.

Comparatively, Scott (2019) reported an average prestress loss of 20% in concrete sleepers aged 25 years, while Remennikov and Kaewunruen (2015) observed a loss of approximately 60% in aged concrete sleepers with unspecified service duration, attributing the deterioration primarily to poor sleeper condition. In the present study, despite the sleepers appearing visually intact, an average prestress loss of 82.5% after more than 40 years in service is notably high. It is important to note that cracks observed beneath the rail seat areas, along with signs of corrosion on the prestressing wires, suggest that localised deterioration may have affected the internal stress distribution. These defects could have compromised the effective force transfer within the wires due to cross-sectional variability, thereby contributing to the observed reduction in residual prestress.

The results for Sleeper 1 and Sleeper 5 were excluded from the calculation of the mean residual prestress force due to anomalies arising from an irregularity during the cutting process and a measurement omission, respectively. Notably, different strain results were recorded for sleepers with two strain gauges (SGs) installed along the same wire axis, identified as North and South. Generally, the Southern fixed SGs yielded higher strain measurements, except for the outcomes in Sleeper 1, where the Northern SGs recorded higher values. The expectation was for both strain gauge measurements to produce the same results as were observed in previous studies. Instead, the values varied considerably, except for Sleeper 2. The variability in strain measurements of SGs fixed on the same axial wire could be attributed to the following factors not accounted for:

i. Asymmetrical placement of SGs relative to the cut - this observation relates to the 10 mm axial offset in the placement of SGs on either side of the sleeper's centre point. The transition from using a bolt cutter to a grinder equipped with a 3 mm-thick steel cutting disc introduced asymmetry in the cutting process, causing the cut to be skewed towards one side. This asymmetry likely contributed to the significant uneven stress release observed after cutting. General observation from this study indicated a bias towards the Southern SGs. Since strain measurements are sensitive to proximity to the point of force release, the gauge nearest to the cut typically exhibits a more pronounced response due to the sudden release of axial force, whereas a gauge positioned further away is likely to experience a delayed or diminished change in strain.

ii. Thermal effects from grinding – frictional heat generated from cutting contact between the grinder and the prestressing wire can introduce various thermal effects that could affect the SG readings, undermining or exaggerating mechanical stress. As noted in (i) above, the asymmetric nature of the cut could lead to uneven heat distribution resulting in a local thermal expansion or contraction response of the material (Callister, 2007). Grinding can also introduce residual stresses due to the applied mechanical force and localised heat produced during cutting (Suresh, 1998). The observed effects of grinding in the study are discussed in Section 4.4.3.3.

iii. An additional observation was the partial severing of a prestressing wire at the far edge of Sleeper 1 and Sleeper 14 by the grinder during concrete removal, which was obscured by residual debris. This likely altered the initial strain state through force redistribution or premature stress release due to the affected anchorage on one side or different boundary conditions.

4.2.2.3 Residual Prestress of Aged and New Sleepers

To validate the methodology outlined in Section 4.2.2.2 for determining the prestress force in aged sleepers, a comparable experimental procedure was applied to similar-type sleepers manufactured in 2006 that had never been in service. As these sleepers had only been subjected to their self-weight from being stacked on top of each other at the storage yard, they were assumed to represent the as-new condition. The results presented in Figure 4.12 indicate that the prestress levels in the 17-year-old concrete sleepers, as determined from measured strain data, varied moderately but remained significantly below the theoretical design stress of 1 020 MPa in all cases.

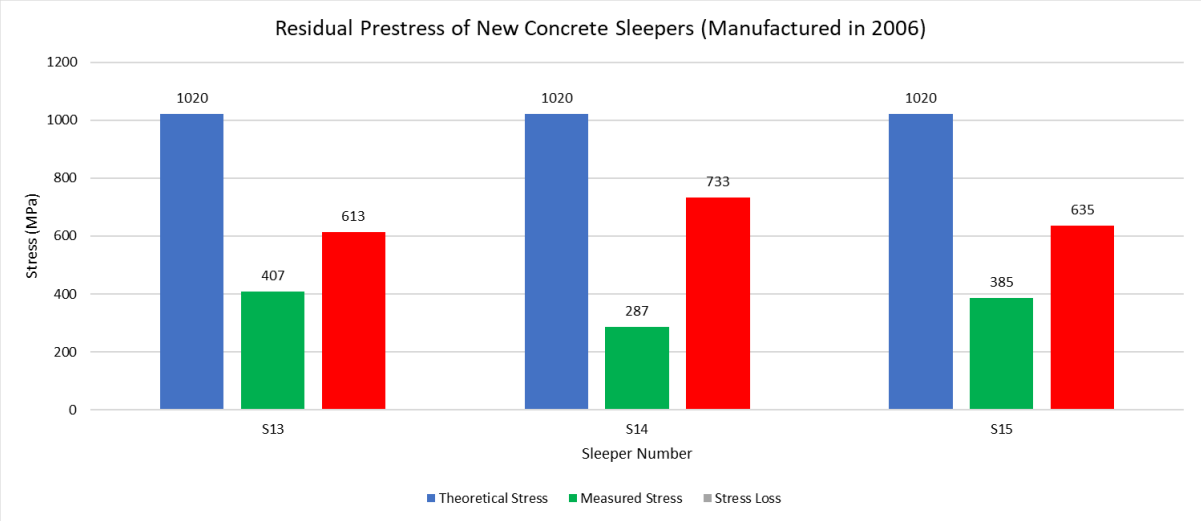

Figure 4.12: The residual prestress of aged concrete sleepers

The mean strain measured at the sleeper centre was -1 797.7 μm/m, corresponding to a mean residual prestress of 359.4 MPa. This represented an average loss of 64.8%. The data exhibited a range of 600 μm/m and a standard deviation (STDEV) of 319.1 μm/m. This is indicative of the high variability of the dataset. The coefficient variation (CV) was found to be 17.78%. The high dispersion of data relative to the mean may be attributed to several factors, including random before-service exposure factors such as weather conditions and cumulative effects of other sleepers whilst stacked at the storage yard.

As expected, the measured strains for the new sleepers were higher than those recorded for the old sleepers. However, the calculated prestress from the experimental strains was lower than anticipated for the sleepers that had never been used. According to BBG7855, the prestress level at transfer, after factoring all losses, should remain approximately consistent. Similar to Sleeper 1, Sleeper 14 exhibited the same cross-sectional reduction damage by the grinder on the far edge, thus reducing the resultant measured strains (i.e., asymmetry boundary conditions).

4.4.3 General Observations

4.4.3.1 Strain Gauge Sensitivity Analysis

An interesting observation on the correlation between the sensitivity of the strain gauge, expressed in terms of resistance tolerance, and the measured strain, was made. Although there is no clearly defined relationship, it appeared that the further away the strain gauges were from the resistance tolerance thresholds, i.e., 120 ± 0.35% Ω, the lower the measured strain results. This phenomenon was the same for both aged and new sleepers, as illustrated in Figure 4.13. About 35% of the measured strain gauges' resistance fell within the 0.35% tolerance. The reasons for this could be attributed to the experimental site and environmental conditions at the time of testing. Whilst the strain gauges were prepared in a closed space, they were mounted on an open site. Although efforts to clean the wires as thoroughly as possible were made, there was a slight wind blowing, which could have added a bit of dust immediately after cleaning, thus affecting the cleaned surface contact between the wires and the strain gauges.

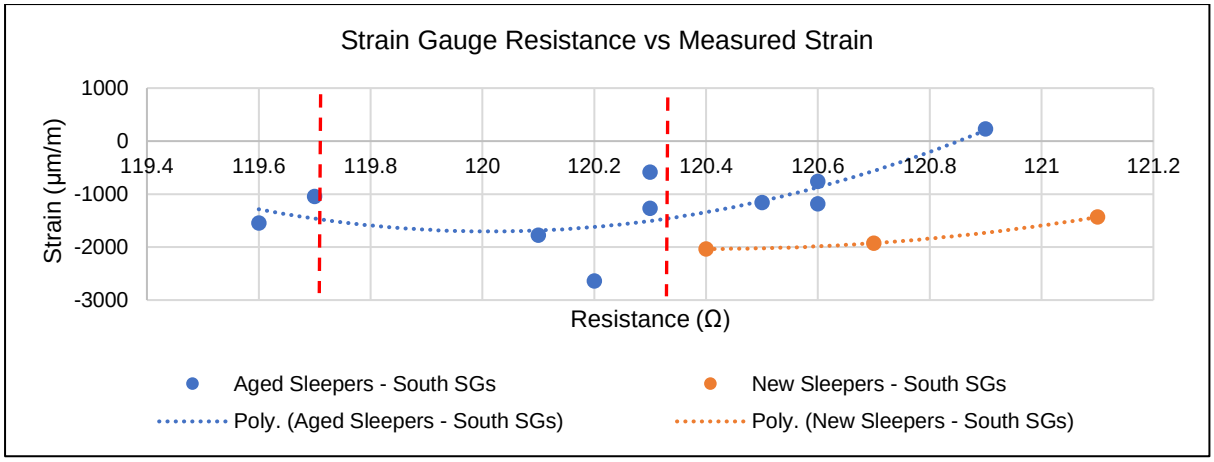

Figure 4.13: A graphical representation of the measured strains in relation to strain gauge resistance

4.4.3.2 Load Distribution

It was decided during the experiments to instrument all four exposed wires on Sleeper number 12 (S12), considering that Sleeper number 5 (S5) was erroneously cut before taking measurements. This was done to provide information on the stress redistribution on uncut wires when one or more wires are cut. Should the wires have provided the same results, the second wire of Sleeper 5 would have been instrumented and tested.

Hypothetically, an equal stress increase redistributed from the cut wire(s) to all uncut wires would be expected. Instead, successive/progressive reduction of stress was noticed as the wires were cut, as shown in Figure 4.14. The reduction could suggest the possibility of slippage of each wire at the onset of load increment. It is for the reason of stress differences that S5 was omitted from the instrumentation and testing.

Moreover, the different strain gauge results obtained from wires in the same concrete sleeper may indicate that the assumption made that all wires carry equal stress, may not be valid. This could potentially lead to underestimations or inaccurate results.

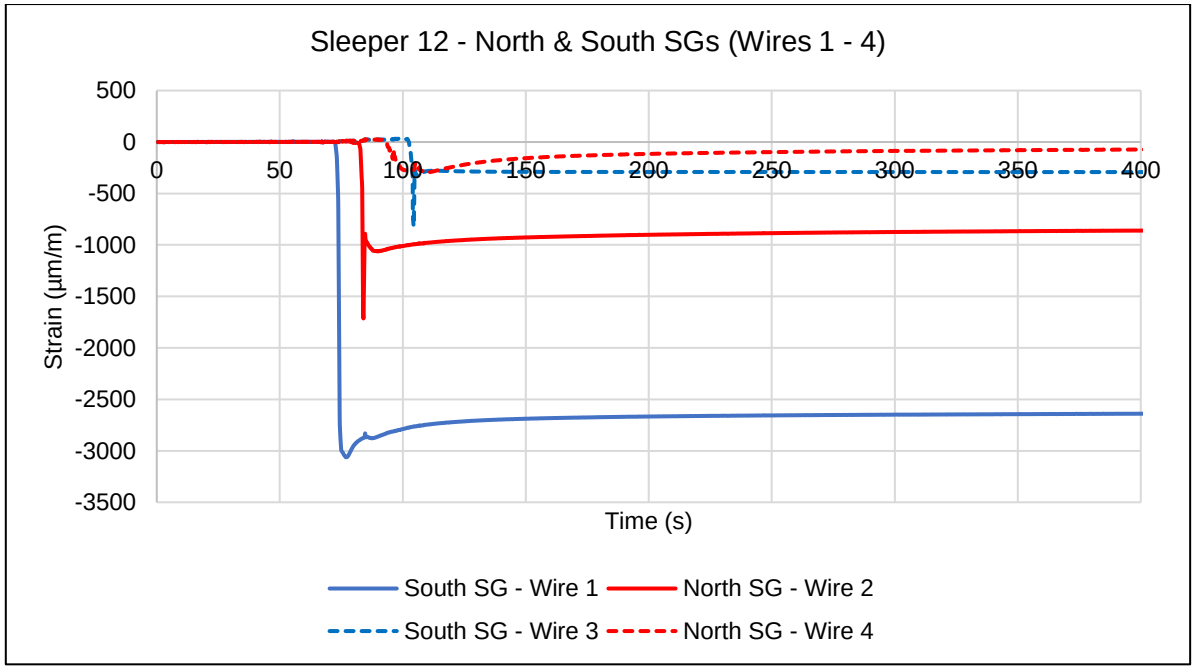

Figure 4.14: Sleeper number 12 - Stress distribution of all cut exposed four wires

4.4.3.3 The Cutting Method: Bolt Cutter vs Grinder

The initial plan involved using the bolt cutter to cut prestressed wires for all sleepers. However, during testing of Sleeper number 1 (S1), the bolt cutter approach was discontinued in favour of an angle grinder. The change was necessitated by the bolt cutter's limited accessibility to the instrumented wire, which was obstructed by concrete and adjacent exposed wires. Consequently, the wires were merely crimped instead of achieving a clean and complete cut, ultimately undermining the desired cutting effectiveness. Despite the partial cut of the prestressing wire in S1, interesting measurable strain readings were recorded, as demonstrated in Figure 4.15.

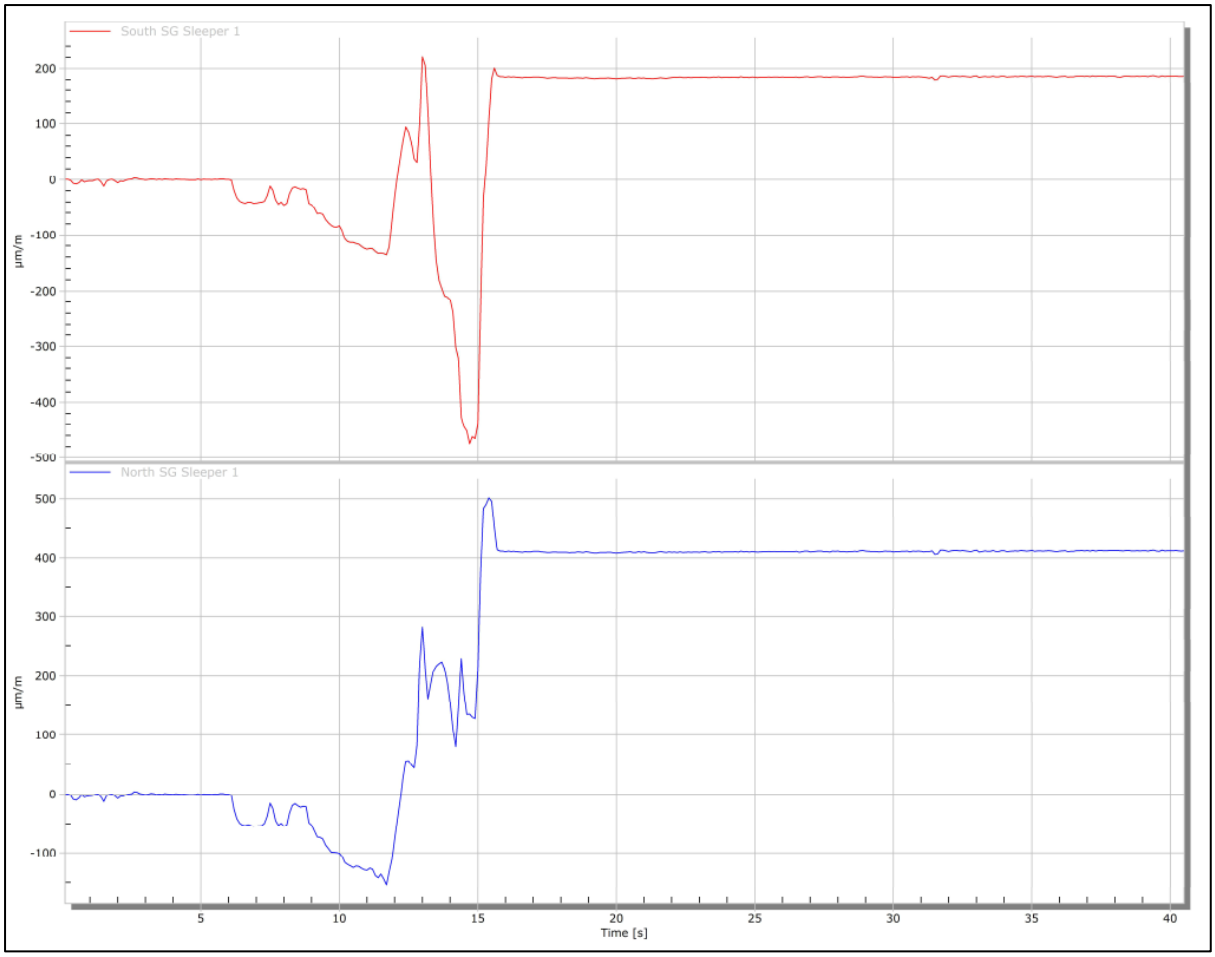

Figure 4.15: Sleeper Number 1 - Results of the bolt cutter method for south and north strain gauge analysis

The strain measurements obtained from the South and North strain gauges (SG), as illustrated in Figure 3.7, exhibited positive values at equilibrium, indicating the presence of tensile forces. Before reaching equilibrium, both SGs displayed a comparable oscillatory behaviour within the time (t) interval between 5 seconds (s) and 13 seconds. At t = 13 s, a simultaneous peak in the positive strain direction was recorded for both gauges. Between t = 13 s and t = 15 s, an unequal reduction in strain values was observed, characterised by a relatively minor decrease in the Northern SG and a more pronounced decrease in the Southern SG. The subsequent inflection at t = 15 s in the positive direction suggests the presence of residual tensile stress on both sides, which eventually converges to a stable equilibrium at their respective final positive strain values. The South SGs reached a steady state at 180 µm/m and the North SG reached 410 µm/m.

Noting the partial cut of the prestressing wire in Sleeper number 1 (S1), the cut was completed using the angle grinder. Before re-testing, the measured strain on S1 was zeroed, thus erasing the record of the bolt cutter method. It was noted that whilst the state of equilibrium could be

reached instantaneously with the use of the bolt cutter, a slight delay occurred with the grinder cutting method. The time lag could be attributed to the heat generated from dry cutting, which interfered with the normalised temperature between the strain gauge and the prestressed wire. Nonetheless, adequate measuring time was allowed with the grinder strategy for temperature normalcy and the steady state to be attained. Figure 4.16 depicts the results of the grinding method that was adopted to finish cutting off the wire on S1.

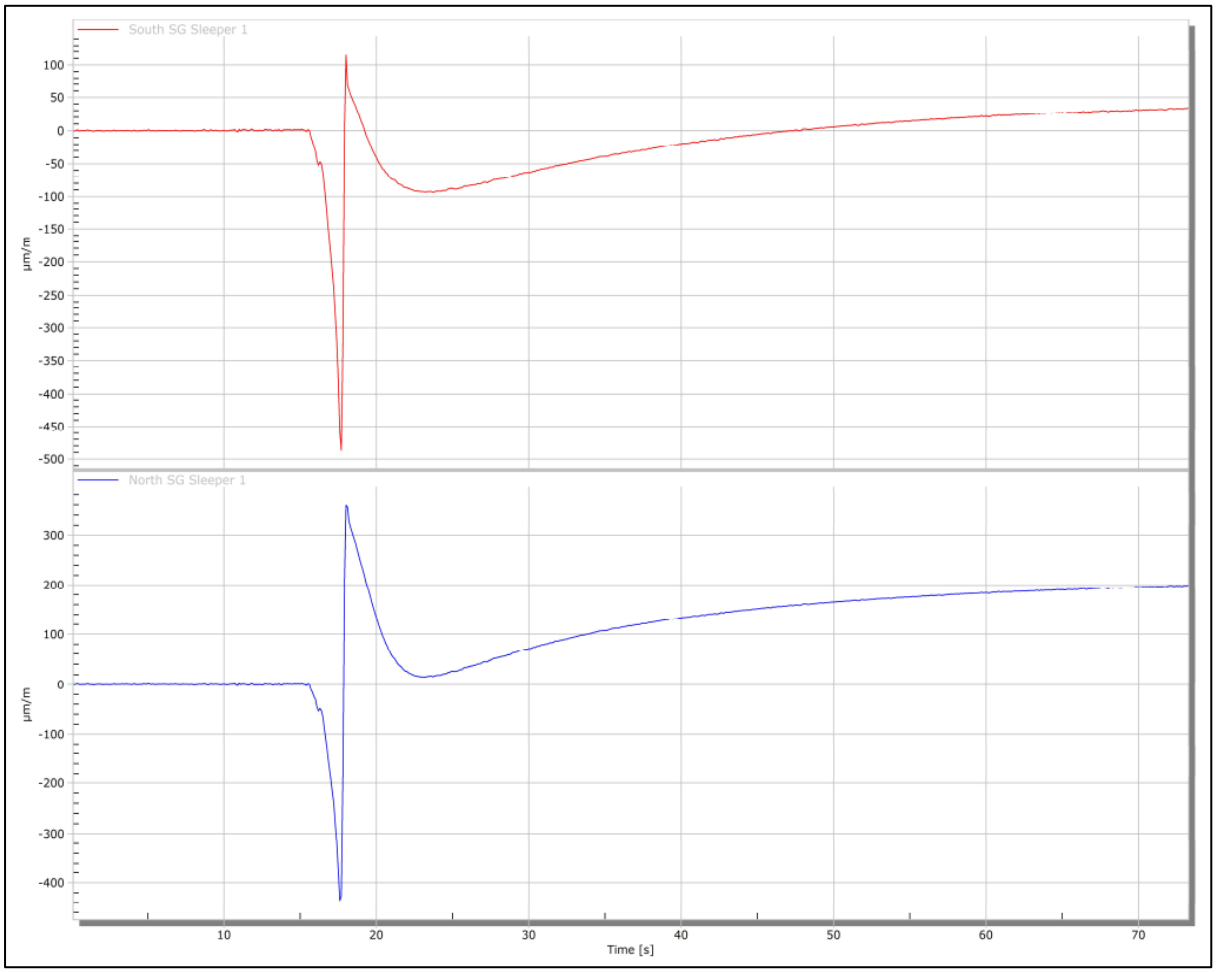

Figure 4.16: Sleeper number 1 - Results of the grinder method for south and north strain gauges

The equilibrium state observed after the application of the grinder cutting method yielded an unexpected outcome. Instead of achieving a negative strain equilibrium, which is typically indicative of axial contraction resulting from prestress release, the observed values exhibited a positive equilibrium strain, suggesting net expansion. This irregular response may be attributed to the thermal effects from the use of the grinder. This phenomenon underscores the sensitivity of the dynamic relaxation technique to the cutting method when assessing prestress loss in concrete sleepers.

4.5 Summary

The findings from the visual condition assessment, material strength tests, and experimental results for both the old and new concrete sleepers were detailed in Chapter 4. The old sleepers exhibited various concrete defects, including cracking, minor abrasion, breakages, and chipping. Notably, corrosion was also observed attributed to moisture ingress, owing to the presence of flexural and shear cracks. In contrast, the new sleepers demonstrated excellent condition. The material strength assessments indicated that the concrete compressive strength of the old sleepers ranged from 60 to 67 MPa, while the tensile strength of the prestressing steel was approximately 1907 MPa. Furthermore, the mean prestress loss was calculated to be 77% for the old sleepers and 65% for the new sleepers. The following chapter presents the proposed criteria for assessing aged sleepers intended for reuse.

5 PROPOSED ASSESSMENT CRITERIA

5.1 Introduction

This chapter discusses the factors to consider when developing a condition assessment framework for aged concrete sleepers that are nearing the end of their design life and require service life extension. The assessment focuses on solely on defects in the sleeper component.

5.2 Historical Service Performance

Previous performance records of concrete sleepers should be included in the evaluation criteria. Two factors to consider are the tonnage that passed over the sleeper during its service life (Choi et al., 2023)and gauge, which relates to the fatigue due to cumulative train traffic and the track geometry parameter influenced by the fastening system condition.

5.2.1 Traffic Tonnages

The traffic passing through a rail section can be used to estimate the fatigue level induced on the concrete sleepers. This can be done by correlating the number of axles traversing the sleeper with the fatigue load cycles determined for a particular sleeper in the laboratory. Assuming that the fatigue results from laboratory testing represent the fatigue strength limit, the cumulative axle loading passing over the sleeper is expected to be below the fatigue strength limit. The relationship between the number of axle loads passing over the concrete sleeper and the number of stress cycles is expressed by the following equation:

$$An \leq N$$

Where: An - cumulative number of axle loads passed that over the concrete sleeper

N - number of stress cycles until fatigue limit as determined in the laboratory

To establish the fatigue stress envelope curve for concrete sleepers, extensive research is needed to determine the fatigue life at different stress ranges. To model the real site conditions, the selected test stress levels should be reflective of the expected axle loads over the concrete sleeper.

5.2.2 Gauge Parameter

The gauge is a track geometry parameter that refers to the distance between the two rails, measured from the inner rail crown level. It is important to review the historical geometry condition data obtained through automated inspection, with a focus on the state or performance of the gauge parameter. If the assessment indicates that the gauge parameter is out of specification, additional effort should be made to investigate the cause of the defective condition. This can be achieved by examining the maintenance, inspection and repair records.

The evaluation should determine whether the faulty gauge was caused by flawed fastening systems in the concrete sleepers or excessive side metal wear on the rail.

To support this evaluation, an extensive visual assessment should be conducted around the shoulder cast-irons of the sleepers to identify defects that could compromise the structural integrity of the cast-irons. These defects may include structurally significant cracking, extreme chipping of concrete around the rail seat zone, as well as severe corrosion of the shoulder cast-irons.

5.2.3 General Maintenance Information

In addition to the factors explained in Sections 5.2.1 and 5.2.2, it is also important to consider the broader historical track maintenance data when assessing damages on concrete sleepers. This involves reviewing track maintenance, inspection and repair reports to understand the types of damage sustained by the sleepers over their useful life. It is important to recognise that railway tracks are complex systems where the proper functioning of one component depends on others. For example, poorly maintained ballast or prolonged track tamping can affect the stress distribution under the sleepers, leading to flexural cracking at the sleeper centre or rail seat area, which can result in partial or complete dysfunctionality.

The concrete sleeper supply strategy involves creating an excess of sleepers in anticipation of future demand. Consequently, the manufactured sleepers are not always immediately installed in tracks. This approach requires infrastructure managers to maintain accurate records of the dates sleepers are put into operation and the cumulative tonnages over their time in use. The concrete sleepers may remain new and unused for months to a few years due to logistical activities that take place between manufacturing and installation, including maintenance requests, procurement events, and transportation to further locations by rail. However, in cases where sleepers are urgently needed for emergency reasons, they may be acquired and installed immediately.

5.3 Safety

The safety performance of concrete sleepers is inextricably linked to their structural integrity, making it a crucial aspect to consider. Structural damage to the sleeper is of utmost significance as it can compromise its stability and safety.

5.3.1 Residual Prestress Force

Reviewed literature and findings from this study have demonstrated that railway sleepers lose prestress over time during their useful life. Therefore, it is important to determine the residual prestress of aged sleepers to ensure that the required bending moments at the rail seat area and mid-span section are adequate. The dynamic relaxation method described in Chapter 3

can be used as an onsite method to indicate the remaining prestress force of the sleeper wires. The reinforcement of concrete sleepers should comply with the design requirements of the BBG8755 specification (Transnet Freight Rail, 2021), as described in Section 4.4.1, which addresses initial and final stresses.

If sleepers exhibit significantly lower prestress force than required, further investigation into the condition of the prestressing wires should be undertaken in terms of corrosion profiling or checking for possible bond slippages. Non-compliant prestress values should be considered as unsuitable.

5.3.2 Exposed Prestressed Wires and Concrete Breakage

Concrete sleepers can be damaged during train operations or track maintenance, which may lead to the exposure of prestress wires. When inspecting concrete sleepers, it is important to note any exposed prestress wires and their condition. Sleepers with exposed wires should not be classified for second hand use. If still in use, they must be promptly removed. The location of the wire exposure on the sleeper does not matter as the risk of corrosion remains high regardless of position. Corrosion can lead to a reduction in the prestress capacity of concrete sleepers.

In addition to wire exposure, concrete sleepers should also be inspected for breakage, which may manifest as chipping or delamination. Sleepers with significant chipping or delamination should not be reused due to reduced concrete cover and distortion of the sleeper's geometry. In severe cases, the concrete may break entirely, exposing the prestress wires as shown in Figure 5.1.

Figure 5.1: Significant concrete chipping and spalling have occurred, resulting in the exposure of corroded prestressed wires.

5.3.3 Cast Iron Shoulder

It is essential to conduct a thorough assessment of the cast-iron shoulders as they play a critical role in the functioning of the entire fastening system. The cast-iron directly interacts with the Pandrol springs (e-clips) and partially with the gauge insulators, making it imperative to focus on the structural integrity of the component and its interface with other parts (refer to Figure 5.2 for a detailed depiction of the fastening unit parts).

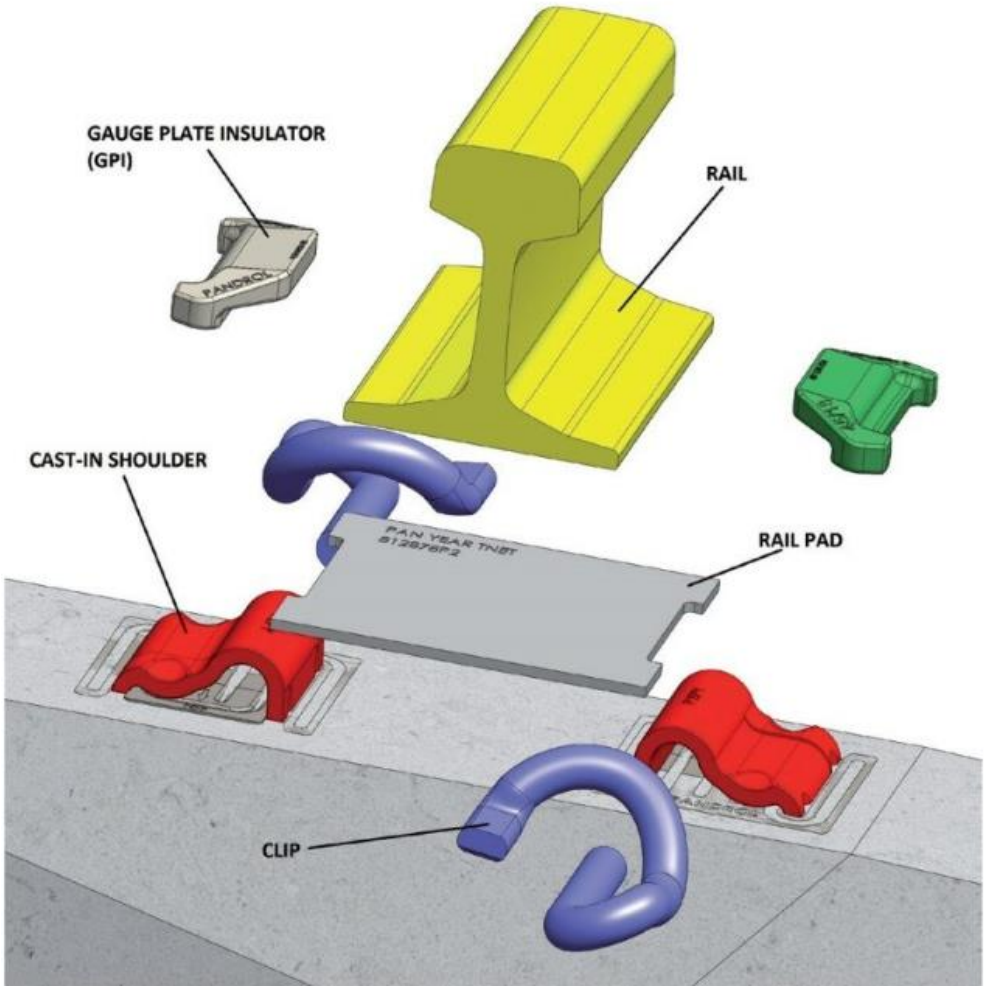

Figure 5.2: The railway track superstructure unit – Denoting the components of the fastening system (Fischer et al., 2015)

Visual evaluation should be carried out to check for signs of corrosion and distortions around the centre leg housing of the cast-iron. It is important to note that the centre leg housing facilitates the insertion of the e-clip, which is crucial for fixing the rail to the sleeper. Any deformities in the centre leg housing could lead to difficulties in fitting or forceful insertion of the e-clip. In addition to external examination, the inspection of the centre leg housing should extend to its internal surface where it comes into contact with the e-clip. Regular installation and removal of the e-clip for maintenance purposes can result in slight metal wear, potentially

enlarging the tunnel or housing and compromising the required tightness for friction. It should be noted that if the cast-iron shoulders are damaged, this could render the entire sleeper unusable, irrespective of the concrete condition. For further insights into potential issues, refer to Figure 5.3, which provides a typical example of a deformed cast-iron centre leg housing.

Figure 5.3: Deformed cast iron shoulder due to impact from a derailed locomotive wheel

5.4 Durability

When considering extending the service life of concrete sleepers, it is important to account for their durability. Common durability issues such as surface abrasion, cracking and corrosion must be carefully evaluated.

5.4.1 Surface Abrasion

The abrasion on concrete sleeper surfaces is usually most severe on the underside, moderate on the rail seat area, and minor on the sides. The extent and significance of abrasion damage can be determined by considering wear uniformity, depth, and exposure of the aggregates. It is important to bear in mind the two-fold effect of abrasion on concrete sleepers. Firstly, the loss of concrete mass reduces the concrete cover, which is required to protect the prestressing steel against corrosion attack. Secondly, the uniform or non-uniform reduction in the cross-sectional depth due to abrasive actions results in imperfect geometry, directly decreasing the service life of the sleeper under equivalent loading conditions of the concrete sleeper (Li, Kaewunruen & Ruilin, 2022).

Research has demonstrated a significant correlation between the mechanical properties of concrete and its resistance to surface deterioration. This is particularly relevant for concrete sleepers, where durability under conditions of repeated loading and environmental exposure is essential. Of particular interest is the inverse relationship between abrasion resistance and compressive strength, often quantified as abrasion depth. Empirical data consistently indicate that higher compressive strength correlates with a decreased depth of material removal due to abrasive action, thereby enhancing surface durability (Mindess, Young & Darwin, 2003; Neville, 2011).

It is imperative to meticulously examine the surface abrasion in the rail seat area, where a rail slope of 1:20 is mandated. The evaluation of the rail seat area should focus on determining the depth of abrasion and assessing whether the observed surface wear exhibits uniformity. A visual assessment can be conducted using the proposed functional condition scale rating (FCSR) presented in Table 5.1.

Table 5.1: Condition rating for surface abrasion

Functional	**Condition Remark**	
1: Good	Fairly new with very little signs of surface wear.	
2: Fair	Noticeable signs of light and uniform surface wear.	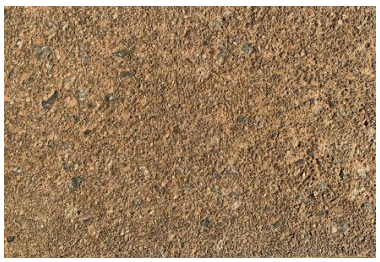
3: Poor	Surface severely worn and can no longer provide the intended service. Exposed aggregates. Irregular surface.	

5.4.2 Surface Cracking

The inspection of railway concrete sleepers is a critical process that should be carried out systematically to thoroughly assess both structural and non-structural cracks. The primary objective of this inspection is to identify, locate, measure the dimensions, and determine the significance of the cracks with respect to the structural integrity of the concrete sleepers. It is essential to focus on critical zones, such as the rail seat area, centre, and shoulder sections of the sleepers during the crack assessment. Cracks at the rail seat and centre parts of the sleepers are typically oriented vertically or diagonally and are usually caused by high flexural and shear stresses. On the other hand, the concrete sleeper shoulders often exhibit longitudinal cracks, possibly due to excessive prestressing.

It is important to note that cracks may appear in mapped patterns or random directions and can be localised or widespread. When the cause of the cracks is unclear, it is recommended to document the location and widths on a sketch or take a picture for review by experts. Further investigation, including laboratory testing for Alkali Aggregate Reactions (AAR), may be necessary. Although AAR has not been reported as a problem for railway concrete sleepers in South Africa since 1985, it should still be visually assessed. Extensive repair of affected sleepers and updates to manufacturing specifications have been made to address AAR (Grabe & Oberholster, 2000).

Other than crack type, size, more precisely width, is a key factor in ascertaining the severity of concrete cracks. Concrete cracks can vary in width from very thin hairline cracks to larger gaps. Hairline cracks typically do not exceed a width of 0.10 mm and can be observed upon closer inspection. Various standards specify permissible crack widths for concrete sleepers under service conditions. International standards, including UIC 713 (2004) and EN 13230-2 (2009), establish a threshold of 0.3 mm for the maximum allowable crack width during service. Crack widths greater than this limit raise concerns regarding the structural integrity and long-term durability of the sleeper. The severity of the reaction to cracking is influenced by its location, especially when it occurs in structurally critical areas such as the rail seat or prestressing tendon regions. In these cases, the recommended course of action may range from continuous monitoring to the complete removal and rejection of the affected sleeper. Furthermore, both UIC 713 (2004) and EN 13230-2 (2009) explicitly prohibit the acceptance of sleepers exhibiting crack widths exceeding 0.5 mm in the rail seat zone.

The general maintenance principle of concrete sleepers is that a crack constitutes damage or failure, necessitating replacement or monitoring of the sleeper. However, as Murray (2010) explained, if the sleeper can fulfil the function of holding the rail firmly in position, it does not necessarily indicate failure at the appearance of some cracks. Therefore, a three-tier class

crack evaluation criterion is established based on the severity of the crack width and its consequence to operation. The adopted crack width limits include 0.10 mm for a hairline crack and 0.3 mm for the accepted structural crack threshold. The narrowness of the 0.10 mm crack width hinders the accumulation of dust or debris, potentially slowing crack propagation (Murray, 2015). During the crack assessment, the sleeper may need to be cleaned with a regulated waterjet to expose cracks filled with dirt. Table 5.2 presents the crack evaluation criteria for concrete sleepers.

Table 5.2: Crack evaluation criterion for concrete sleepers

k Severity Class	Crack Width (mm)	Crack Classification	Sleeper Condition	Operational Action
Class I	0.10 ≤	Thin Crack	One or very few cracks are just visible to the naked eye.	Sleeper is fully usable in the track
Class II	0.10 > w ≤ 0.3	Medium Crack	Visible cracks. Minor spalling of concrete and little other damage, i.e., chipping.	Sleeper reusable in light axle load rail lines
Class III	> 0.3	Wide Crack	Wider cracks. Sleeper disintegration	Sleeper is not to be used

Crack widths can be determined using two main methods: direct observation and non-destructive methods. Direct observation involves manual measurement using a crack comparator, which is a small, hand-held microscope equipped with a scale or lens closest to the surface being viewed. Alternatively, a clear card with lines of specified width marked on it can also be used for measurement (see Figure 5.4). Conversely, non-destructive methods employ advanced techniques such as ultrasonic and image scanning to assess crack widths.

Figure 5.4: An illustration of the manual crack width gauge card

5.4.3 Corrosion of Prestressing Wires

Due to the low concrete cover for the sleeper wires at the extreme top and bottom surfaces of the sleeper wires, as well as the diverse exposure environments, it is crucial to prioritise conducting comprehensive durability tests related to the corrosion of prestressing wires. These tests should specifically focus on assessing chloride content, carbonation depth, and sulphate contamination.

For a thorough evaluation of chloride profiles, carbonation depth, and sulphate profiles, it is strongly recommended that meticulous laboratory testing be conducted using core samples extracted from the sleepers. The coring of sleepers and determination of chlorides and carbonation depth should strictly adhere to the acceptable standards. The carbonation depth should be considered critical, i.e., the carbon depth required to initiate corrosion, when it equals the concrete cover, according to BS EN 14630. For chloride content, a comparison with recommended maximum levels in codes of practice can be made, such as SANS 10100-2 (2014). Table 5.3 outlines the factors to consider when assessing the overall condition of old sleepers.

Table 5.3: Critical factors to evaluate in the assessment of aged concrete sleepers for potential reuse or disposal (Adapted from: Choi et al., 2023)

Description	Evaluation Items	Methodology	Inspection Coverage	Inspection Time	Aged Sleeper Acceptance Criterion Thresholds
Historical Service Performance	Accumulated Tonnage	Traffic Data	Entire Section/All Sleepers	After Removal	< Target load cycles (to be determined)
	Gauge	Maintenance Data (Track Geometry)	Entire Section/All Sleepers	Before Removal	< Max Standard Deviation Gauge limit (evidence attributing gauge defect to sleepers)
Strength (Safety)	Prestressed Loss	Dynamic Relaxation	4 Sections/All Sleepers	After Removal	= 0.60 f_s ; *if* ≤ 0.60 $f_{s,}$ conduct bending moment tests
	Exposed Prestressed Wires	Field Visual Inspection	Entire Section/All Sleepers	Before and After Removal	Prestressed Wires not Exposed
	Deformed cast-iron	Field Visual Inspection	Entire Section/All Sleepers	Before and After Removal	Non-deformed Cast Iron
	Surface Cracks and Breakage of Concrete	Visual Inspection	Entire Section/All Sleepers	Before and After Removal	- Minor Cracks - Minor chipping on edges, not longer than 200 mm or deeper than 15 mm
Durability	Rebound Hardness Test	Non-Destructive Testing	4 Sections/500m	Before and After Removal	≥ Specified 60MPa
	Depth of Carbonation or Chlorination	Laboratory Test	2 Sections/500m	After Removal	-Penetration < 2mm (10% of Concrete Cover)
	Surface Cracks	Visual Inspection	Entire Section/All Sleepers	Before and After Removal	< 0.3 mm
	Abrasion	Visual Inspection	Entire Section/All Sleepers	After Removal	Functional condition rating of 1 or 2 as per the proposed assessment criterion

Note: Table 5.3 is based on the study by Choi et al. (2023) and has been expanded to include two assessment components detailed in the last two columns: the time in which inspection must be conducted and the threshold criteria for each evaluation factor. The time aspect considers the period in the life of the sleeper when the condition assessment should take place, whether before or after removal. This is because assessing the condition of sleepers can be challenging due to their position both in and out of the track. For instance, it may not be possible to visually assess the full extent of sleeper condition while they are buried in the ballast. It is also easier to conduct typical destructive material testing, such as depth of carbonation and chlorination tests, on sleepers that have been removed from the track. Additionally, determination of prestress loss is recommended for strength requirement testing. While Choi et al. (2023) suggested some of the evaluation items as optional, this study considered all parameters mandatory for assessing old sleepers that are being considered for reuse.

5.5 Summary

A comprehensive evaluation of structural performance is required, particularly regarding prestress loss and the residual strength of the concrete, as well as the primary durability parameters such as carbonation, chloride penetration, and abrasion resistance. This assessment is essential to ascertain the recyclability of concrete sleepers beyond their initial lifespan. Additionally, data concerning the historical load history and environmental exposure of the sleepers is necessary for an accurate evaluation of their current condition and long-term performance. Collectively, these tests establish a solid basis for assessing the structural safety and integrity of reused sleepers in secondary applications.

6 CONCLUSIONS AND RECOMMENDATIONS

Concrete sleepers are one critical components of railway infrastructure, serving an essential role in the safety, stability, and operating efficiency of the rail system. Through a combination of visual examination, dynamic relaxation testing, and material strength assessments, the study has demonstrated significant structural degradation in the sleeper specimens tested in the study, beyond their 40-year design lifespan. The major findings highlight the necessity for a holistic assessment approach to determine the viability of reusing old sleepers, integrating both qualitative observation and quantitative measurements to inform lifecycle management decisions.

6.1 Visual Condition Assessment

Examination of P2 concrete sleepers, obtained from a single operational environment, revealed defect patterns originating from both service-related and environmental conditions. Concrete abrasion was noticeable at the rail seat area and more pronounced at the sleeper base, where sleeper-ballast interactions are concentrated. A hardened plastic-like paste material was identified on the rail seat surface and was termed the “sleeper-pad residue”. This residue, likely formed through a thermo-mechanical process during service, poses a potential risk by decreasing the frictional surface between pads and concrete, thereby altering load distribution dynamics.

Flexural cracks, originating at the sleeper base and propagating vertically (70–80 mm in height with widths of 0.1–1.0 mm), indicated that repeated overloading that exceeded the sleeper’s bending and shear capacity. While chipping along the surface of the edges was considered non-structural, its recurrence highlights the cumulative impact of maintenance practices and operational handling. Steel components, including prestressed wires and cast-iron shoulders, exhibited areas of sporadic corrosion. Localised severe corrosion was observed in prestressing wires, whereas uniform surface corrosion on cast-iron shoulders was deemed structurally insignificant.

6.2 Material Strengths

The concrete specimens achieved a mean compressive strength range of 60 to 67 MPa, surpassing the specified 60 MPa minimum This is indicative of exceptional resistance to crushing forces and long-term durability in high-load environments. Although the surface roughness was accounted for in the study by taking more rebound values to average out the variability, core samples should be taken to correlate the compressive strengths.

The prestressed steel wires demonstrated a mean ultimate tensile strength of 1907 MPa, aligning with high-tensile applications. These findings confirm the original design specifications, highlighting the inherent capacity of the materials to withstand the operational demands of railway systems.

6.3 Prestress Loss

The study demonstrated that railway concrete sleepers experience significant reductions in initial prestressing force over time, due to various factors. Through application of the dynamic relaxation method to measure strains in prestressing wires, average prestress losses were calculated at 77% for aged sleepers and 65% for new sleepers. Statistical analysis revealed considerable variability and dispersion within the dataset. The corresponding coefficients of variation (49.9% and 17.78%) underscore the significance of the testing methodology employed and uncontrolled variables, including pre-service handling, environmental exposure, operational conditions and the presence of defects such as cracking and corrosion.

The observed prestress loss in both new and aged sleepers is likely to the result of multiple contributing factors. Analysis of the relationship between measured strain and corresponding measured resistance revealed that values further from the tolerance range corresponded with lower strain measurements. Only 35% of the tested sleeper samples met the allowable strain gauge resistance specification of 120 ± 0.35% Ω. This finding suggests that environmental factors—particularly relevant given the in-situ testing conditions—and procedural aspects may have influenced the measurements.

The utilisation of grinding equipment for both concrete removal and prestressing wire cutting presented several methodological challenges, including asymmetrical strain gauge placement resulting from the 3 mm cutting disc thickness, localised thermal effects, and variations in anchorage conditions. These factors, either individually or collectively, may have substantially impacted the reproducibility of prestress measurements.

Despite the relatively recent manufacture of some concrete sleepers, they remain susceptible to long-term mechanisms such as concrete creep and steel relaxation, both of which contribute to prestress loss. The observed 65% prestress loss in unused sleepers was particularly unexpected, considering they had not been in service and exhibited no visible deterioration. It is noteworthy that they had only been subjected to self-weight loading whilst in storage at the maintenance yard.

Given the generally low prestressing forces obtained using the dynamic relaxation technique, the following measures are recommended to improve future testing reliability:

- Quality assurance can be achieved by ensuring that all strain gauges fall within the acceptable resistance range, thereby enhancing the comparability of the measured strain values.
- The installation process for strain gauges should be standardised to consider the impact of the cutting method employed, specifically regarding the resultant cutting gap, to minimise measurement variability caused by asymmetry. Moreover, in cases where the surface of steel wires exhibits irregularities, such as indentations, ribbing, or twisting, the designated areas for fixation should remain consistent.
- The effect of thermally invasive cutting techniques warrants further examination, or at minimum, reassessment due to potential thermal effects. Furthermore, the adoption of alternative cold cutting methods is strongly advised.
- During concrete removal, careful control must be exercised to avoid disrupting boundary conditions. Cracking or fragmentation of concrete and damage to prestressing wire at anchorage points should be prevented through implementation of less invasive concrete removal techniques.

6.4 Proposed Assessment Criteria

A structured evaluation framework was proposed to determine the potential reusability of aged concrete sleepers. This framework encompasses three primary parameters: historical service performance, safety, and durability. Each parameter is associated with a distinct performance measure, which may be either qualitative or quantitative, and includes well-defined compliance thresholds.

Given the sleepers' exposure to cyclic loading, susceptibility to fatigue damage and harsh environmental conditions, it is imperative that the historical performance of concrete sleeper is considered. This assessment class focuses on two critical factors: the cumulative traffic loads the sleepers have supported and the gauge parameter. The cyclic stress that a sleeper experiences from initial deployment until potential fatigue failure can be correlated with the tonnage of rail traffic it has supported. Similarly, the gauge parameter provides valuable insights regarding the condition and integrity of fastening components.

The second category for assessment of aged sleepers, safety, addresses both the sleepers' structural integrity and longevity. In this context, safety is associated with component strength and structural capacity. A structurally sound system that is free from defects can reliably perform its intended function. The third category pertains to the durability of the material. While durability is a key consideration in design, it should also form an essential component of the evaluation metrics for aged concrete sleepers considered for reuse. This

recommendation is based on findings from visual inspections, which revealed evidence of cracking, abrasion, and corrosion damage to both the concrete and prestressing wires.

6.5 Life Cycle Management of Concrete Sleepers

To ensure the effective management of concrete sleepers throughout their service life, it is advised that a detailed defect-descriptive approach be adopted in visual condition assessments, rather than relying solely on generic functional rating systems. The defect-descriptive methodology entails the identification of specific defects, precise documentation of their locations on the sleeper components, and the quantification of their severity.

Railway infrastructure managers are encouraged to integrate advanced inspection technologies, such as ultrasonic testing and imaging systems, into their assessment protocols. The utilisation of such methods facilitates the acquisition of accurate information pertaining to the condition of sleepers, thereby supporting precise and reliable evaluations. The adoption of these advanced inspection processes empowers railway authorities to make informed decisions concerning maintenance actions and replacement policies, with the aim of improving the safety and efficiency of railway operations. Furthermore, the application of the criteria outlined in Chapter 5 and summarised in Table 5.3 for the assessment of second-hand concrete sleepers is highly recommended. The classification of sleepers designated for reuse is more effectively carried out before their removal from service, thereby preserving essential historical information that may be lost after decommissioning and relocation.

6.6 Future Research

It is likely that the assumptions made in the study to simplify the analysis might have affected experimental measurements. Several interesting observations were noted, prompting further exploration. The following areas are proposed for future research:

- Study the effect strain gauge orientation on measured strain results in prestressing wires.
- Research prestress loss in concrete sleepers of different ages, both in and out of service, sampling sleepers with various physical defects.
- Investigate the effect of varying prestressing wire exposure lengths, instead of the fixed 150 mm length used in this study.
- Investigate the effect of bent wires on measured prestress forces.
- Study how different prestressing wire cutting methods (like bolt cutters and grinders) effect measured strains.
- Explore the effects of sleeper pad residue on frictional properties between new pad material and concrete surface at the rail seat.

- Establish the correlation between prestress loss and flexural bending moments at rail seat and centre section of the sleeper.
- Determine the target fatigue load at which the sleeper fails or loses its functionality

REFERENCES

Abdel-Jaber, H., & Glisic, B. (2019). Monitoring of prestressing forces in prestressed concrete structures—An overview. *Structural Control and Health Monitoring*, *26*(8), pp. 1–27. https://doi.org/10.1002/stc.2374

ACI Committee 209. (2008). *Prediction of creep, shrinkage, and temperature effects in concrete structures*. (ACI 209R-92, Reapproved 2008). Farmington Hills, MI: American Concrete Institute.

Alexander, M. G., Bentur, A., & Mindess, Sidney. (2017). *Durability of concrete: Design and Construction* (1st Edition). CRC Press.

Amhudo, R. L., Tavio, T., & Putu Raka, I. G. (2018). Comparison of compressive and tensile strengths of dry-cast concrete with Ordinary Portland and Portland Pozzolana Cements. *Civil Engineering Journal*, *4*(8), pp. 1760. https://doi.org/10.28991/cej-03091111

American Railway Engineering and Maintenance-of-Way Association (AREMA), (2006). *Manual for railway engineering*. (4th Edition). Lanham, MD: AREMA.

Bhatt, P. (2011). *Prestressed Concrete Design to Eurocodes* (1st Edition). CRC Press. https://doi.org/https://doi.org/10.1201/b12

British Standards Institution (BSI). (2012). *BS 5896:2012 – High tensile steel wire and strand for the prestressing of concrete*. London: British Standards Institution

Callister, W. D. (2007). *Materials science and engineering: An introduction* (7th Edition). Wiley.

Camille, C., Kahagala, D., Mirza, O., & Clarke, T. (2022). Full-scale static and single impact testing of prestressed concrete sleepers reinforced with macro synthetic fibres. *Transportation Engineering*, *7*, 100104. https://doi.org/10.1016/j.treng.2022.100104

Caro, L. A., Martí-Vargas, J. R., & Serna, P. (2013). Prestress losses evaluation in prestressed concrete prismatic specimens. *Engineering Structures*, *48*(3), pp. 704–715. https://doi.org/10.1016/j.engstruct.2012.11.038

Choi, J.-Y., Shin, T.-H., Kim, S.-H., & Chung, J.-S. (2023). Structural Integrity Assessment of Concrete Sleepers by Modal Test Technique. *Materials*, *16*(16), pp. 1–16. https://doi.org/10.3390/ ma16165614

Dunaiski, P. E. (1985). *The response of prestressed concrete sleepers to torsional loading.* The Civil Engineer in South Africa, 27(11), 575–581.

European Committee for Standardisation (CEN), 2009. CEN. (2009). *EN 13230-2: Railway applications – Track – Concrete sleepers and bearers – Part 2: Prestressed monoblock sleepers*.

Fischer, S., Eller, B., Koda, Z., & Nemeth, A. (2015). Railway Construction. Universitas-

Gyor Nonprofit Kft.

https://www.researchgate.net/publication/282246421_Railway_construction

Gebeyehu, L. B. (2017). Capacity analysis of railway concrete sleeper. *Civil and Environmental Research*, *9*(6), pp. 76–83.

Grabe, H., & Oberholster, R. (2000). Programme for the treatment and replacement of ASR affected concrete sleepers in the Sishen-Saldanha railway line. *Proceedings of the 11th International Conference on Alkali-Aggregate Reaction in Concrete*, *June 2000*. Québec City, Canada. Québec: Centre de recherche interuniversitaire sur le béton, pp.1059–1068

Gräbe, P. J., Mtshotana, B. F., Sebati, M. M., & Thünemann, E. Q. (2016). The effects of under-sleeper pads on sleeper-ballast interaction. *Journal of the South African Institution of Civil Engineering*, *58*(2), pp. 35–41. https://doi.org/10.17159/2309-8775/2016/v58n2a4

Gylltoft, K. (1987). *Concrete railway sleepers*.

Hay, J. G. (1962). Concrete sleepers and fastenings on the South African railways. *The Civil Engineer in South Africa*, *4*(6), pp. 112–118.

Hoffmann, K. (1989). An introduction to measurements using strain gages. Darmstadt: Hottinger Baldwin Messtechnik GmbH.

Hurst, M. K. (1988). Prestressed Concrete Design. In *Prestressed Concrete Design*. https://doi.org/10.4324/9780203476840

International Union of Railways (UIC). (2004). *UIC Code 713: Design of monoblock concrete sleepers. 2nd Edition.*

International Union of Railways (UIC). (2021). *Circular practices in the railway and ways forward - Reuse Project Final Report*. https://uic.org/IMG/pdf/reuse_project_final_report.pdf

Jhatial, A. (2022). Synergic influence of degrading mechanisms and induced loading by prestressing on the concrete: state of the art. *Environmental Science and Pollution Research*, *29*(3). pp. 3184–3198. https://doi.org/10.1007/s11356-021-17151-9

Kaewunruen, S., & Remennikov, A. M. (2006). Rotational capacity of a railway prestressed concrete sleeper under static hogging moment. *Construction and Professional Practices - Proceedings of the 10th East Asia-Pacific Conference on Structural Engineering and Construction, EASEC 2010*, *5*, pp. 399–404.

Khayal, O. (2019). Utilisation of dynamic relaxation method in solving ordinary and partial differential equations of rectangular engineering structures. *International Journal of Mechanical and Civil Engineering*, *02*(10), pp. 1–16.

Kraľovanec, J., Bahleda, F., Prokop, J., Moravčík, M., & Neslušan, M. (2021). Verification of actual prestressing in existing pre-tensioned members. *Applied Sciences (Switzerland)*, *11*(13), p 5971. https://doi.org/10.3390/app11135971

Kralovanec, J., Moravcík, M., & Jost, J. (2021). Analysis of prestressing in precast prestressed concrete beams. *Civil and Environmental Engineering*, *17*(1), 184–191. https://doi.org/10.2478/cee-2021-0019

Li, D., Kaewunruen, S., Robery, P., & Remennikov, A. M. (2020). Parametric studies into creep and shrinkage characteristics in railway prestressed concrete sleepers. *Frontiers in Built Environment*, *6*, pp. 1–10. https://doi.org/10.3389/fbuil.2020.00130

Li, D., Kaewunruen, S., & Ruilin, Y. (2022). Remaining fatigue life predictions of railway prestressed concrete sleepers considering time-dependent surface abrasion. *Sustainability*, *14*(18), pp. 1–22. https://doi.org/10.3390/ su141811237

Lombard, P. C., & Wildenboer, L. A. (1981). Concrete sleepers and fastenings on the South African railways. *The Civil Engineer in South Africa*, *23*(2), pp. 33–45.

Lutch, R. H., Harris, D. K., & Ahlborn, T. M. (2009). Prestressed concrete ties in North America. *AREMA Annual Conference*, *906*, pp. 1–39.

Markovski, G., Ćećez, M., University, C., Bijedić, D., Mostar, in, & Šahinagić-Isović, M. (2012). Shrinkage strain of concrete-causes and types. *Građevinar*, *64*(9), pp. 727–734. https://doi.org/https://doi.org/10.14256/JCE.719.2012

Mehta, P. K., & Monteiro, P. J. M. (2006). *Creep. in: Concrete: Microstructure, Properties, and Materials.* (3rd Edition). McGraw-Hill.

Mindess, S., Young. J. F. and Darwin. D. (2003). *Concrete* (2nd Edition.). Prentice Hall.

Muchinsky, P., & Stevens, N. (2012). Rational design method for prestressed concrete sleepers. *Proceedings of the Institution of Mechanical Engineers, Part F: Journal of Rail and Rapid Transit*, *226*(2), pp. 155–173. https://doi.org/https://doi.org/10.1177/0954409711418754

Murray, M. (2015). Heavy haul sleeper design - a rational cost-saving method. In S. In Kalay & S. Cathcart (Eds.), *Proceedings of the 11th International Heavy Haul Association Conference*, pp. 1160–1169).

Murray, M. H. (2010). Renewing concrete sleepers – How long can they last? *Conference on Railway Engineering*, pp. 197–202.

Mutungi, W. N. (2023). *Creep in concrete. In: H.M. Saleh, A.I. Hassan & M. Mhadhbi, eds. Reinforced Concrete Structures – Innovations in Materials, Design and Analysis,* pp. 1–15. London: IntechOpen.

Nawy, E. G. (2009). *Reinforced concrete: a fundamental approach*, p. 915. https://books.google.com/books?id=fHCDqh_7-oEC&pgis=1

Neville, A. M. (2011). *Properties of concrete* (5th Edition). Pearson Education Limited.

Ngamkhanong, C., & Kaewunruen, S. (2018). Influence of prestress losses on the dynamic over static capacity ratios of railway concrete sleepers. *International Conference on Interdisciplinary Approaches.*, pp. 925–930. https://doi.org/10.5281/zenodo.1405563

Otter, J., Cassell, A., & Hobbs, R. (1966). Dynamic relaxation. *Proc. Instn Civ. Engrs*, *35.* P 6986.

Papadrakakis, M. (1978). Gradient and relaxation nonlinear techniques for the analysis of cable supported structures. *Unpublished Doctoral Thesis, City, University of London*. http://openaccess.city.ac.uk/21924/ Link to published version.

Remennikov, A., & Kaewunruen, S. (2006). Experimental investigation on dynamic railway sleeper/ballast interaction. *Experimental Mechanics*, *46*(1), pp. 57–66. https://doi.org/10.1007/s11340-006-5868-z

Remennikov, A., & Kaewunruen, S. (2015). Determination of prestressing force in railway concrete sleepers using dynamic relaxation technique. *Journal of Performance of Constructed Facilities*, *29*(5), pp. 1–7. https://doi.org/10.1061/(ASCE)CF.1943-5509.0000634

Republic of South Africa (2023). Roadmap for the Freight Logistics System in South Africa. *Pretoria, South Africa: Republic of South Africa*

Scott, J. D. (2019). Experimental evaluation of remaining prestress force and centre negative bending-moment in railroad ties removed from track after 25 years of service*. PhD Thesis*. Kansas State University, Manhattan, Kansas, United States.

Standards Australia (2012). *AS 1085.14–2012: Railway track material – Part 14: Prestressed concrete sleepers*. Sydney: Standards Australia.

South African Bureau of Standards (SABS), (2007). *SANS 2001-CC1:2007 – Construction works – Part CC1: Concrete works (structural)*. Pretoria: SABS.

South African Bureau of Standards (SABS), (2014). *SANS 10100-2:2014 – The structural use of concrete – Part 2: Materials and execution of work*. Pretoria: SABS.

Suresh, S. (1998). *Fatigue of Materials*. Cambridge University Press.

Taherinezhad, J., Sofi, M., Mendis, P. A., & Ngo, T. (2013). A review of behaviour of Prestressed concrete sleepers. *Electronic Journal of Structural Engineering*, *13*(1), pp. 1–16.

Transnet Freight Rail. (2021). *BBG8755: Specification for monolithic prestressed concrete sleepers used on 1065 mm gauge railway track*. Track Technology Management.

Wallah, S. E. (2010). Creep Behaviour of Fly ash-based geopolymer concrete. *Civil Engineering Dimension*, *12*(2), pp. 73–78. https://doi.org/10.9744/ced.12.2.73-78

Wildenboer, L. A., Erasmus, P. J., Stephan, H. B., & Rauch, H. P. (1989). Railway track structure: Recent developments and breakthroughs. *The Civil Engineer in South Africa - Railways and Harbour Division*, *January*.

Zakeri, J. A., & Sadeghi, J. (2007). Field investigation on load distribution and deflections of railway track sleepers. *Journal of Mechanical Science and Technology*, *21*(12), pp. 1948–1956. https://doi.org/10.1007/bf03177452

Zakeri, J., & Rezvani, F. H. (2012). Failures of railway concrete sleepers during service life. *International Journal of Construction Engineering and Management*, *1*(1), pp. 1–5. https://doi.org/10.5923/j.ijcem.20120101.01

APPENDICES

APPENDIX A: ETHICS CLEARANCE

APPENDIX B: RESIDUAL PRESTRESS

Sleeper Number	SG Mount Position	Measured Resistance (Ω)	Measured Strain (μm/m)	E_{steel} (GP_a)	$\delta_{measured}$ (MP_a)	$\delta_{theoretical}$ (MP_a)	Prestress Loss at t = 40 years	Remarks
1	South	120.9	215	200	-83	1 140	107%	Started the test with a bolt cutter, which could not fully cut the wire, then a grinder was used. The strain results obtained from the bolt cutter and grinder cutting methods were added to give the ultimate strain for the complete cut wire. A delay in reaching the equilibrium position was observed with the use of the grinding method. The wire on the south side was slightly cut at the edge during the concrete removal process.
	North	120.8	610	200	0	1 140	100%	
2	South	120.6	-1 185	200	221	1 140	81%	
	North	120.7	-1 026	200	0	1 140	100%	
3	South	120.6	-763	200	102	1 140	91%	
	North	120.9	-255	200	0	1 140	100%	
4	South	120.5	-1 158	200	172	1 140	85%	
	North	120.6	-559	200	0	1 140	100%	
5	South	120.6	Not Recorded	200	Not Recorded	Not Recorded	Not Recorded	Mistakenly cut prior to testing
	North	120.2	Not Recorded	200				
6	South	119.6	-1 543	200	309	1 140	73%	
7	South	120.3	-1 267	200	253	1 140	78%	
8	South	120.3	-586	200	117	1 140	90%	
9	South	119.7	-1 047	200	209	1 140	82%	
10	South	120.1	-1 776	200	355	1 140	69%	
11	North	121.1	-385	200	77	1 140	93%	
12.1	South	120.2	-2 640	200	528	1 140	54%	All four exposed wires were connected/one after the other
12.2	North	120.6	-861	200	172	1 140	85%	
12.3	South	120.6	-292	200	58	1 140	95%	
12.4	North	120.2	-73	200	15	1 140	99%	

Sleeper Number	SG Mount Position	Measured Resistance (Ω)	Strain (μm/m)	E_{steel} (GP_a)	$\delta_{measured}$ (MP_a)	$\delta_{theoretical}$ (MP_a)	Prestress Loss at t = 17 years	Remarks
13	South	120.4	-2 034	200	407	1 020	60%	
14	South	121.1	-1 434	200	287	1 020	72%	Affected anchorage/Partially cut wire
15	South	120.7	-1 925	200	385	1 020	62%	

The mean prestress loss for aged concrete sleepers was calculated using data from sleepers numbered 2 to 12. For sleeper number 12, the focus was exclusively on the first wire. Sleepers numbered 1 and 5 were omitted from the analysis. Additionally, the values from the North affixed strain gauges (SGs) were excluded, and only the highest values from the South affixed SGs were utilised. This decision was based on the premise that the results from the two wires should have been consistent, as evidenced by the findings from Sleeper number 2 and corroborated by previous research. The results of the statistical analyses conducted are presented below.

Aged Concrete Sleepers										
Strain (με)	**Mean (με)**	**Median (με)**	**Standard Deviation (με)**	**Range (με)**	**Minimum (με)**	**Maximum (με)**	**1st Quartile (Q1) - (με)**	**3rd Quartile (Q3) - (με)**	**Interquartile Range - (με)**	**Coefficient of Variation (%)**
-1185	-1273.0	-1171.5	635.5	2255	-2640	-385	-1543	-586	957	49.9
-763										
-1158										
-1543										
-1267										
-586										
-1047										
-1776										
-385										
-2640										

APPENDIX C: CONDITION ASSESSMENT FINDINGS

Visual assessment of all concrete sleeper samples was conducted, and the findings are presented below. The sleeper member was sectioned into areas of interest aligned to the mode of failure associated with the respective areas of interest. The sleepers exhibited a common deterioration mechanism around the rail seat area, where sleeper pad residuals and vertical cracking initiating from the bases of the sleepers, noticeable up to a height of between 100 – 120mm, were observed.

Member Section	Condition	S_1	S_2	S_3	S_4	S_5	S_6	S_7	S_8	S_9	S_10	S_11	S_12
Cast Iron	Rust/Corrosion	√	√	√	√	√	√	√	√	√	√	√	√
	Deformation	x	x	x	x	x	x	x	x	x	x	x	x
Rail Seat Area	Abrasion	√	√	√	√	√	√	√	x	x	x	x	x
	Sleeper Pad Residual	√	√	√	√	√	√	√	√	√	√	√	√
	Cracking	√	√	√	√	√	√	√	√	√	√	√	√
Centre Area	Cracking	x	x	x	x	x	x	x	x	x	x	x	x
Shoulder Area	Edge Chipping	√	√	√	√	√	√	√	√	√	√	√	√
	Longitudinal Cracking	x	x	x	x	x	x	x	x	x	x	x	x
Sleeper Base (All Round)	Cracking	√	√	√	√	√	√	√	√	√	√	√	√
	Abrasion underneath	√	√	√	√	√	√	√	√	√	√	√	√
	Edge Chipping	√	√	√	√	√	√	√	√	√	√	√	√
Sleeper Top (All Round)	Edge Chipping	√	√	√	√	√	√	√	√	√	√	√	√

APPENDIX D: MATERIAL PROPERTIES

Determination of the Mean Rebound Value Resilience

Rebound Test Location	Sleeper Section	Sleeper 1	Sleeper 2	Sleeper 3	Mean Rebound (Resilience) Value per Test Zone, Nα	Median Rebound (Resilience)	Deviation from Mean	Squared Deviation	Variance	Standard Deviation	Lower Bound (Resilience)	Upper Bound (Resilience)	Outliers	Coefficient Variation (CV)
Shoulder Section (Left)	$Upper_1$	46.00	46.00	51.00	50.75	50.75	4.75	22.56	16.31	4.04	42.67	58.83	0	7.96%
	$Center_1$	56.00	50.00	50.50			-5.25	27.56						
	$Lower_1$	51.50	49.00	51.50			-0.75	0.56						
	$Upper_2$	48.00	48.50	50.00			2.75	7.56						
	$Center_2$	57.00	52.00	52.00			-6.25	39.06						
	$Lower_2$	50.00	51.00	53.50			0.75	0.56						
Rail Seat Section (Left)	$Upper_1$	48.00	53.00	56.20	52.59	52.75	4.59	21.06	7.62	2.76	47.23	58.27	0	5.25%
	$Center_1$	52.50	56.00	49.90			0.09	0.01						
	$Lower_1$	50.00	55.00	53.00			2.59	6.70						
	$Upper_2$	49.00	52.50	56.00			3.59	12.88						
	$Center_2$	51.00	54.50	54.00			1.59	2.52						
	$Lower_2$	51.00	52.00	53.00			1.59	2.52						
Intermediate Section	$Upper_1$	51.00	57.00	52.00	53.48	53.50	2.48	6.16	10.07	3.17	47.15	59.85	0	5.93%
	$Center_1$	53.00	55.00	56.00			0.48	0.23						
	$Lower_1$	50.00	54.00	53.00			3.48	12.12						
	$Upper_2$	55.00	53.00	51.00			-1.52	2.31						
	$Center_2$	57.00	53.50	55.00			-3.52	12.38						
	$Lower_2$	54.50	52.00	54.00			-1.02	1.04						
	$Upper_3$	49.00	55.00	53.00			4.48	20.08						
	$Center_3$	52.00	53.50	56.00			1.48	2.19						
	$Lower_3$	51.50	55.00	53.00			1.98	3.93						
	$Center_1$	49.00	53.00	56.00			1.75	3.06						
	$Lower_1$	46.00	56.50	55.00			4.75	22.56						
	$Upper_2$	49.00	58.00	54.00			1.75	3.06						
	$Center_2$	50.00	52.00	57.00			0.75	0.56						

	$Lower_2$	48.00	55.00	55.00			2.75	7.56						

Rebound Test Location	Sleeper Section	Sleeper 1	Sleeper 2	Sleeper 3	Mean Rebound (Resilience) Value per Test Zone, Nα	Median Rebound (Resilience)	Deviation from Mean	Squared Deviation	Variance	Standard Deviation	Lower Bound (Resilience)	Upper Bound (Resilience)	Outliers	Coefficient Variation (CV)
Rail Seat Section (Right)	$Upper_1$	55.00	53.80	51.50	52.24	52.50	-4.25	18.06	4.87	2.21	48.09	56.91	46	4.22%
	$Center_1$	52.00	54.00	53.00			-1.25	1.56						
	$Lower_1$	53.00	53.00	50.00			-2.25	5.06						
	$Upper_2$	51.70	50.00	50.00			-0.95	0.90						
	$Center_2$	52.50	46.00	53.50			-1.75	3.06						
	$Lower_2$	50.00	53.00	52.00			0.75	0.56						
Shoulder Section (Right)	$Upper_1$	50.00	61.50	55.50	54.38	55.00	0.75	0.56	6.23	2.50	50.01	59.99	46.0; 48; 49; 49; 61.5	4.59%
	$Center_1$	49.00	53.00	56.00			1.75	3.06						
	$Lower_1$	46.00	56.50	55.00			4.75	22.56						
	$Upper_2$	49.00	58.00	54.00			1.75	3.06						
	$Center_2$	50.00	52.00	57.00			0.75	0.56						
	$Lower_2$	48.00	55.00	55.00			2.75	7.56						

Conversion table of concrete strength value of test zone

Rebound Value	MPa								
	Impact Direction					Horizontal	Impact Direction		
	-90	90	60	45	30	0	-30	-45	-60
20	14.9	10.3	10.3	10.3	10.3	10.3	13.1	13.7	14.3
21	16.2	10.3	10.3	10.3	10.3	11.4	14.3	14.9	15.5
22	17.4	10.3	10.3	10.3	10.3	12.5	15.4	16.0	16.7
23	18.8	10.3	10.3	10.3	10.4	13.7	16.7	17.4	18.0
24	20.0	10.3	10.3	10.5	11.6	14.9	17.9	18.6	19.3
25	21.5	10.3	10.8	11.6	12.7	16.2	19.2	20.0	20.8
26	22.8	11.0	12.0	12.8	14.0	17.5	20.6	21.4	22.1
27	24.5	11.9	13.3	14.0	15.3	18.9	22.1	22.8	23.6
28	25.9	13.4	14.6	15.4	16.7	20.3	23.5	24.3	25.0
29	27.6	14.8	16.0	16.7	18.0	21.8	25.0	25.9	26.7
30	29.1	16.2	17.5	18.2	19.6	23.3	26.5	27.4	28.2
31	30.9	17.6	18.9	19.6	21.0	24.9	28.2	29.1	30.0
32	32.5	19.1	20.8	21.2	22.7	26.5	29.8	30.7	31.5
33	34.4	20.8	22.0	22.7	24.3	28.2	31.6	32.5	33.5
34	36.1	22.4	23.6	24.5	26.0	30.0	33.3	34.2	35.2
35	38.2	24.1	25.2	26.0	27.8	31.8	35.2	36.1	37.1
36	39.9	25.9	27.1	27.9	29.5	33.6	36.9	37.9	38.9
37	42.0	27.8	28.8	29.6	31.4	35.5	38.9	39.9	41.0
38	43.9	29.6	30.7	31.6	33.5	37.5	40.7	41.8	42.8
39	46.1	31.6	32.5	33.5	35.4	39.5	42.8	43.9	45.0
40	48.1	33.6	34.6	35.5	37.5	41.6	44.8	45.9	47.0
41	50.4	35.5	36.5	37.5	39.5	43.7	47.0	48.1	49.2
42	52.5	37.7	38.7	39.7	41.8	45.9	49.0	50.2	51.3
43	52.5	39.7	40.7	41.8	43.9	48.1	51.3	52.5	53.6
44	57.0	42.0	43.0	44.1	46.3	50.4	53.4	54.6	55.8
45	59.5	44.1	45.2	46.3	48.5	52.7	55.8	57.0	58.2
46	59.5	46.5	47.6	48.7	51.0	55.0	58.0	59.2	60.0
47	59.5	48.7	49.9	51.0	53.4	57.5	58.0	59.2	60.0
48	59.5	51.3	52.5	53.6	56.0	60.0	58.0	59.2	60.0
49	59.5	53.6	54.8	56.0	58.5	60.0	58.0	59.2	60.0
50	59.5	56.8	57.5	58.8	60.0	60.0	58.0	59.2	60.0

Stress Conversion Best Fit Equation

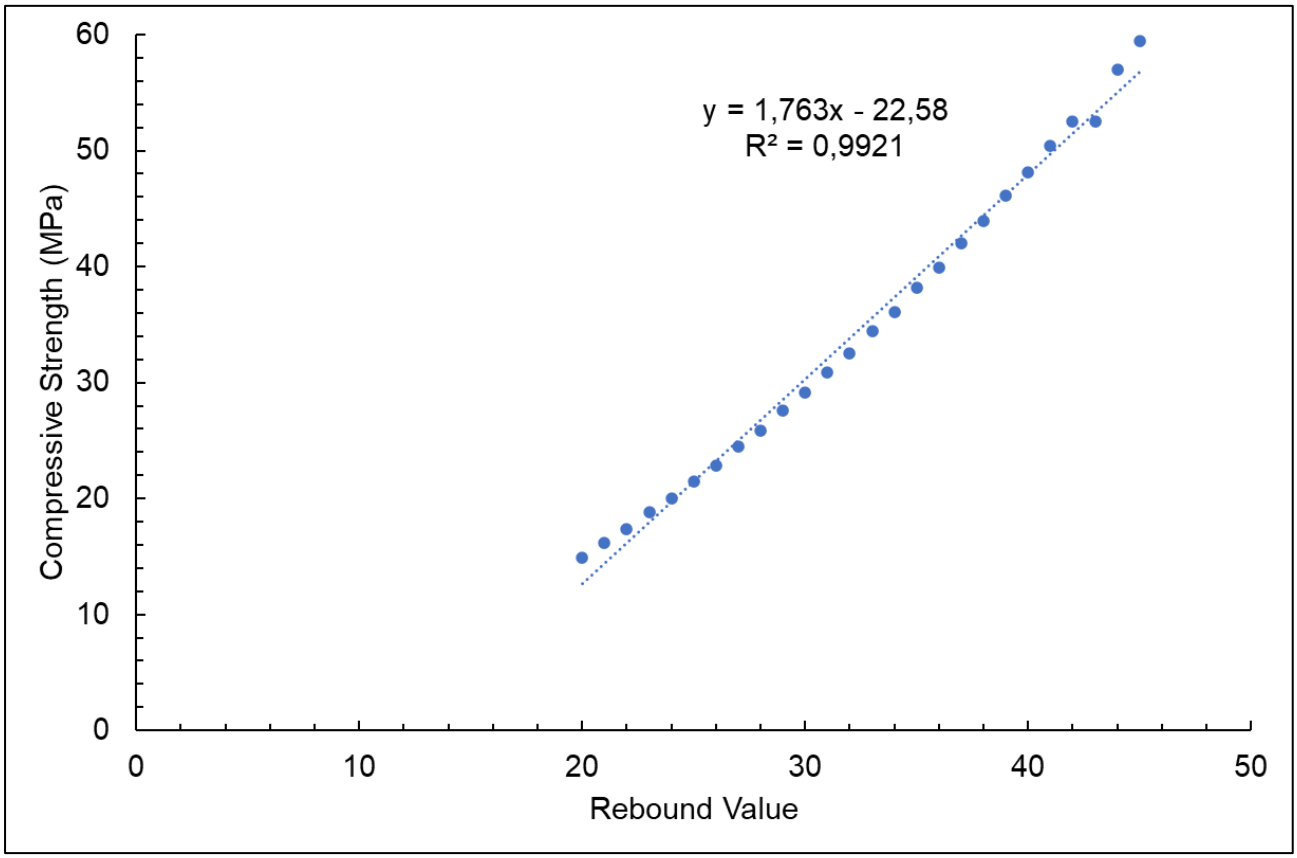

Estimated Concrete Sleeper Compressive Strength

Rebound Test Location		Sleeper 1	Sleeper 2	Sleeper 3	Mean Rebound (Resillience) Value per Test Zone, Nα	Correction Value	N = Nα + Correction Value	Stress Conversion (MPa): Eqn. of Best Fit Line
Shoulder Section (Left)	$Upper_1$	46.00	46.00	51.00	50.75	-3.50	47.25	60.72
	$Center_1$	56.00	50.00	50.50				
	$Lower_1$	51.50	49.00	51.50				
	$Upper_2$	48.00	48.50	50.00				
	$Center_2$	57.00	52.00	52.00				
	$Lower_2$	50.00	51.00	53.50				
Rail Seat Section (Left)	$Upper_1$	48.00	53.00	56.20	52.59	-3.50	49.09	63.96
	$Center_1$	52.50	56.00	49.90				
	$Lower_1$	50.00	55.00	53.00				
	$Upper_2$	49.00	52.50	56.00				
	$Center_2$	51.00	54.50	54.00				
	$Lower_2$	51.00	52.00	53.00				
Intermediate Section	$Upper_1$	51.00	57.00	52.00	53.48	-3.50	49.98	65.54
	$Center_1$	53.00	55.00	56.00				
	$Lower_1$	50.00	54.00	53.00				
	$Upper_2$	55.00	53.00	51.00				
	$Center_2$	57.00	53.50	55.00				
	$Lower_2$	54.50	52.00	54.00				
	$Upper_3$	49.00	55.00	53.00				
	$Center_3$	52.00	53.50	56.00				
	$Lower_3$	51.50	55.00	53.00				
Rail Seat Section (Right)	$Upper_1$	55.00	53.80	51.50	52.24	-3.50	48.74	63.34
	$Center_1$	52.00	54.00	53.00				
	$Lower_1$	53.00	53.00	50.00				
	$Upper_2$	51.70	50.00	50.00				
	$Center_2$	52.50	46.00	53.50				
	$Lower_2$	50.00	53.00	52.00				
Shoulder Section (Right)	$Upper_1$	50.00	61.50	55.50	54.38	-3.50	50.88	67.13
	$Center_1$	49.00	53.00	56.00				
	$Lower_1$	46.00	56.50	55.00				
	$Upper_2$	49.00	58.00	54.00				
	$Center_2$	50.00	52.00	57.00				
	$Lower_2$	48.00	55.00	55.00				

D3: STEEL TENSILE STRENGTH TESTING RESULTS

TEST: TENSILE	SPECIFICATION: * BS EN 10002-1:2001							METHOD: VML-QTY-MTD-0001		
Sample	Dimension (mm)	Area (mm^2)	Gauge (mm)	Yield Load (kN)	Max Load (kN)	Yield Stress (MPa)	UTS (MPa)	Elongation (%)	ROA (%)	Fracture Position
Specification and customer requirements:						NMS	NMS	NMS		
Test Direction										
Wire Sample - 1	3.60	10.18	20	13.60	19.36	1337	1902	18	45	-
Wire Sample - 2	3.60	10.18	20	12.89	19.65	1267	1931	20	44	-
Wire Sample - 3	3.60	10.18	20	14.42	19.21	1417	1887	17	42	-

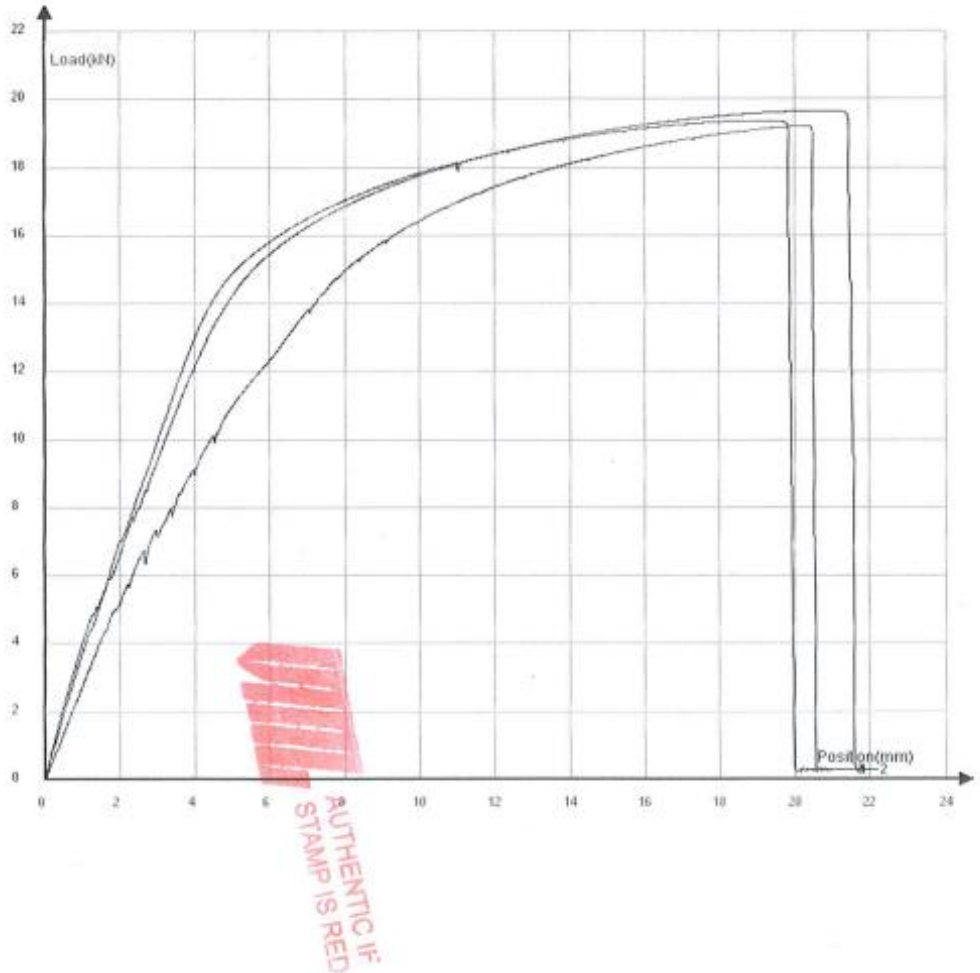

APPENDIX E: ANNUAL SLEEPER INSPECTION FORM

RAILWAY INFRASTRUCTURE ASSET CONDITION ASSESSMENT DOCUMENT

			Track Discipline	**BBC 8175 Revision 2** MICA Reference: 16: Sleepers
Functional Location	Station From	Station To		Depot
Asset Description		Line		Line Code
Inspected by	Grade	Employee No.	Signature	Date

ANNUAL SLEEPER CONDITION ASSESSMENT FORM

km From*	km To*	Visual Condition Assessment: Score 1 - 5	Year Installed	Additional Comments

* Assessed sections to be no longer than 1 km in length

Visual Condition Assessment: Score	Description of Asset or Component Condition
1: New/ Excellent	Relatively new with limited signs of wear or use and requires only routine preventive maintenance
2: Good	Numerous signs of wear or use but requires only routine preventive maintenance
3: Fair	Shows considerable deterioration and requires regular rehabilitation and corrective preventive maintenance
4: Poor	Approaching the end of its usefull service life and requires replacement in the near future
5: Unserviceable	Can no longer provide the intended service, is beyond rehabilitation and requires immediate replacement

APPENDIX F: EXPERIMENTAL RESULTS

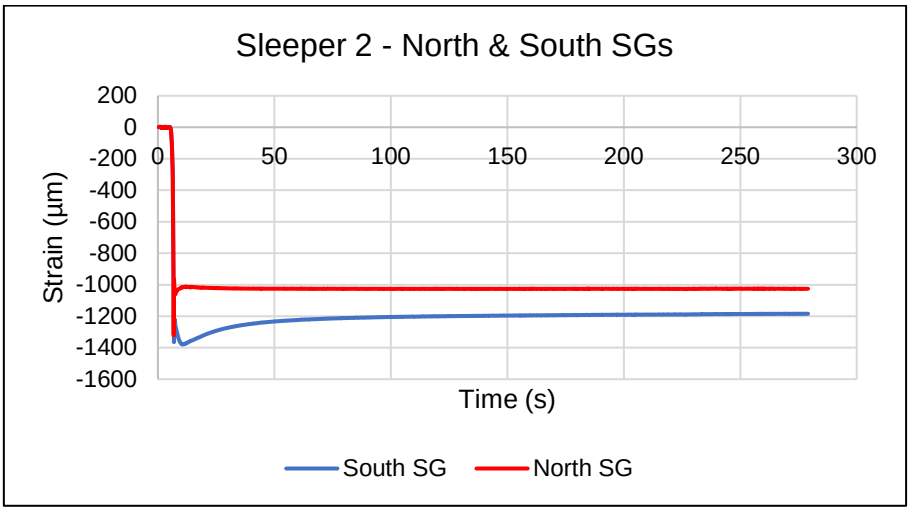

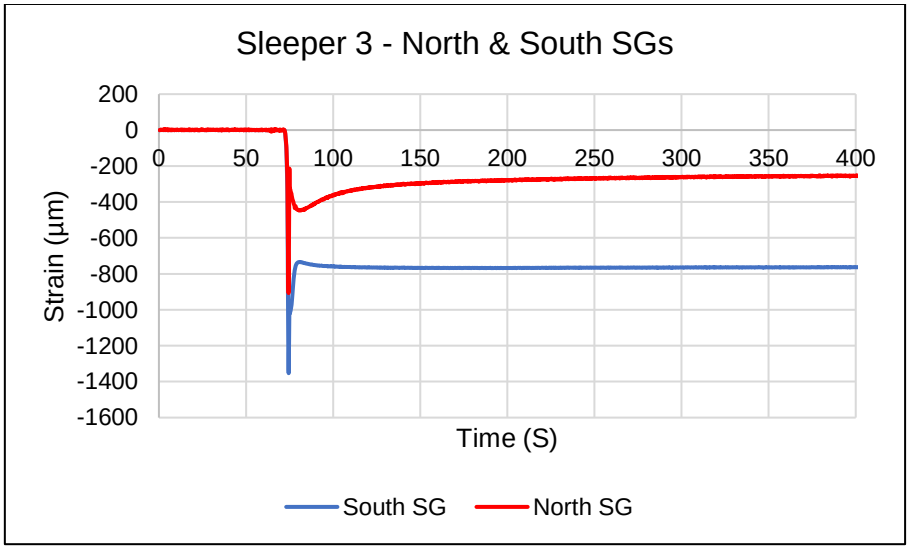

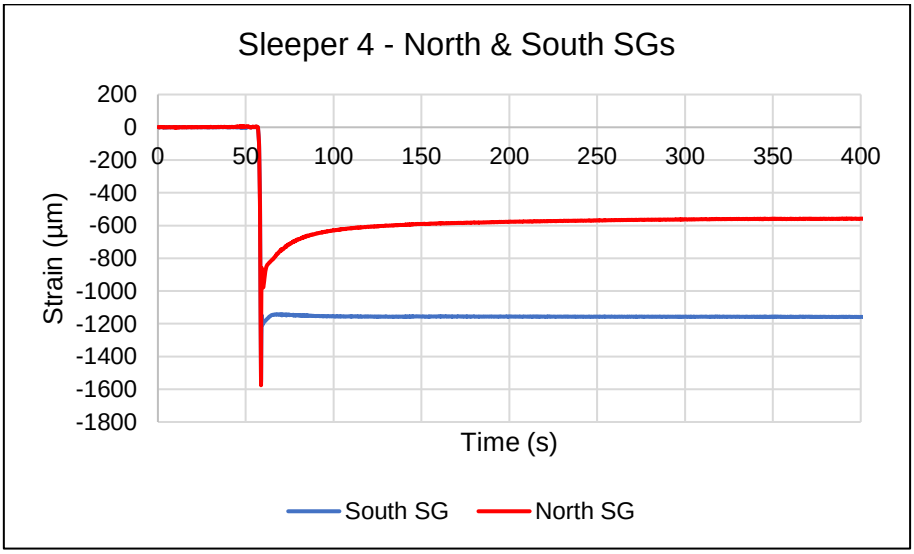

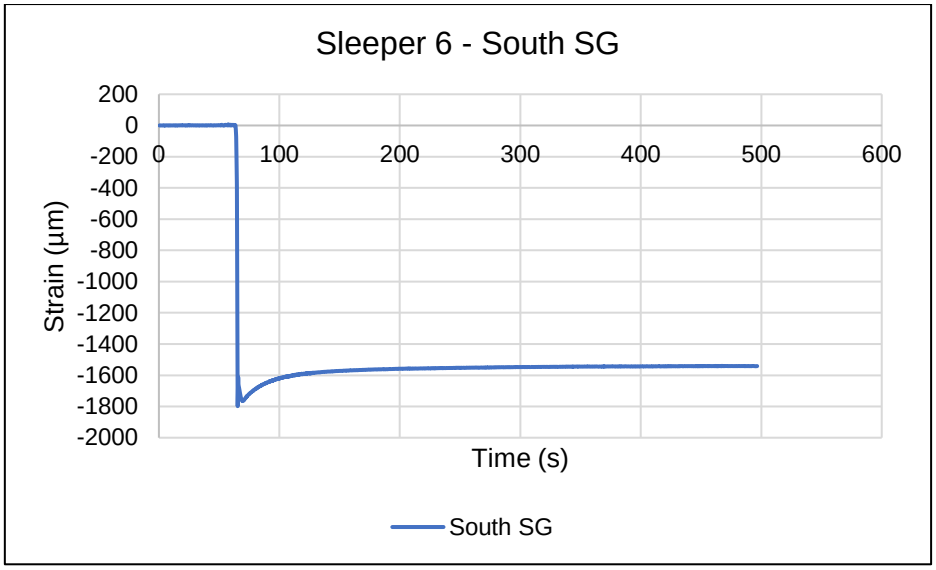
Sleeper 6 - South SG
200
0
-200
-400
-600
-800
-1000
-1200
-1400
-1600
-1800
-2000
0
100
200
300
400
500
600
Strain (µm)
Time (s)
South SG

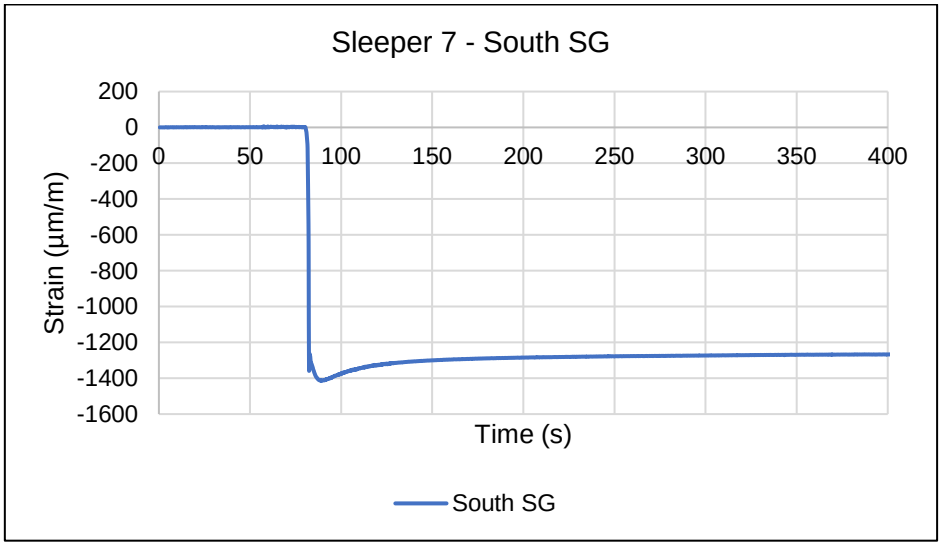
Sleeper 7 - South SG
200
0
-200
-400
-600
-800
-1000
-1200
-1400
-1600
0
50
100
150
200
250
300
350
400
Strain (µm/m)
Time (s)
South SG

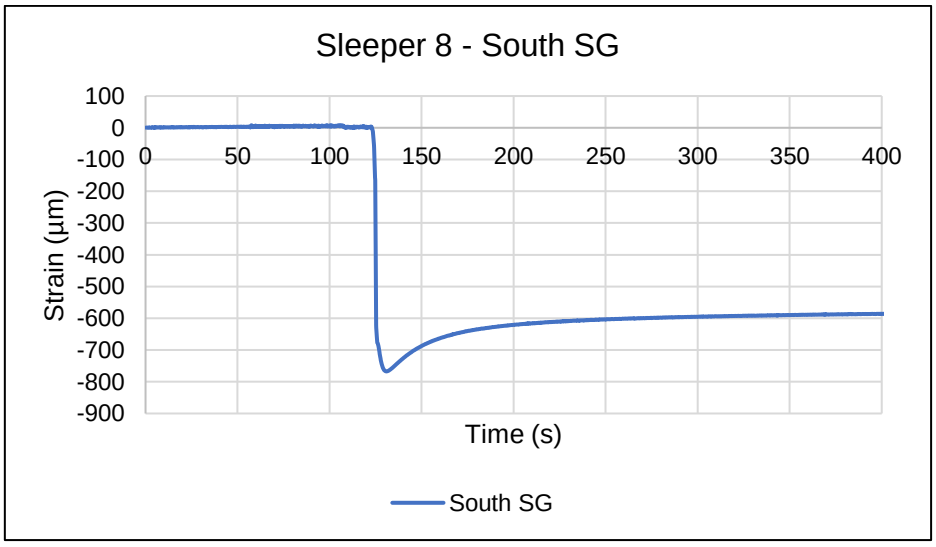
Sleeper 8 - South SG
100
0
-100
-200
-300
-400
-500
-600
-700
-800
-900
0
50
100
150
200
250
300
350
400
Strain (µm)
Time (s)
South SG

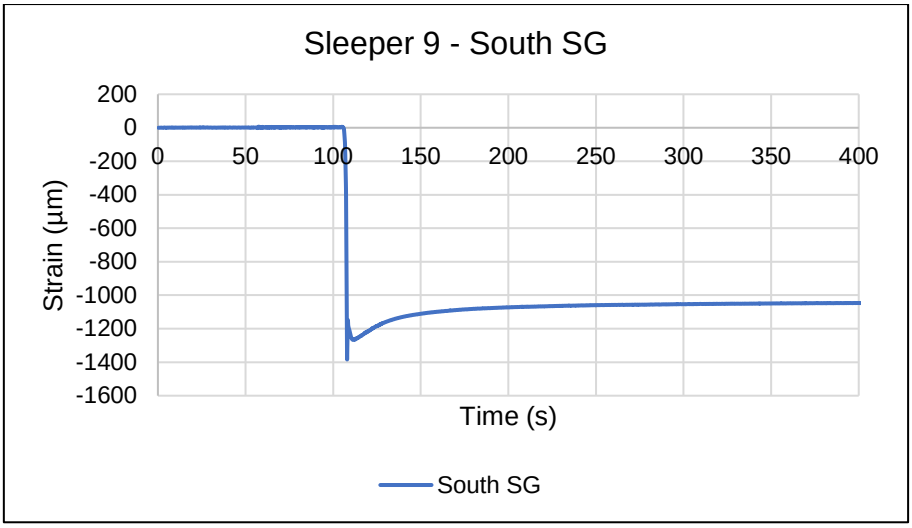
Sleeper 9 - South SG
200
0
-200
-400
-600
-800
-1000
-1200
-1400
-1600
0
50
100
150
200
250
300
350
400
Strain (µm)
Time (s)
South SG

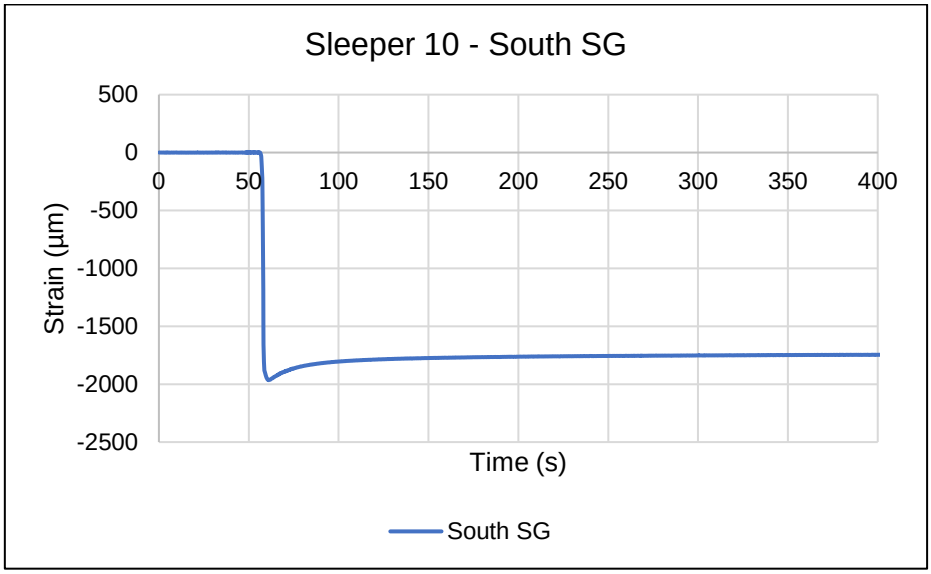
Sleeper 10 - South SG
500
0
-500
-1000
-1500
-2000
-2500
0
50
100
150
200
250
300
350
400
Strain (µm)
Time (s)
South SG

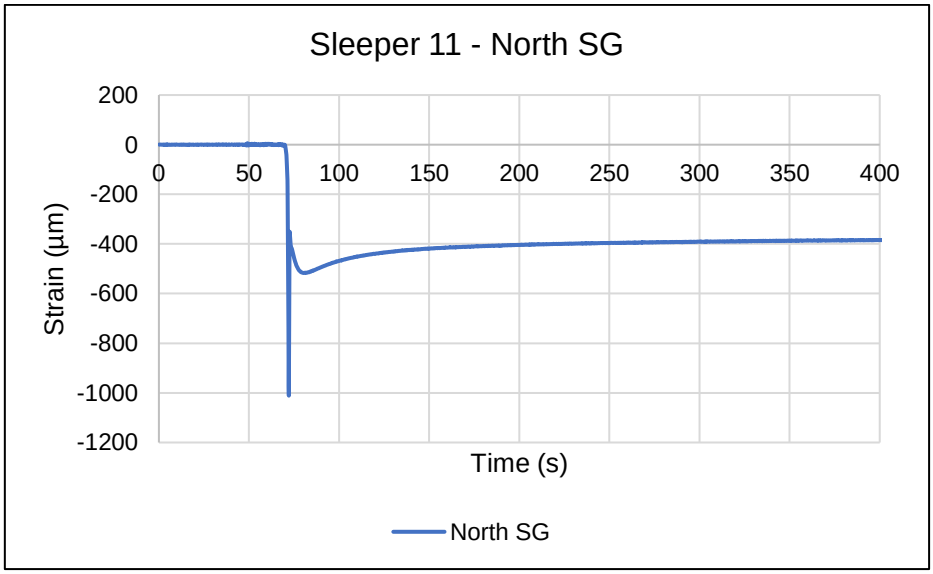
Sleeper 11 - North SG
200
0
-200
-400
-600
-800
-1000
-1200
0
50
100
150
200
250
300
350
400
Strain (µm)
Time (s)
North SG

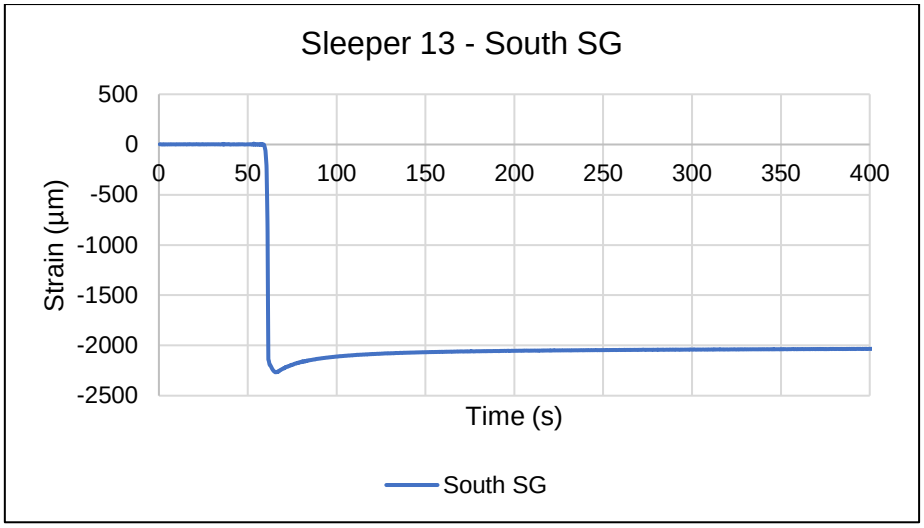
Sleeper 13 - South SG
500
0
-500
-1000
-1500
-2000
-2500
0
50
100
150
200
250
300
350
400
Strain (µm)
Time (s)
South SG

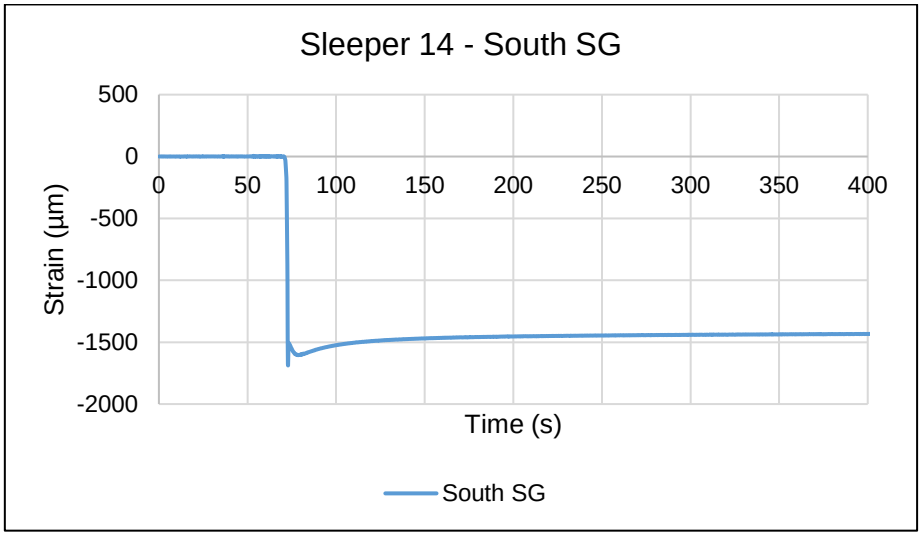
Sleeper 14 - South SG
500
0
-500
-1000
-1500
-2000
0
50
100
150
200
250
300
350
400
Strain (µm)
Time (s)
South SG

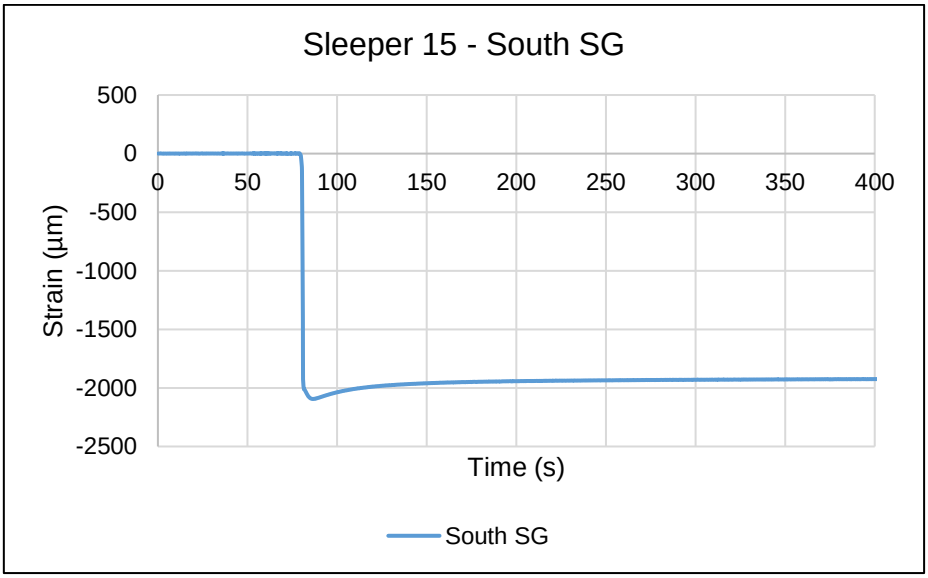
Sleeper 15 - South SG
500
0
-500
-1000
-1500
-2000
-2500
0
50
100
150
200
250
300
350
400
Strain (µm)
Time (s)
South SG

APPENDIX G: STRAIN GAUGE

HBM

Dehnungsmeßstreifen
Strain Gauges
Jauges d'extensométrie

Typ **1.5/120LY13**

Stückzahl Quantity Quantité	10	mit with avec	☐	ohne without sans	X	Applikationshilfe Application aid Support d'aide à l'application

Widerstand Resistance Résistance	120.00	[Ω]	± 0.35 [%]
k-Faktor Gauge factor Facteur k	1.90		± 1,5 [%]
Querempfindlichkeit Transverse Sensitivity Sensibilité transverse	0.7	[%]	

Temperaturkompensation: Angepaßt für
Temperature Compensation: Compensated for
Compensation de température: Compensation pour

α = 23.0 [10^{-6}/°C]

☐ Stahl / Steel / Acier
X Aluminium
☐ Sonstige / Other / Autre

Temperaturkoeffizient des k-Faktors Temperature coefficient of gauge factor Coefficient de température du facteur k	126 ± 10 [10^{-6}/°C] (-10....+45 °C)
Artikel Nr. Part No. No. de Réf.	1-LY13-1,5/120
Folienlos Lot Lot de la feuille	A249/03/03
Herstellungslos Batch Lot de fabrication	EV6798700/1

Alle technischen Daten nach OIML IR 62, bei Beachtung der abweichenden Toleranzangaben auch nach VDI/VDE 2635. Geben Sie bei Rückfragen bitte DMS-Typ und Herstellungs-Los an.

All technical data in accordance with OIML IR 62, also compliant with VDI/VDE 2635 if deviating tolerances are observed. In case of further inquiries please indicate gauge type and batch number.

Toutes caractéristiques techniques selon OIML IR 62 et VDI/VDE 2635 pour les indications différentes de tolérance. Pour toutes questions, indiquer le type de la jauge ainsi que le lot de fabrication.

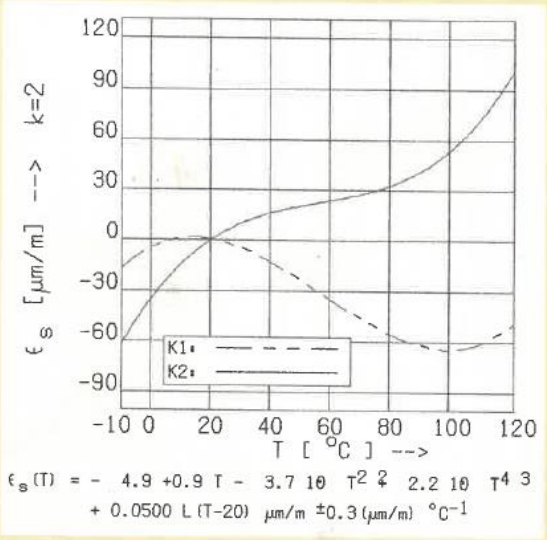

$\epsilon_s(T) = -\ 4.9 + 0.9\ T - 3.7\ 10\ T^{2}\ 2 + 2.2\ 10\ T^{4}\ 3$
$+\ 0.0500\ L\ (T-20)$ µm/m ±0.3 (µm/m) $°C^{-1}$

Temperaturgang der Dehnungsmeßstreifen bei Applikation auf Werkstoffen mit umseitig angegebenem Wärmeausdehnungskoeffizienten α. Gemessen bei kontinuierlicher Temperaturänderung.

Kennlinie 1: DMS ohne Anschlußbändchen

Kennlinie 2: DMS mit Anschlußbändchen (30 mm einfache Bändchenlänge). Bei gekürzten Bändchen liegt der Temperaturgang zwischen Kennlinie 1 und 2. Die numerische Darstellung erlaubt, den Temperaturgang für jede Bändchenlänge exakt zu errechnen.
T = Temperatur in °C L = einfache Bändchenlänge in mm

The **Thermal output** refers to strain gauges when bonded to materials with the coefficient of thermal expansion α given overleaf. Values are measured at a continous temperature progression.

Curve 1: Gauges without connecting leads

Curve 2: Gauges with connecting leads (simple lead length of 30 mm). If the leads are shorter, then the thermal output lies between curve 1 and 2. The numeric approximation allows the calculation of the thermal output for any lead length.
T = temperature in °C L = simple lead length in mm

Comportement en température des jauges d'extensométrie appliquées sur des matériaux dont les coefficients de dilatation thermique α sont indiqués au verso. Mesuré au cours d'une variation continue de la température.

Courbe 1: Jauges sans fils de sortie

Courbe 2: Jauges avec fils de sortie (longueur unitaire du fil de 30 mm). Lorsque les fils sont plus courts, le comportement en température se trouvera entre les deux courbes 1 et 2. Le dernier terme de l'équation détermine avec exactitude l'influence des fils de sortie.
T = température en °C L = longueur unitaire des fils en mm

HOTTINGER BALDWIN MESSTECHNIK GMBH
Postfach 4235 · Im Tiefen See 45 · D-6100 Darmstadt
Telefon: (06151) *803-0 · Telefax: (06151) 894896
Telex: 419341 · Telegramm: Messtechnik Darmstadt

vw-d 1.90 – 30.0 wd